TÉCNICO LISBOA

Investigation of offshore wind farm layout optimization regarding wake effects and cable topology

Bryce Murray Wade

Thesis to obtain the Master of Science Degree in

Energy Engineering and Management

Supervisor: Prof. Ricardo Balbino dos Santos Pereira

Examination Committee

Chairperson: Prof. José Alberto Caiado Falcão de Campos

Supervisor: Prof. Ricardo Balbino dos Santos Pereira

Member of the Committee: Eng. Tiago Mendes Duarte

October 2018

I declare that this document is an original work of my own authorship and that it fulfils all the requirements of the Code of Conduct and Good Practices of the *Universidade de Lisboa*.

To those working towards a sustainable future.

Acknowledgements

I would like to express my sincere gratitude to my supervisor Ricardo Pereira for his guidance and support throughout this thesis. His technical knowledge and superior command of the English language were instrumental in the final product.

I would additionally like to thank Bart Ummels for his willingness to provide insights into the offshore wind industry which helped shape my thesis.

I must also thank InnoEnergy and the ENTECH program who provided such a valuable experience over the past two years filled with new knowledge, new perspectives and new friendships.

Finally, I would like to also express my deepest appreciation to my family and friends near and far who provided support, both emotional and technical, throughout the duration of the thesis.

Cameron, you deserve your own line of recognition for your programming expertise that helped me out of a few sticky situations.

Thank you all.

Abstract

Offshore wind energy is emerging as a large contributor to installed renewable energy capacity. In order to continue the momentum of its development, the offshore wind industry is looking to continually lower the levelized cost of electricity (LCOE). One area being explored in an effort to lower the LCOE of offshore wind generation is the optimization of the wind farm layout. Many of the offshore wind farm layout designs that exist today are structured in a rectilinear form where turbines are spaced evenly along columns and rows. This thesis explores the economic advantages of removing rectilinear constraints and optimizing the positions of the individual turbines within an offshore wind farm.

At the core of achieving the thesis objective was the development of a model that is capable of simulating an existing offshore wind farm by converting representative wind farm data into an LCOE. The positions of the turbines within the wind farm can be modified using an optimization framework with the intent to minimize the LCOE. The model comprised of the Jensen Wake Model, a hybrid cable layout heuristic and an NREL cost scaling model. The wind farm layout was optimized using a genetic algorithm.

The cost estimation model and optimization framework were applied into two case studies to analyze the results of the wind farm layout optimization of two wind farms, Horns Rev and Borssele. In both case studies the optimized layouts provided higher AEP, shorter intra-array collection cable lengths and ultimately a lower LCOE than the baseline rectilinear layouts.

Keywords

Offshore Wind Energy, Wind Farm Layout Optimization Problem, Wake Effects, Cable Topology, Genetic Algorithm

Resumo

A energia eólica offshore está emergindo como um grande contribuinte para a capacidade instalada de energia renovável. A fim de continuar o ímpeto de seu desenvolvimento, a indústria eólica offshore procura reduzir continuamente o custo nivelado da eletricidade (LCOE). Uma área que pode contribuir para reduzir o LCOE da geração eólica offshore é a otimização do layout do parque eólico. Muitos dos projetos de layout de parques eólicos offshore que existem hoje são estruturados de forma retilínea, onde as turbinas são espaçadas uniformemente ao longo de colunas e linhas. Esta tese explora as vantagens económicas de remover restrições retilíneas e otimizar as posições das turbinas individuais dentro de um parque eólico offshore.

O objetivo central desta tese é alcançar o desenvolvimento de um modelo que seja capaz de simular um parque eólico offshore existente, convertendo dados representativos de parques eólicos em um LCOE. As posições das turbinas dentro do parque eólico podem ser modificadas usando uma estrutura de otimização com a intenção de minimizar o LCOE. O modelo foi composto pelo modelo Jensen Wake, uma heurística de layout de cabo híbrido e um modelo de escalonamento de custo NREL. O layout do parque eólico foi otimizado usando um algoritmo genético.

O modelo de estimativa de custos e a estrutura de otimização foram aplicados em dois casos de estudo para analisar os resultados da otimização do layout de dois parques eólicos, Horns Rev e Borssele. Em ambos os estudos de caso, os layouts otimizados proporcionaram maior AEP, menor comprimento de cabo de coleta e, tambem, menor LCOE do que os layouts retilíneos de linha de base.

Palavras-chave

Energia Eólica Offshore, Problema de Otimização de Layout de Parque Eólico, Wake Effects, Topologia de Cabo, Algoritmo Genético

Table of Contents

List of Figures

List of Tables

List of Acronyms

AC	Alternating Current
AEP	Annual Energy Production
AOE	Annual Operation Expenses
BLC	Bottom Lease Cost
CFD	Computational Fluid Dynamics
COS	Cost of Steel
DC	Direct Current
EW	Esau-Williams
FCR	Fixed Charge Rate
GA	Genetic Algorithm
GDP	Gross Domestic Product
HVAC	High Voltage Alternating Current
HVDC	High Voltage Direct Current
ICC	Initial Capital Cost
LCOE	Levelized Cost of Electricity
LRC	Levelized Replacement Cost
MVAC	Medium Voltage Alternating Current
NREL	National Renewable Energy Laboratory
OWE	Offshore Wind Energy
OWFACLP	Offshore Wind Farm Array Cable Layout Problem
OWFLO	Offshore Wind Farm Layout Optimization
O&M	Operation and Maintenance
POS	Planar Open Savings
VRP	Vehicle Routing Problem
WDL	Wake Dissipation Length
WFLOP	Wind Farm Layout Optimization Problem

List of Symbols

$tan\delta$	Insulation loss factor
η_{CC}	Collection Cable Efficiency
ϑ	Wind Direction
ρ	Density of Fluid
A_{turb}	Swept Area of the Turbine Rotor
a	Induction Factor
BCE	Blade Material Cost Estimator
C	Cable Capacity
C_p	Power Coefficient
C_t	Thrust Coefficient
c_w	Weibull Scale Parameter
COS	Cost of Steel
D_o	Rotor Diameter
D_1	Wake Diameter at 1
f	Frequency
$f_w(v)$	Frequency of Occurrence
$GDPE$	Labor Cost Estimator
H	Hub Height
I	Current
k	Wake Decay Constant
k_w	Weibull Shape Parameter
L	Cable Length
N	Number of Turbines
P	Power
P_Ω	Ohmic losses
R	Turbine Radius
R_{ac}	AC Resistance
T	Annual Hours
U	Voltage
u	Wind Velocity at Rotor
U_{turb}	Wind Velocity at Turbine Rotor
U_∞	Free Stream Wind Velocity
v	Wind Speed
v_o	Free Stream Wind Velocity

v_1	Downstream Wind Velocity at 1
w	Weighting Factor
W_d	Dielectric losses

Chapter 1

Introduction

This chapter gives a brief overview of the work developed in the current thesis. Background information on offshore wind energy is provided which leads to an analysis of the problem of improving the economic viability of offshore wind projects by optimizing the wind farm layouts. The objective of the thesis is then defined, followed by a description of the approach taken to achieve the objective.

1.1 Background Information

Developing carbon free sources of electricity has become a global focus in recent decades. As the understanding of the importance of this shift within our energy sector spreads, increased interest and investment have been directed towards renewable energy sources. Wind energy is a leading technology in the development of large-scale renewable energy generation and is a significant percentage of the electricity generation of many nations. [1] [2]

Some nations have pushed wind energy technology by providing incentives for its development, as there are motivations beyond simply economics with regards to energy generation. As nations reach the limits of on-shore wind farm potential, whether it be limited land availability or undesirable locations, they are looking for new opportunities to exploit this vastly untapped resource. This had led to increased investment and interest in offshore wind energy. Offshore wind energy (OWE) utilizes similar technology to its onshore kin, but has distinct advantages of being less disruptive to communities, improved wind conditions, and potential for larger scale turbines and farms. [3]

As the offshore wind energy industry grows, the technology is improving and is making offshore wind energy viable in an increasing number of locations. This includes nations previously not interested in offshore wind energy development for financial reasons. In some locations, OWE is reaching a critical point where it is now being developed without government backing [4]. In order to continue the momentum of its development, the offshore wind industry is looking to continually lower the levelized cost of electricity (LCOE). This is being done by improving the materials and design, the control strategies and the wind farm design and planning. Focusing on these core areas can help OWE surmount the economic hurdles which will result in further development and ultimately contribute more to sustainable electricity grids. [5]

1.2 Problem Analysis

One area being explored in an effort to lower the LCOE of offshore wind generation is the optimization of the wind farm layout. There are multiple parameters that are considered when designing a wind farm array including but not limited to: wake effects, wind profile, bathymetry, soil types, cable installation costs, transmission losses, environmental concerns, permitting restrictions and visual impact. While acknowledging these parameters, many of the resulting wind farm layout designs that exist today are structured in a rectilinear form where turbines are spaced evenly along columns and rows. This is the case for many notable large projects such as Horns Rev, London Array, Gemini Wind Farm and Dudgeon, as well as Barrow, Sheringham Shoal and Walney 1, seen in Figure 1-1.

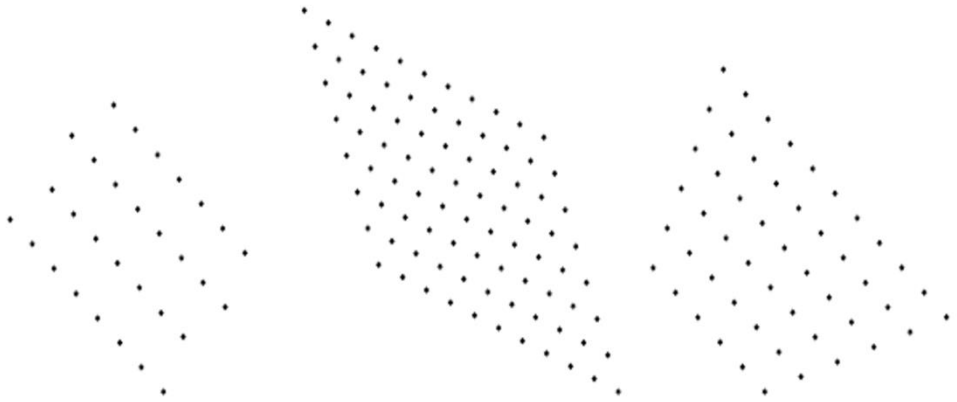

Figure 1-1. Rectilinear offshore wind farm layouts [6]

Wind farm designers have considered the value of minimizing wake effects, as the rows and columns of wind farms are often oriented into an optimal direction based on the local wind climate. However, the inconsistent nature of environmental factors such as the local wind climate, bathymetry, and soil types would conclude that these are not driving factors in the structured layouts. It is the inherent value of aesthetics, the permitting restrictions and other external factors that presumably lead to these traditional layouts. It has been hypothesized through many academic research efforts that keeping rectilinear formats may cost a great deal when measuring the annual energy production over the lifetime of the windfarm [7].

When determining the spacing between turbines in an offshore windfarm layout, there are two key parameters that oppose with regards to profitability; wake effects and the collection cable length. Wake effects can be defined as the kinetic energy deficit caused by an upstream turbine on a downstream turbine, and is directly related to the distance between the turbines [8]. Therefore, the further spaced apart the turbines are from one another within a wind farm, the more overall energy is converted from the wind to electricity. However, the increased spacing between the turbines results in a longer collection cable length required for transmission of the electricity. This increases the collection cable material costs, installation costs and transmission losses. The opposing nature of these design variables result in some layouts being more profitable than others.

Abandoning the rectilinear constraints described above and understanding how the wake effect and cable cost variables are related can be utilized in the wind farm design process to improve the economic viability of offshore wind development.

1.3 Thesis Objective

The objective of this thesis is to explore the advantages of optimizing the positions of the individual turbines within an offshore wind farm. The optimization seeks to minimize the objective function which is the levelized cost of electricity (LCOE) of the wind farm. At the core of achieving the thesis objective was the development of a model that is capable of the following:

- Simulating an existing offshore wind farm by converting necessary input data into a representative LCOE.
- Providing the ability to optimize the positions of the individual turbines within the wind farm in order to lower the LCOE.
- Providing the ability to perform sensitivity analysis for different input parameters for the offshore wind farm that can provide insight to the importance of the different design variables.
- Being improved in future work in an effort to increase the accuracy and effectiveness.

Due to the potential of such a tool and the restraints on time and resources, the scope of this thesis was focused on the development of a valid model that can be used to compare the difference in LCOE from an existing layout to an optimized layout. Assumptions and simplifications that were incorporated are noted throughout the thesis.

1.4 Approach

The approach taken was to extensively review existing research in different areas of offshore wind farm modelling and to select the most appropriate sub-models to combine into a complete framework that produces LCOE estimations from the wind farm characteristics. The different areas of research included work that has simulated offshore wind farm wake effects, simulated cable topology designs, developed representative economic models and provided optimization evaluations. Key determining factors in selecting sub-models included their accuracy, their simplicity and their computational requirements. The accuracy was necessary in order to provide results of value, as compounding sub-components with less accurate results would lead to a final result of little value. The simplicity and computational requirements were considered in order to maintain an achievable scope within the applied time constraints, and because of technical limitations of the simulation computers. The computational requirements played the strongest part in deciding on the wake model, as advanced CFD methods which provide more accurate results require extensive computing power which was not available. When the best design under the given constraints was selected for each sub-component, they were combined into one model. The structured method of assembly for the model allows for future improvements on particular sub-components which could provide more accuracy and new insights in its future use.

MATLAB was selected as the software in which to build the model as its strengths align with the

requirements of this model, it has optimization tools built in, and most importantly it was available and familiar to the author and advisor at the time of execution. The model structure was divided into three components: a physical component, an economic component and an optimization component.

- The physical component takes the physical input parameters such as wind climate data, turbine characteristics and wind farm layout, then utilizes the Jensen Wake model and a cable layout heuristic to provide an annual energy produced (AEP) and cable layout for the wind farm.
- The economic component takes the economic input parameters, such as the various turbine component costs, cable costs and transmission costs, and using scaling models developed by NREL, converts the AEP into a levelized cost of energy (LCOE).
- The optimization component uses a genetic algorithm that considers the turbine positions within a wind farm layout as variables, and minimizes the LCOE by using both the physical and economic components.

The model was validated using measured data from an existing wind farm. Upon validation, the model was used to estimate the difference in LCOE's for different wind farms with the existing and optimized wind farm layouts and conclusions were drawn from the results.

1.5 Thesis Outline

The outline of the report and content of each chapter is described below;

Chapter 2 describes the state of the art of the wind farm layout optimization research.

Chapter 3 introduces the physical component of the model which consists of the turbine and wind characteristics, wake effects, cable topology and wind farm annual energy production.

Chapter 4 discusses the economic component of the model which consists of the different fixed and variable costs, and the economic assumptions included in the final model.

Chapter 5 presents the different methods for model validation and describes the limitations of the model.

Chapter 6 explores the optimization component of the thesis and delves into the optimization framework and parameters.

Chapter 7 provides analysis and evaluates the results of two case studies. The analysis is focused on the value of optimizing offshore wind farm layouts while removing existing layout constraints.

Chapter 8 draws conclusions from the thesis and provides recommendations for future expansion of this work.

Chapter 2

State of the Art

This chapter provides an overview of the state of the art of the wind farm layout optimization problem. It first describes the problem and its origins, and then discusses the different ways in which the research is being advanced.

2.1 Wind Farm Layout Optimization Problem

A wind farm consists of an array of wind turbines that convert the kinetic energy from the wind to electricity. Wind turbines can be arranged within a wind farm in a certain orientation in order to increase the energy the wind farm yields. Traditional layouts are typically in a rectilinear format, identifiable by the turbine's arrangement in equally spaced rows and columns. The majority of the largest wind farms in operation today are in a grid format, rotated in an orientation with respect to the wind direction to maximize energy yield (for the set formation). However there has been a growing field of research into truly maximizing the energy yield for a given wind farm site by abandoning the rectilinear constraints. The area of this research has been termed the Wind Farm Layout Optimization Problem (WFLOP) where interested parties are creating models and using optimization algorithms to better understand how different wind farm orientations can provide higher energy yields under different environmental and physical circumstances. [7]

The WFLOP requires a defined objective function and an optimization strategy. The objective function is calculated based on the design parameters, and is minimized through optimization of the wind farm design. The objective function is most commonly maximum annual energy production (AEP), minimum cost of energy (COE), maximum profit or a combination of them. The optimization strategies use algorithms that iterate through various scenarios in search of satisfying constraints and minimizing the objective function. The optimization algorithms can be categorized into gradient methods [9], genetic algorithms [10] [11], viral algorithms [12], particle swarm algorithms [13] and greedy heuristic algorithms [14]. [15]

The WFLOP was first explored by Mosetti et al. [10] in 1994 by considering a wind farm that did not have a defined desired power output, but a fixed number of potential turbine positions. The wind farm consisted of a 10x10 grid where the wind turbine could be placed in the centre of each quadrant or not in search of the most profitable design based on the objective function, as seen in Figure 2-1.

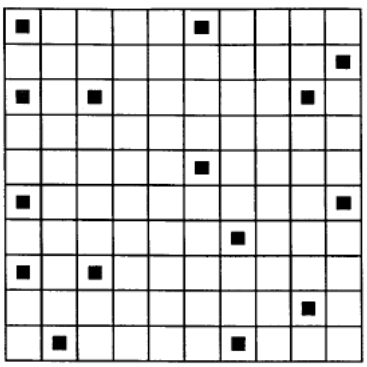

Figure 2-1:Turbine position results for a Mosetti simulation [10]

The objective function defined by Mosetti et al. was a combination of maximizing the power produced while minimizing the installation cost, which resulted in Equation 2-1,

$$Obj_{MOS} = \frac{1}{P_{tot}} w_1 + \frac{cost_{tot}}{P_{tot}} w_2 \quad \text{2-1}$$

Where w_1 and w_2 are the weighing factors. Within their sub-model, Mosetti et al. used the Jensen model to determine the wake deficits within the wind farm. In order to ensure that the Jensen model was valid, the grid sizes were defined to 5D (5 times the diameter of the turbine rotor) in order to ensure the turbines did not interact in the near wake region. (The limitations of the Jensen model are discussed in Section 3.2.)

The cost function implemented was simplified to represent the total cost of the wind farm installation by the number of turbines installed (N), as seen in Equation 2-2.

$$cost = N\left(\frac{2}{3} + \frac{1}{3}e^{-0.00174N^2}\right) \quad \text{2-2}$$

Mosetti et al. used a genetic algorithm (GA) to determine an optimal value to meet the defined objective function by letting a population of 200 individuals evolve for 400 generations. Mosetti. et al. compared the results from the model under three different scenarios: Constant wind speed, constant wind direction; constant wind speed, multiple wind directions; and multiple wind speeds, multiple wind directions. [16]

Since the work of Mosetti et al. there have been numerous attempts to determine the best methods for designing a wind farm layout. The research that followed Mosetti et al. can largely be categorized into two paths: (1) a track focused on the development and testing of different optimization strategies i.e. optimization algorithms, and (2) a track focused on improving the wind farm model accuracy [7]. The second path concentrates on the inclusion of more comprehensive sub-models that consist of an increasing number of parameters in an effort to make the simulations more representative and applicable. Such sub-models address financial prospection, aerodynamics, structural fatigue and degradation, electrical system and grid interconnection, environmental impact and uncertainty and more [7] [17].

The first path was followed by Grady et al. [11] whose objective was to determine the effectiveness of the genetic algorithm optimization procedure in identifying optimal configurations. The objective function was slightly different for their study than that of Mosetti et al., as it evolved to minimize the cost per unit energy produced, as shown in Equation 2-3.

$$Obj = \frac{cost}{P_{tot}} \quad 2\text{-}3$$

A key improvement to Mosetti et al.'s original work was that Grady et al. modified the GA parameters by increasing the number of individuals to 600, created 20 subpopulations and simulated over 3000 generations. By allowing for a larger number of generations, there was an opportunity to achieve a more optimized result at the expense of increased computing time and power required [16].

A non-trivial omission from the Mosetti et al.'s original research into the wind farm optimization was the layout dependent costs [18]. The cost model used by Mosetti et al. was very basic and was solely dependent on the number of turbines installed, under the assumption that the price decreases with the count of wind turbines purchased [15]. There are a number of factors that are dependent on the specific layout of each wind turbine, such as cable cost, that were not accounted for.

A significant contribution to the research focused on improving the performance modelling of wind farms, was the work of Elkinton [19]. The objective of Elkinton's study was to investigate the use of optimization algorithms for offshore wind farm micro-siting. Elkinton approached the wind farm layout optimization problem differently than previous works [10] [11] by considering a continuous space (not a defined grid), with a defined number of wind turbines. The objective function used by Elkinton was minimizing the levelized cost of energy (LCOE), defined by;

$$LCOE = \frac{C_C * FCR + C_{O\&M}}{AEP} \quad 2\text{-}4$$

The variables of the optimization were the coordinates of the wind turbines. Elkinton's study only used the position of two wind turbines as the intent was to develop a more realistic sub models, in particular the cost model, and not focus on the optimization strategies [17].

Elkinton's cost model included for the total investment cost, the operation and maintenance cost, and the AEP, which accounted for wake losses, transmission losses and wind farm availability. Further detail into the cost model can be seen in the reference paper [19]. Elkinton's broader project, the offshore wind farm layout optimization (OWFLO) project focuses intently on modelling the cost of energy (COE) for offshore wind farms and is often used as reference [20].

Pillai et al. [18] advanced the effort of making the results of the offshore WFLOP more dependable by accounting for realistic constraints faced by a wind farm developer. These realistic constraints included variables such as different degrees of layout restrictions which can be imposed by regulatory bodies. The potential layout restrictions were categorized into Array mode (regular grid), Binary mode (defined allowable turbine positions), and Continuous mode (any turbine location is possible). Array mode provides clearly defined navigation channels and is therefore desired by some regulatory bodies, whereas continuous mode has the potential to provide increased efficiency and returns for the wind farm. Binary mode is a compromise which allows for an optimized solution while including positioning

constraints. Pillai et al., while working alongside wind farm developers, developed a sophisticated and detailed LCOE evaluation tool with these constraints and compared its results with that of an existing offshore wind farm. Upon measuring its accuracy (less than 1% error), the model was then used to optimize the existing wind farm layout which resulted in potential reductions in the LCOE between 1-3.5%, depending on the constraints imposed.

Hebert et al. [7] provided a comprehensive review of the state of the art of wind farm design and optimization as of 2014. Hebert et al. reviewed over 150 works and found that the most common objective functions being used were the maximum AEP, maximum instantaneous power conversion and minimum COE, as seen in Figure 2-2.

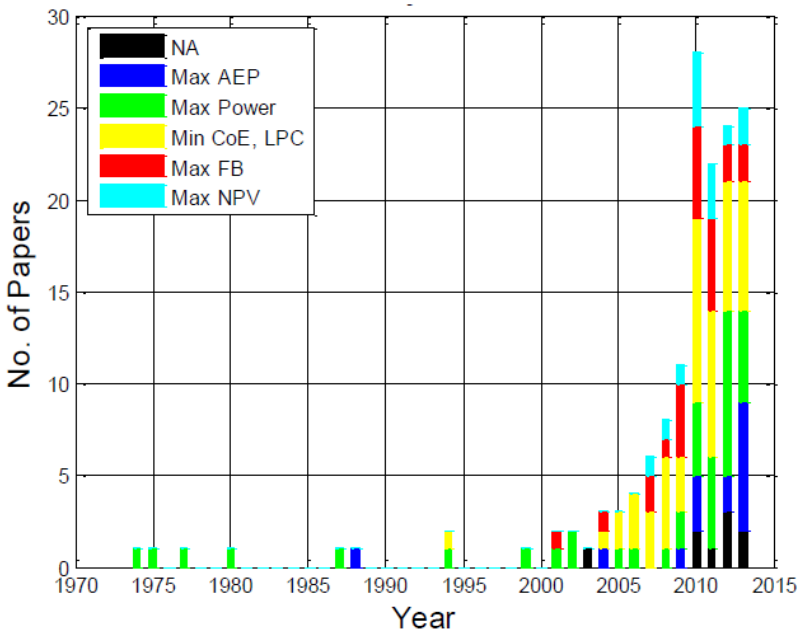

Figure 2-2: Objective function analysis by Hebert et al. [7]

The most common wake model used within WFLOP research to date is the Katic-Jensen model, shown in Figure 2-3. This is in large part due to its modelling simplicity which lessens the computational demand and decreases the simulation time. Hebert et al. concluded that computational technologies are typically the limiting factor for the treatment of the WFLOP problem. Beyond improvement of computational restraints, Hebert et al. concluded that the most important research trends in WFLOP are focused on improving the formulations describing the expected energy conversion of the wind farm, the wind turbine wakes and turbulence impacts, the wind turbine structural fatigue and degradation, the various types of environmental impacts, the overall electrical system losses and reliability and the uncertainty and risk management. Namely, the sub-models and optimization methods must be continually improved to include for more design variable and to require less simplifications in order to provide more accurate results [7].

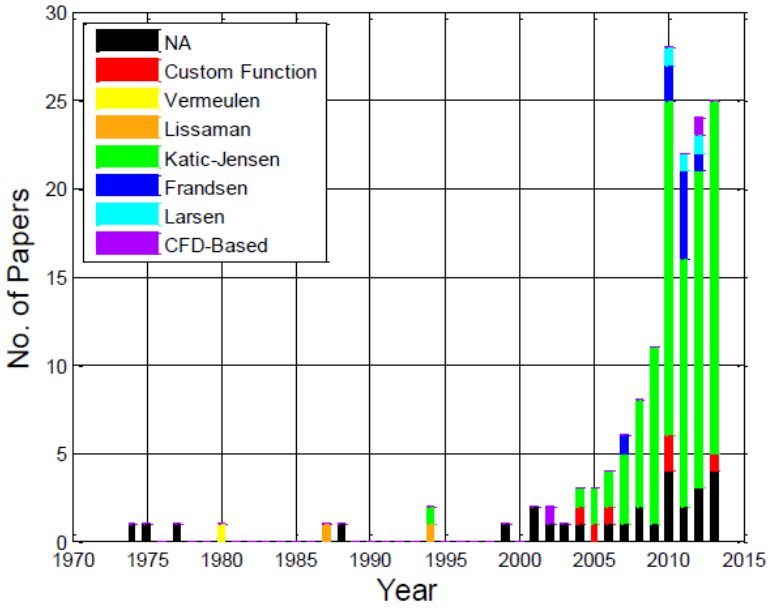

Figure 2-3: Wake model review by Hebert et al. [7]

Pillai et al. more recently proposed that future research should increase the focus on industrial applications and therefore develop more accurate cost models and include more complex and realistic constraints that wind farm developers encounter [18]. This requires increased input and transparency from wind farm developers themselves for the inclusion of current and accurate data, as well as representative physical and economical constraints.

Chapter 3

Physical Model

With the ultimate goal of determining the advantages of optimized wind farm layouts versus existing wind farm layouts with rectilinear constraints, a modelling framework was required in which the different wind farm layouts could be simulated. The modelling framework developed in this thesis is explained easiest by breaking down the three core components. This chapter details the physical component which accounts for the environmental and physical characteristics of the wind farm and provides the annual energy production and collection cable layout. The key sub-components within the physical model are described below.

3.1 Model Inputs

To represent an offshore wind farm there are certain essential parameters by which the wind farm and its environmental conditions can be defined. Section 3.1 describes the necessary input parameters required for the model to represent the simulated wind farm, shown in Figure 3-1.

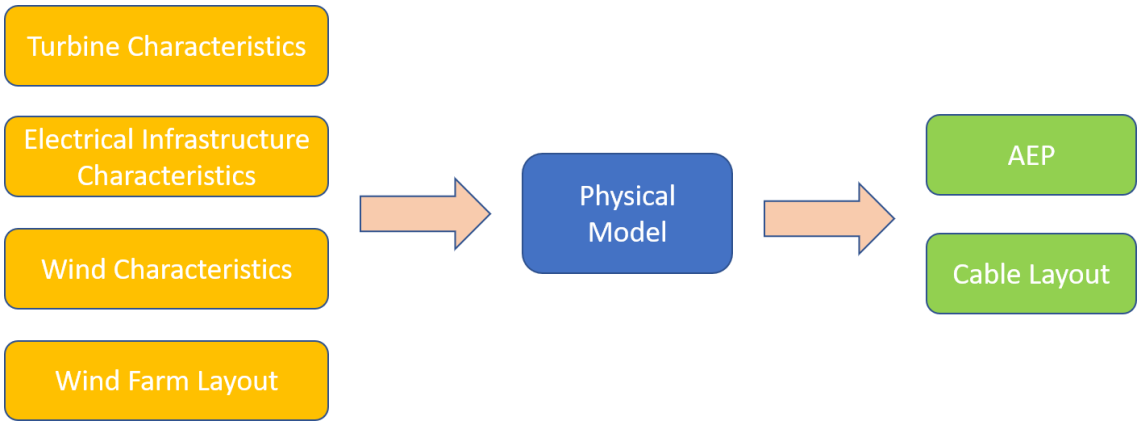

Figure 3-1: Physical model representation

3.1.1 Turbine & Electrical Infrastructure Characteristics

The model is constructed so that the parameters can be modified easily to suit an existing wind farm, with the limitation that the wind farm consists of only one type of wind turbine. It was found through research on many of the existing large-scale wind farms that this assumption of an array of the same turbine model is acceptable.

3.1.1.1 Wind Turbine & Cable Components

Hub height – The hub height is required to properly account for wind velocities that will be experienced by the turbine. Typically, higher hub heights result in higher experienced wind velocities and less influence from the water. For the purpose of this model, the influence of the water on the wind profile is accounted for in the Weibull distribution, though its influence on the wake boundaries was neglected.

Rotor Diameter – Although the rotor diameter is a key factor in determining the power curve (discussed below) and how much energy is extracted from the wind, in the present work it is included since it is a direct input for the Jensen wake modelling.

Intra-Array Cable Capacity – The collection cable design assumes one uniform cable for the whole design (simplification). The intra-array cable characteristics must be set to determine the maximum

number of turbines that can be collected on a single intra-array collection cable.

3.1.1.2 Wind Turbine Power Curve

How much power a wind turbine produces is related in theory to the cube of the incoming wind velocity, as seen in Equation 3-1.

$$P_{turb} = \rho A_{turb} U_{turb}^3 \quad \text{3-1}$$

P_{turb} ……..…Turbine Power [W]

ρ…… Density of Air [kg/m^3]

A_{turb}……Turbine Swept Area [m^2]

U_{turb}……..…Wind Velocity at Turbine [m/s]

However, there are external factors that results in a relationship that is not purely cubic. The wind turbine does not begin producing power until the wind speed reaches a predetermined threshold due to control parameters set by the manufacturer. This threshold is referred to as the cut-in speed, and can be seen in Figure 3-2. The wind turbine is also controlled to stop producing power after the wind reaches velocities that generate high loads. The occurrence of these wind speeds is rare which makes it financially unviable to design turbines to withstand higher loads as the increased output does not compensate for the increased investment. This threshold is referred to as the cut-out speed. [21]

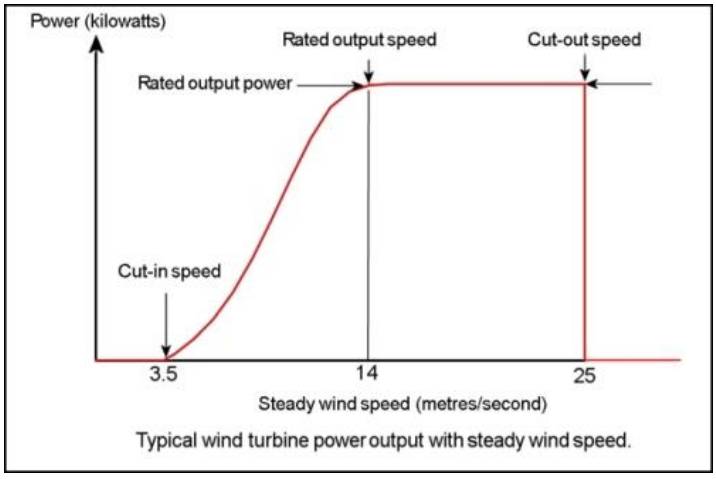

Figure 3-2: Example power curve characteristics [22]

The turbine power curve is limited by an additional factor beyond the wind that is responsible for the curve in Figure 3-2 to not be purely cubic, which is the generator rating. Turbines are equipped with a generator whose maximum power is reached at the wind turbine rated speed. This rated speed is specific to the turbine characteristics as well as the characteristics of the wind farm site [21]. The model

assumes that the turbines are full span pitch-controlled, variable-speed turbines [23] which means that beyond the rated wind speed, the wind turbine is controlled so that the power output plateaus at the rated power of the generator. An accurate power curve is essential in determining the annual energy output (AEP) for a wind turbine, especially for wind speeds between the cut-in and rated speed where slight changes in wind speeds can result in significant changes in power output. The result of such importance is that the accurate power curves of many turbines are considered proprietary by the manufacturer. There is also often a discrepancy between published power curves and the actual measured power curves. This can be a source of error when using a general power curve within a model to compare with measured data from an existing wind farm. [24]

3.1.1.3 Wind Turbine Thrust Curve

When determining the power output for an entire wind farm, the wind velocity deficits caused by upstream wind turbines on downstream wind turbines is required. As discussed later in Section 3.2, the wakes and resulting wind deficits from upstream wind turbines are directly related to the thrust coefficient of the upstream wind turbine. The thrust coefficient is related to the pitch of the blades which is exemplified in the thrust curve shown for a pitch-controlled variable-speed turbine in Figure 3-3. Prior to the rated wind speed, the thrust coefficient remains relatively flat. Once the turbine experiences the rated wind speed and control is required to not surpass the generator rating, the thrust coefficient declines as the blades are pitched into the wind to reduce the power input. As an accurate power curve is critical to determining the power output from a single turbine, an accurate thrust curve is critical to determining the wake effects and the power output for an array of wind turbines.

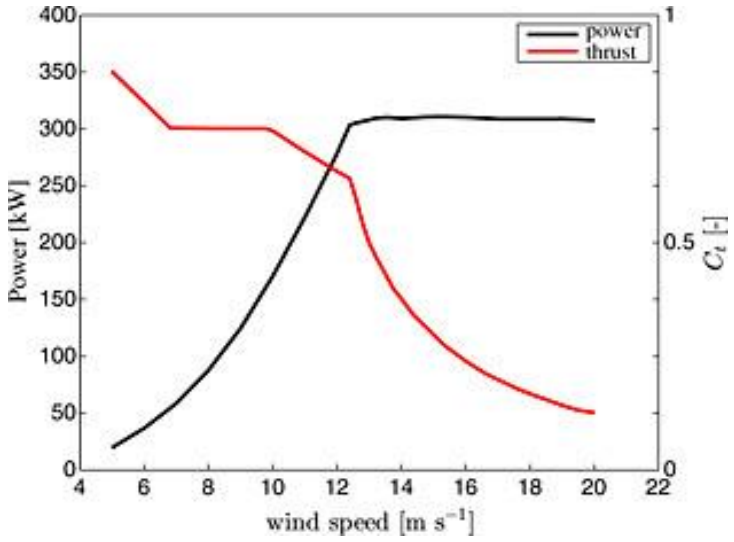

Figure 3-3: Example power and thrust coefficient curve [25]

3.1.2 Wind Characteristics

A key parameter in estimating the annual energy production of a wind turbine is estimating the wind

itself, both the distribution of the wind velocities and the distribution of the wind direction. Gathering wind data through long term meteorological observations is an important step in the analysis of a wind site, as is processing this data and using it to estimate the future wind climate.

3.1.2.1 Wind Velocity Distribution

The Weibull distribution is an industry accepted and recommended probability distribution that can represent the wind velocity distribution for a given site. The two parameter Weibull probability model was determined to fit real wind data better than the lognormal, gamma and Rayleigh models, per Garcia et al. [26].

The probability density function of the Weibull distribution is given by Equation 3-2,

$$f_w(v) = \frac{k_w}{c_w}\left(\frac{v}{c_w}\right)^{k_w-1} e^{-\left(\frac{v}{c_w}\right)^{k_w}} \quad \text{3-2}$$

$f_w(v)$ ……..…Frequency of Occurrence [-]

v…… Wind Speed [m/s]

k_w…….……Shape Parameter [-]

c_w……..…..…Scale Parameter [m/s]

where $f_w(v)$ is the probability of observing wind speed v [27].

For an assessment of the climate, the shape factor k_w and scale factor c_w can be applied to create a Weibull distribution that matches the measured wind data. Once the probabilities are determined for each wind speed, they can be multiplied by the number of hours in a year to identify the number of hours each year that a turbine is expected to experience a given velocity. This information is then used to determine the estimated energy yield by multiplying by the appropriate power value for each wind speed on the power curve, as seen in Equation 3-3.

$$AEP = T\int_{v_o}^{v_\infty} P(v)\, f_w(v) dv \quad \text{3-3}$$

AEP ……Annual Energy Production [kWh]

T……..…… Annual Hours [h]

P……Wind Turbine Power [kW]

The current model uses the shape factor and scale factor as inputs and uses the Weibull probability density function to provide the wind velocity distribution. Equation 3-3 is only applicable for a single wind

turbine that does not experience wake effects from other wind turbines in a wind farm. When considering the power production of a wind farm, the direction from which the wind approaches must also be included.

3.1.2.2 Wind Velocity Distribution

The wind rose is a spatial representation of the variation of the wind direction for a given site. It indicates how often the wind approaches a wind farm from a given direction. This is an important factor in wind farm layout design as determining the most dominant wind directions helps in orienting the wind farm in order to minimize wake effects and maximize energy production [28]. Statistically the wind direction data can be binned in a radial format, with the greater number of bins giving more precise directional data.

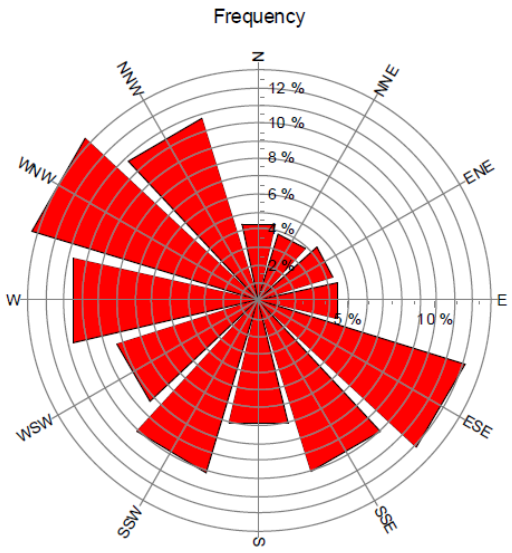

Figure 3-4: Wind rose (30° bins) – Horns Rev wind farm [24]

With the proper equipment and data processing, each wind direction can be associated with a Weibull distribution providing an accurate estimation for the wind distribution in a given year. This results in increased confidence in the annual energy production estimates. Equation 3-4 shows the inclusion of the wind directions into Equation 3-3.

$$AEP = T \int_{\vartheta_o}^{\vartheta_{360}} \int_{v_o}^{v_\infty} P(v)\, f_w(v) dv d\vartheta \qquad 3\text{-}4$$

ϑ ……Wind Direction [°]

3.1.3 Wind Farm Layout

To analyze the turbine placement of existing wind farm layouts and develop a tool that can optimize the

turbine positions to provide a lower LCOE, an accurate representation of the wind farm layout is essential. The parameters and constraints involved in the development of the model are discussed within the following subsections.

3.1.3.1 Parameters

When determining the positions of the turbines within an offshore wind farm there are multiple parameters that are considered. Many of the parameters are specific to the wind farm site, which can be referred to as macro-siting; physical boundary constraints, environmental concerns, permitting restrictions, shipping restrictions and aesthetics. There are also many parameters that apply to the location of each of the individual wind turbines to be positioned, which can be referred to as micro-siting; wake effects, cable and transmission costs, water depth and soil characteristics. Not all of the parameters mentioned are exclusive to only macro or micro-siting, but are considered for both.

Due to the variability and complexity that the inclusion of all of these parameters would result in, several assumptions for current modelling were made. For the parameters that are specific to the location of the wind farm itself, the following assumptions were made;

- The outer perimeter of the existing wind farm was kept constant when applying the optimization function.
- The environmental concerns, permitting restrictions and shipping restrictions were all neglected and provided no value or restrictions in the optimization. It should be noted however that general costs associated with permitting and other administrative tasks were considered as a fixed cost for the wind farm in the economic model.
- Aesthetics were not considered of any value throughout the optimization process. As aesthetics do play a role when the wind farms are within the public eye, a tool such as this would provide more value to wind farms further offshore where they are of less concern.

For the parameters that are specific to the location of each individual turbine, the following assumptions were made;

- The water depth and soil types were considered to be the same for each turbine location in the wind farm. The assumption was made because all sites are different and developing a tool to incorporate bathymetry and soil characteristics data would be extensive, as would acquiring the data to represent this. This level of complexity of both creating an accurate tool and gaining access to this data is beyond the scope of this thesis. However, based on the strict rectilinear layouts of existing wind farms, it is assumed that existing designs pay little attention to the water depth and soil characteristics for each specific turbine location (micro-siting). It is important to distinguish however, that water depth and soil characteristics do play a significant role in overall wind farm site location (macro-siting).

One parameter that is included in the model as a fixed cost (independent of turbine position) and not a variable cost (turbine position dependent), was the cost of operation and maintenance. An argument can be made that the positions of the turbines affect the overall cost of operations and maintenance due

to the turbine location variation causing variations in the wake effects. The variations in the wake effects may result in increased / decreased turbulence experienced by a wind turbine which could affect its required maintenance. With this said, operation and maintenance costs are often estimated by using an overall percentage of the total initial investment (fixed costs) for large offshore wind installations due to its unpredictable nature [23]. Therefore, for the purpose of this model, the operation and maintenance cost were considered independent of the layout of the wind turbines.

3.1.3.2 Wind Farm Optimization Physical Constraints

Although the overall objective of the thesis clearly outlined the intent to remove constraints on the positions of the individual turbines within the wind farm, the model was designed to provide flexibility and the option of different turbine position constraints.

The optimization framework that was implemented is best applied when the wind farm perimeter boundaries are strict and the restrictions on specific wind turbine positioning is not. This option provides the flexibility of positional constraints for each turbine akin to the approach introduced by Pillai [18], or no specific turbine placement constraints beyond the physical constraints required by the wake model. These physical constraints required by the wake model include turbines maintaining three diameters spacing between each other to avoid near wake conditions, which is critical for the implementation of the Jensen Wake Model [8] described below in Section 3.2.

3.2 Wake Model

A key function of the physical model is to determine the array efficiency based on the input parameters. The array efficiency can be defined as the ratio of the actual energy output of a given array of wind turbines versus the sum of the energy output of an equal number of wind turbines without the effects on one another. If all turbines experienced free stream wind conditions, as if they were on their own, the array efficiency would be 100%. However, when grouped together, wind turbines have a negative influence on one another due to the wakes caused by each turbine. Wake effects are at the core of the physical model and will be discussed at length in the following sections.

3.2.1 Wake Effects

As a turbine extracts energy from the wind and converts it to electrical energy, it leaves a wake behind which can be seen in Figure 3-5 below. The wake is characterized by reduced wind speeds and increased turbulence in the flow [21]. The wake from a turbine expands and gradually returns to the free stream condition as it continues downstream. If the wake of a turbine intersects with the swept area of another turbine downstream prior to reaching the free stream condition, the downwind turbine is considered to be shadowed by the upstream turbine [29]. If a turbine is shadowed, it experiences a lower wind velocity than the free stream, which can result in less energy conversion than if the turbine

was not shadowed. Understanding the magnitude of these losses and how to minimize them is paramount in order to maximize the return on investment of an offshore wind park.

Figure 3-5: Wakes at Horns Rev wind farm made visible by weather conditions [30]

3.2.2 Wake Effect Properties

Wake effects are considered of increased relevance in offshore wind turbine arrangements than onshore wind turbine arrangements due to the increased restrictions for onshore turbine placement caused by topography, residents and the environment [31]. Typically, the only obstruction of the wind for a given turbine in an offshore wind farm is other turbines, which may be arranged accordingly.

Wind turbine wakes themselves can be classified as either near wake or far wake which are characterized by how close to the wake-causing turbine the position is [32]. For instance, the near wake region is up to two to three turbine diameters downstream from the turbine. The near wake region is characterized by having the wind velocity directly disturbed by the turbine geometry. The far wake region is anything beyond the near wake region, or further than three diameters [33].

The far wake has two main mechanisms that define the flow conditions which are convection and turbulent diffusion. In the far wake region turbulence is a more dominating factor than in the near wake region. When incorporating wake effects into a model for an offshore wind farm, the far wake becomes more important than the near wake due to the larger distances between the turbines [16]. As the focus of this thesis was on the design of offshore wind farms, far wake models were considered, and more precisely the Jensen (Park) Model.

3.2.3 Jensen Model

The Jensen Model is one of the oldest and most widely used wake prediction models. A benefit to the use of the Jensen model is that it is a relatively simple model that is less computationally demanding

than others and has still been proven to provide comparably accurate results [16] [32] [34].

The Jensen model assumes a linearly expanding wake and is only applicable in the far wake region as the model ignores characteristics found in the near wake region, namely vortex shedding [8] [16]. This was an important constraint included in the physical model. No turbine was permitted within three diameters of one another.

3.2.3.1 Single Wake Effect

A key assumption to the Jensen single wake model is that mass[1] is conserved in the direction of the turbine axis [8]. As such, the Jensen model is derived using the conservation of mass equation for a given control volume, which can be expressed as shown in Equation 3-5.

$$D_0^2 u + (D_1^2 - D_0^2) v_0 = D_1^2 v_1 \qquad 3\text{-}5$$

D_o ……Rotor Diameter $[m]$

D_1 ……Wake Diameter at x $[m]$

v_o ……Free Stream Wind Velocity $[m/s]$

v_1 ……Downstream Wind Velocity at x $[m/s]$

u ……Wind Velocity at Rotor $[m/s]$

The original Jensen model determined the wind velocity within the wake by Equation 3-6. Katic et al. later expressed the wake effect within the Jensen model as a function of the thrust coefficient rather than the induction factor [8]. This Katic-Jensen modification was used within this thesis and its derivation is as follows.

$$\frac{v_1}{v_0} = 1 - \frac{2a}{\left(1 + \frac{kx}{D_0}\right)^2} \qquad 3\text{-}6$$

a ……Induction Factor [–]

k ……Wake Decay Constant [–]

The induction factor a is defined as the initial velocity deficit, which can be expressed as a function of the thrust coefficient of the turbine, as seen in Equation 3-7.

[1] Katic et al. [8] incorrectly state “momentum is conserved” in their model.

$$a = \frac{1 - \sqrt{(1 - C_t)}}{2} \qquad 3\text{-}7$$

C_t ……Thrust Coefficient [–]

Incorporating Equations 3-6 and 3-7, the total velocity deficit of the wind velocity due to the wake effects at a position x can be given by Equation 3-8.

$$1 - \frac{v_1}{v_0} = \frac{1 - \sqrt{1 - C_t}}{\left(1 + \frac{2\,\mathrm{k}\,x}{D_0}\right)^2} \qquad 3\text{-}8$$

To account for when a turbine experiences only a portion of the linearly defined wake, a simplification was implemented using a binary partial wake model. When the rotor area is partially in the wake of another turbine, it was assumed that if half or more of the turbine's swept area was affected by the wake, then the full wake would be considered. If less than half of the turbine's swept area was affected by the wake, the wake would not be considered. This assumption yields a better approximation when the wind directions have an increased number of bins, and can be less accurate with a decreased number of bins due to the potential magnitude in the difference between wakes considered and not.

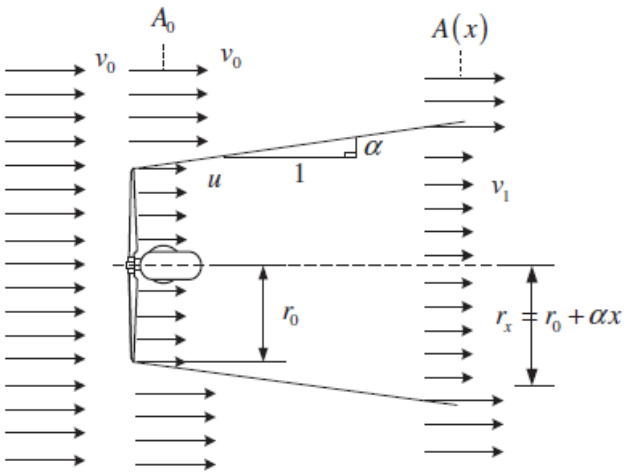

Figure 3-6: Jensen's single wake model $(k = \alpha)$ [29]

3.2.3.2 Multiple Wake Effects

Equation 3-8 describes the ratio of the velocity deficit for a single turbine in the wake of another. With a

large number of turbines assembled into an array in the form of an offshore wind farm, there is a likelihood that wakes will interact and that a downstream turbine will be in the wake of more than one upstream turbine. When having multiple wakes interacting with one another, it is assumed that the kinetic energy deficit of a mixed wake is equal to the sum of the energy deficits for each wake acting on a given position. This can be expressed by Equation 3-9 for a turbine in the wake of two others who experience a wake velocity of v_1 and v_2 [8].

$$\left(1-\frac{v_3}{v_0}\right)^2=\left(1-\frac{v_1}{v_0}\right)^2+\left(1-\frac{v_2}{v_0}\right)^2 \qquad 3\text{-}9$$

v_3 ……Wind Velocity at Turbine 3 $[m/s]$

Which can be generalized for multiple turbines by:

$$v_i=v_o\left[1-\sqrt{\sum_{i=1}^{N_t}\left(1-\frac{v_i}{v_o}\right)^2}\right] \qquad 3\text{-}10$$

This approach of using Equations 3-9 and 3-10 is valid for both scenarios seen in Figure 3-7 and Figure 3-8.

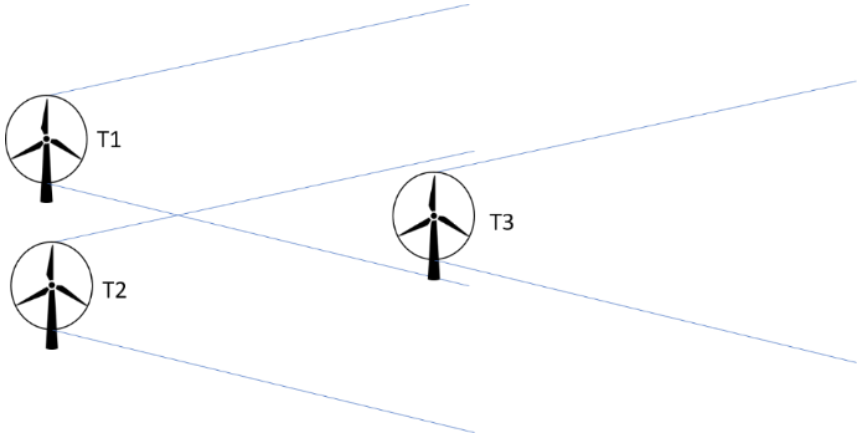

Figure 3-7: Multiple wake effects – Example A

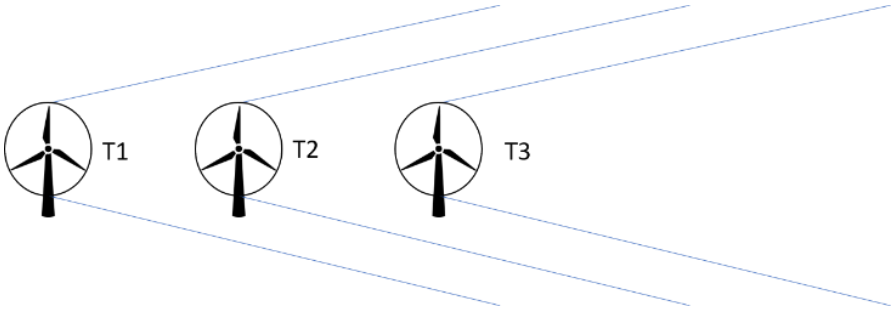

Figure 3-8: Multiple wake effects – Example B

In Figure 3-7, both Turbine 1 and Turbine 2 cause wakes that interact downstream and affect Turbine 3. In Figure 3-8, both Turbine 1 and Turbine 2 cause wakes that affect Turbine 3, however in this scenario Turbine 2 doesn't experience the free stream velocity. Even in this scenario, Equation 3-10 is valid and the free stream velocity is used to calculate the combined wake effects for Turbine 3 [35].

The Jensen & Katic model was selected over more complex models for this thesis, as it is a simple model that is widely implemented in many software applications and has been validated through wind farm analysis software [34]. In addition, the Jensen model fits best with the computational restraints of this thesis.

3.3 Electrical System

Two major components of the electrical system of an offshore wind farm are the intra-array collection system and the transmission system. Both of these components are considered significant contributors to the Initial Capital Cost of a wind farm as seen in wind farm cost breakdown in Figure 3-9.

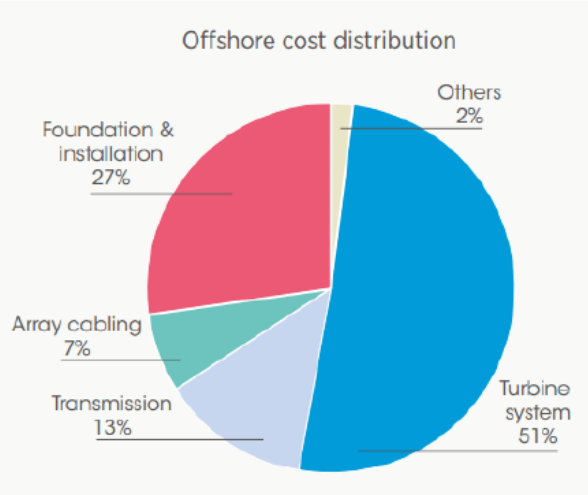

Figure 3-9: Capital cost breakdown for typical offshore wind farm [36]

Lundberg [37] classified the electrical layouts for offshore wind farms into six categories: Small AC, Large AC, AC/DC, Small DC, Large DC and series DC. An analysis presented by Madariaga [38] indicates that as of 2012, 85% of the existing wind farms have a large AC layout. A large AC wind farm can be characterized by a medium voltage AC (MVAC) collection system supplying a transformer which increases the voltage for transmission to high voltage AC (HVAC) and then transmits the power to shore and ultimately the grid. A traditional layout of a large AC wind farm can be seen below in Figure 3-10.

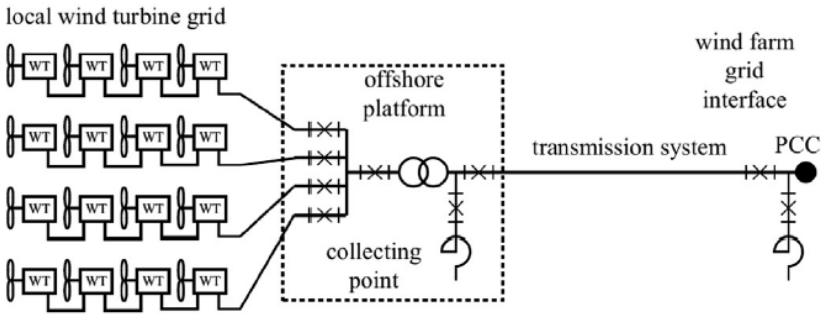

Figure 3-10: Traditional AC wind farm layout [38]

As the electrical system is a significant cost component to offshore wind farms, much research into the other classifications of wind farms has been done since the analysis by Lundberg. Increased focus has been placed on HVDC transmission in particular as wind farms increase in size, power output and distance from shore. As all of these three parameters increase, HVDC becomes increasingly desirable [39]. However, due to the prominence of large AC wind farms, the model developed in this thesis assumes that the wind farm being simulated is a large AC classification. With this said, if a wind farm uses HVDC transmission but still uses AC collection cables, the model is still valid with a few simple modifications to the cost parameters which will be discussed further in Chapter 4.

It is important to make a distinction between the collection system and transmission system when including them in an OWFLOP. The collection system is dependent on the position of the individual turbines, where as the transmission system is independent of the turbine positions.

3.3.1 Intra-Array Collection Cables

The collection system gathers the electricity from each individual turbine and connects it to a substation. The subsea cables drop from the individual turbines to the seabed and are typically buried 1 to 2 meters underground. Current collection systems are typically medium voltage, and depending on the project can range from 10 to 66 kV. There are a number of design strategies for the layout of collection cables, each with their own strengths and drawbacks.

3.3.1.1 Radial Design

The simplest design strategy for a collection system is the radial design, which connects a series of turbines on a single cable. The number of turbines per cable is determined by the maximum power output from each turbine and the maximum rated capacity of the cable. This design seen in Figure 3-11 is widely adopted for smaller wind farms. The radial design is considered to be advantageous because it uses minimal cable, but its drawback is that it does not account for any redundancy [41]. Redundancy is the duplication of critical components within a system that increases the reliability of said system. In this case, redundancy would include additional cables that would provide an alternate means of transmission for the turbines if the first cable were to fail, which is known as a ring design.

Figure 3-11: Radial cable connection design [41]

3.3.1.2 Ring Design

The ring design can take a number of different forms and in general is considered preferable when redundancy and reliability is a priority in the design of the collection system. A single-sided ring takes a similar form to the radial design, however the last turbine is connected directly back to the substation with a cable of equal capacity, as seen in Figure 3-12. This provides 100% redundancy in the design, but doubles the amount of cable. A double-sided (with potential for more “sides”) ring design is similar to the single-sided design but instead of the last turbine connecting directly to the substation, it connects to the end of another string, as seen in Figure 3-13. This design provides redundancy and reduces the cable length relative to the single-sided ring design, but it requires an increase in cable capacity to handle the full power output of the turbines from each string if there is a fault in one. [41]

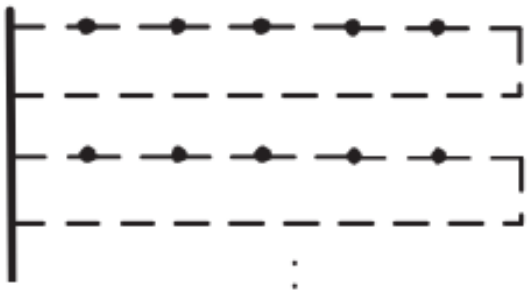

Figure 3-12: Single- sided ring cable connection design [41]

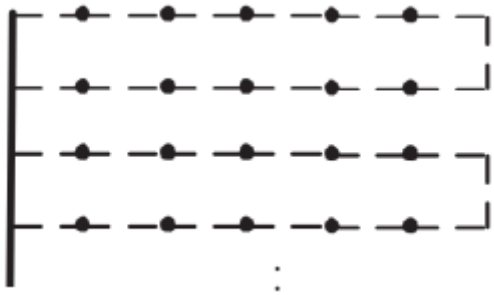

Figure 3-13: Double-sided ring cable connection design [41]

3.3.1.3 Star Design

The star design, as seen in Figure 3-14, provides increased security and reduces the rating of the cables required. Its drawback is that it can require longer cable lengths and more complicated electrical components. The star design provides security rather than redundancy. If the cable connecting one turbine faults, that turbine is disconnected and does not provide any power, though only that turbine is disconnected and not all ‘down-string’ turbines. [41]

Figure 3-14: Star cable connection design [41]

3.3.1.4 Branch Design

The branch design is less common for offshore wind farm designs, but is frequently used in communication networks and has desirable features for use in collection cable design. The branch design, as seen in Figure 3-15, provides opportunity for lower cost and higher reliability than the currently most common approach, the radial design. [40]

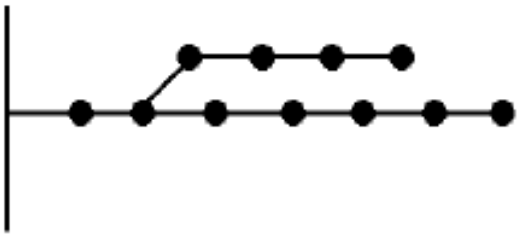

Figure 3-15: Branch cable connection design [40]

3.3.2 Array Cable Layout Problem

The goal of the Offshore Wind Farm Array Cable Layout Problem (OWFACLP) is to minimize the total cable cost for a set of defined turbine and substation locations by finding the optimal intra-array cable topology without violating any constraints [6]. The OWFACLP is considered a Non-deterministic Polynomial-time hard (NP-hard) problem in combinatorial optimization. Solving a problem of this type for a large number of variables (large wind farms) is complex and can be computationally expensive when using classical mathematical optimization methods. Sophisticated heuristics have been developed that provide an acceptable approximation of an optimal solution and do so in a much more computationally efficient manner [6]. For the application of the OWFACLP within the current model, while taking into consideration its role as a sub-component of a larger model, a heuristic approach provides a sufficiently accurate result in an acceptable time frame.

Selecting which type of heuristic would be most effective in the model depends directly on the layout strategy employed. The branch design was selected from the layout strategies listed in Section 3.3.1 as it had similarities to the common radial design but provided potential for lower costs, lower losses and higher reliability. The selection of the design strategy is difficult for a model whose intent is to be used for general application, as the design strategy is very much dependent on the designer's preferences for redundancy, reliability and risk. However, what is important for this model is that the design strategy is consistent between simulations of existing layouts and optimized layouts to provide a fair comparison.

The assumption that the wind farm consists of only one turbine model, which was made within the wake model, is also applicable to the cable design. This allows for the cable capacities to be represented as a number of turbines, rather than current or power, which minimizes that data and calculations necessary. A key constraint employed in the OWFACLP is that no cables can cross one another as this is a logistics constraint for construction and maintenance.

3.3.2.1 Planar Open Savings (POS) Heuristic

The POS heuristic was developed by Bauer and Lysgaard [6] and is one of the most efficient heuristic algorithms for the radial internal connection of offshore wind farms [40]. POS heuristic computes layouts on average only 2% more expensive than the optimal wind farm layouts defined in the study [6].

Additionally, through comparisons with real-world offshore wind farm installations, Bauer and Lysgaard found that their results provided layouts that were as high as 13% cheaper than the installed layout.

The POS heuristic is an adaptation from the Clarke and Wright Savings Heuristic used to solve the Vehicle Routing Problem (VRP). The POS heuristic begins with an initial solution of every wind turbine being connected directly to the substation. In every step the savings heuristic considers merging two routes (cables) into one cable. The savings associated with this merge are logged, and in every step the heuristic greedily chooses the merge with the highest savings resulting in a route not exceeding the defined capacity [6]. The heuristic continues until all savings are achieved under the given constraints and capacities and a near optimal solution is reached.

3.3.2.2 Esau-Williams (EW) Heuristic

The EW heuristic is a saving procedure which, similar to that of the POS heuristic, starts from a star tree formation of the turbines and substation connections. In each iteration, the merging of two routes is determined by the option that provides the largest savings [42]. Relative to the POS heuristic, the EW provides more freedom and possibilities for merging routes since there is no limitation on the position of the turbines in their corresponding routes. The main characteristic of the EW heuristic is that it attempts to connect the turbines further from the substation into clusters first, and then upon a cable reaching its full capacity, the algorithm continues with creating a new cluster closer to the substation [40].

3.3.2.3 Implemented Hybrid Solution

Katsouris [40] tested the different heuristics under different cable layout strategies (radial and branched), and different substation positions (located inside or outside the wind farm perimeter), as shown below in Table 3-1. Katsouris found that a hybrid solution, which incorporates the POS heuristic and the EW heuristic, provides the best results when using branched topology cable design with the substation positioned within the wind farm. This hybrid solution was selected as the base design for the present model. In addition, the hybrid method was employed because it provided more flexibility to the model as it contained the POS and EW heuristics, and therefore the model could be easily modified to provide the best algorithm for the given conditions.

Table 3-1: Heuristic preferences for cable topology designs [40]

	Single Cable Type		**Multiple Cable Types**	
Position of Substation	**In**	**Out**	**In**	**Out**
Radial Topology	POS	POS	POS	POS
Branched Topology	EW	EW	Hybrid	Hybrid
Overall	EW	POS	Hybrid	POS

More details on the inner workings of these heuristic algorithms can be found in Appendix A.

3.3.3 Electrical Losses in Intra-Array Layout

When transmitting power through cables there are two types of losses that occur; Ohmic losses (Equation 3-11) and Dielectric losses (Equation 3-12) [43]. Ohmic losses are also known as copper losses and are the result of the resistance of the cable.

$$P_{\Omega} = R_{ac} I^2 \qquad 3\text{-}11$$

P_{Ω} ……..…Ohmic losses $[W/m]$

R_{ac}……AC Resistance $[\Omega/m]$

I…… Current $[A]$

The dielectric losses pertain to the electrical characteristics of the insulated cable. When exposed to alternating current, the dielectric insulation acts as a capacitor, and the electric dipoles are realigned with each voltage direction. The power loss is in the form of heat that is produced from the current required to realign the electric dipoles [43].

$$W_d = 2\pi f C U^2 tan\delta \qquad 3\text{-}12$$

W_d ……Dielectric losses $[W/m]$

f……..……..……Frequency $[Hz]$

C……..…… Cable Capacity $[F/m]$

U…….. Voltage $[V]$

$tan\delta$……...Insulation loss factor [-]

It is important to include for the power losses in the collection cables as they directly impact the AEP of the wind farm based on the different cable layouts. In order to include both ohmic and dielectric losses, a simplification was necessary, as including the power flow for the entire wind farm internal network [44] was beyond the scope of this thesis.

To determine the losses in the collection cables, a value for the transmission efficiency was obtained for Horns Rev wind farm with the estimated cable length of the existing design. When modifying the cable layout, the losses were determined by calculating them relative to the change in total cable length. Equation 3-13 shows the simplified loss calculation that was included in the model.

$$P_{CL} = (1 - \eta_{CC}) \left[\left(\frac{L_{new} - L_{old}}{L_{old}} \right) + 1 \right] * AEP \quad \text{3-13}$$

P_{CL}……Collection Cable Losses [kWh]

η_{CC} ……Collection Cable Efficiency [%]

L_{new}……Improved Cable Length [m]

L_{old}……Original Cable Length [m]

The assumption that the cable length reduction is directly correlated with the collection cable losses reduction is an estimation, however it was considered more appropriate to include the losses in the form of an estimation than to not include at all. When applying this simplification to wind farms other than Horns Rev, from which the cable efficiency was obtained, it is important to consider the cable characteristics as the losses are related to the cable voltage rating, current rating and length. External software can be used to generate a more accurate estimation in future versions.

3.4 Annual Energy Production (AEP)

The AEP for a wind turbine is the total energy that is converted from the wind to electricity over the duration of a year. Equation 3-14 defines the total power available in the wind.

$$P_{wind} = \frac{1}{2} \rho A_d U_\infty^3 \quad \text{3-14}$$

P_{wind} ……Power Available in Wind [W]

ρ……Density of the air [kg/m^3]

A_d……Turbine Swept Area [m^2]

U_∞……Velocity of the Wind [m/s]

The amount of power that the wind turbine is capable of extracting from the wind is given by Equation 3-15. Further information on the derivation of the following equations are outlined by Burton [21].

$$P_{turb} = 2\rho A_d U_\infty^3 a(1-a)^2 = \rho A_d U_{turb}^3 \quad \text{3-15}$$

P_{turb} ……Turbine Power [W]

U_{turb}……Velocity at Turbine Rotor [m/s]

a……Induction Factor [-]

The total power that can be extracted from the wind relative to the total power available in the wind is the definition of the power coefficient.

$$C_P = \frac{P_{turb}}{\frac{1}{2}\rho U_\infty^3 A_d} = \frac{Power\ Extracted}{Power\ Available} \quad \text{3-16}$$

C_P ……Power Coefficient [-]

The maximum aerodynamic C_P for a wind turbine is theoretically 0.593, which is named the Betz limit. This maximum value has not been physically attainable, and most C_P for existing wind turbines are closer to 0.45 - 0.50. The power equations for a turbine are what defines its power curve described in Section 3.1.1 above. The AEP of a turbine (see Equation 3-17) can be determined by integrating the power for each wind scenario experienced over the duration of a year by applying the power curve of a wind turbine with the annual wind distribution experienced.

$$AEP_{turb} = T \int_{\vartheta_o}^{\vartheta_{360}} \int_{v_o}^{v_\infty} P(v)\, f_w(v) dv d\vartheta \quad \text{3-17}$$

AEP ……Annual Energy Production [kWh]

T…… Annual Hours [h]

ϑ ……Wind Direction [°]

v…… Wind Velocity [m/s]

$P(v)$……Wind Turbine Power [kW]

$f_w(v)$ ……Frequency of Occurrence [-]

The AEP for an entire windfarm is simply the summation of the AEP for each turbine in the wind farm, as seen in Equation 3-18.

$$AEP_{windfarm} = \sum AEP_{turb} \quad \text{3-18}$$

The array efficiency is considered the total AEP from the windfarm which experiences wake effects divided by the AEP of an identical wind farm without consideration for wake effects. Maximizing array efficiency through micro-siting of the wind turbines maximizes the AEP of the wind farm.

An additional factor when calculating the AEP for a wind farm is the availability. The availability of a wind turbine is the amount of time for which a wind turbine is available to operate when maintenance and repair time is considered [21]. For a wind farm, the availability is considered the average of the availability of the turbines within. In order to compare model estimations with measured data, it is important to account for the availability of the wind farm over the measured period.

3.5 Physical Model Summary

The physical model applies the input parameters outlined in Section 3.1 to the wake model described in Section 3.2 and to the cable layout heuristics in Section 3.3 to provide the wind farm cable topology and its annual energy production. The AEP and total collection cable length are used in the economic model outlined in Section 4 to determine the levelized cost of electricity for the wind farm. As the expectation is for the physical model to be run many times throughout a single optimization, simulation time was a key consideration in the implementation of the wake model and the nested optimization of the cable layout topology.

Chapter 4

Economic Model

The purpose of the economic model is to provide a Levelized Cost of Electricity (LCOE) from the outputs of the physical model; the AEP and collection cable layout. When determining the cost of a wind farm in the form of an LCOE, the designer must consider several elements of the process: Initial Capital Cost (ICC), operations and maintenance (O&M), levelized replacement cost (LRC) and annual energy production (AEP). The ICC is the largest component of the economic model and it is the focus of Sections 4.2 and 4.3. The LCOE and the rest of the variables it is comprised of are discussed in Section 4.4.

4.1 Wind Farm Cost Models

As outlined in Chapter 2, there is a growing interest in the optimization of the layout design for offshore wind farms. Prior to achieving valuable optimization results, consistent and accurate economic cost data are required on the most significant aspects involved in the planning, construction, operation and decommissioning of the wind farm. Obtaining representative economic data for offshore wind farms is difficult and uncertainty comes from the following factors [45]:

- Variable competitiveness in the supply chain,
- Volatility in the commodities prices, in particular the costs for the turbines, cables and foundations,
- Prices given in different currencies and years,
- Different metocean and seabed conditions,
- Different distances between the wind farm and the nearest harbour capable of providing installation and maintenance services.

There are varying levels of depth for different cost models that have been developed, a number of which were summarized and referenced by Gonzalez-Rodriguez [45]. The complexity of the cost model and the level of detail it provides is only as accurate as the information that is available to insert into the model. The cost model developed by Zaaijer [35] for example is very extensive and requires precise data about the wind farm regarding the materials and designs for many of the components, such as the tower, blades, nacelle, foundation etc. Although a model of this complexity has the potential to provide more accurate results, finding enough publicly available data for specific wind farms to validate the model was beyond the scope of this thesis.

The National Renewable Energy Laboratory (NREL) in the United States published a report where they had been working to develop a reliable tool for estimating the cost of both onshore and offshore wind generated electricity [23]. The tool provided cost scaling measures that were related to only a few base parameters, namely the wind turbine dimensions and power rating. Although this cost model is unlikely to be as accurate as one requiring much more input data such as Zaaijer, the input data required for this model is more readily available and therefore within the scope of this thesis.

The NREL cost scaling model required slight modifications to be implemented into the economic model. A key component to the overall model and its optimization capabilities is that it involves two contrasting parameters, the wake effects and the intra array cable length. Because the cable length is an optimization parameter, the cost of the intra-array electrical system must be dependent on the cable length and not solely dependent on the turbine and wind farm size. Therefore, an additional cost model that provides a cost function for the intra-array electrical system that is dependent on the cable length must be integrated.

The component of the economic model that is the most relevant for this thesis is the ICC. The ICC and

how it is implemented into the model developed for the thesis can be explained easiest by breaking it down into two distinct categories; fixed costs and variable costs. The fixed costs are considered to be all costs that are dependent on parameters that are unchanged within the optimization process. The variable costs are all those costs that are dependent on parameters that are changed within the optimization process, most notably the turbine positions and the total intra-array cable length. A representation of the economic model can be seen in Figure 4-1.

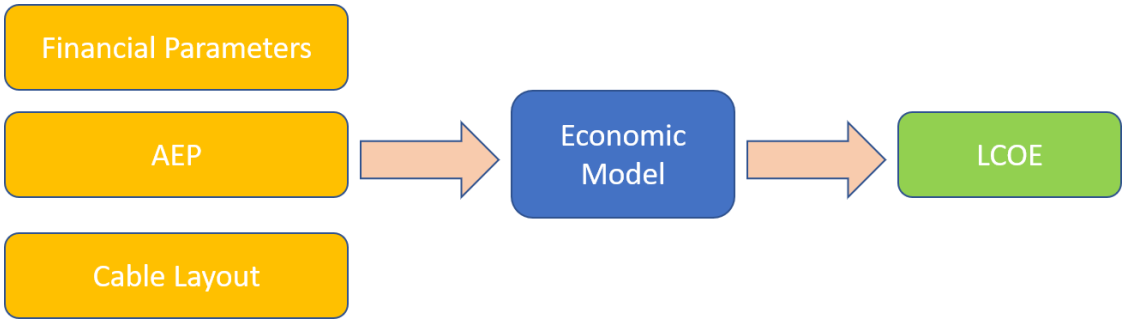

Figure 4-1: Economic model representation

4.2 Fixed Costs

The Wind Turbine Design Cost and Scaling Model developed by Fingersh et al. (NREL) [23] was selected to be the basis of the economic model for all of the fixed costs because of the simplicity of the parameters required. The model is intended to provide reliable cost projections for wind generated electricity based on different turbine and wind farm sizes. This was an important characteristic for implementation into a model that intends to be used for a variety of wind farm and wind turbine sizes. It is understood that at the time of publishing the Fingersh (NREL) model, the components directly related to offshore technology were in their infancy and the forecasts are considered extremely rough. The cost estimates are projected based on only the turbine power rating, rotor diameter, hub height, as well as a few inflation and cost of material variables, all of which remain unchanged throughout the optimization process. The overall cost model has developed cost scaling functions for each of the major components and sub-components. These component and sub-component functions along with key variables will be discussed in the following section.

The following considerations were accounted for when implementing the NREL cost scaling model;

- The NREL scaling model is a tool that uses simple scaling relationships to project the cost of wind turbine components and subsystems for different wind turbine sizes and configurations. The model focuses on the three-bladed, upwind, pitch-controlled, variable-speed wind turbine. Therefore, all turbines being used in the model, must be of this configuration. It is believed that this will be the main configuration used in the wind energy

sector in the foreseeable future. Changes to this would require modifications to the model, which are expected in time.

- The model originally provides results that are in 2002 US dollars, and there is an input for inflation rates that provide results in US dollars of the current time frame.
- NREL model cost equations also comprised of equations and data from the Wind Partnerships for Advanced Component Technology (WindPACT) projects and the Low Wind Speed Technology (LWST) projects.
- The ICC is the sum of the turbine system cost and the balance of station cost.

Further explanation of each formula can be found at the reference [23] regarding how the cost scaling factors were empirically derived.

4.2.1 Turbine System Cost

Fingersh et al. break down the turbine system cost into the rotor, drive train & nacelle, controls and tower. The cost function that represents each, as well as a representative value of the overall wind farm cost, will be presented for each component below. All dimensions are in meters, masses in kilograms, power in kilowatts and costs in US dollars. All values are per turbine and must be multiplied by the total number of turbines to get the total wind farm cost. The original turbine system formulas are based on a mature turbine design and a 50 MW wind farm installation. The turbine system costs are representative of onshore wind turbines and then adjusted afterwards to represent offshore wind turbines. A wind farm installation of 50 MW is not representative of typical large offshore wind farms, and it is uncertain how large the economies of scale effect is on wind farms over 50 MW. The increased capacity of offshore wind farms is accounted for in the balance of station costs in Section 4.2.2 as factors are based on a 500 MW wind farm.

4.2.1.1 Rotor

The rotor consists of three turbine blades, a hub, pitch system and nose cone.

Table 4-1: Rotor Component Costs

Rotor Components	Cost
Blades	$3 * \frac{[(0.4019 * R^3 - 955.24) * BCE + 2.7445 * R^{2.5025} * GDPE]}{1 - 0.28}$
Hub	$4.25 * (0.954 * (0.1452 * \mathrm{R}^{2.9158}) + 5680.3)$
Pitch System	$2.28 * (0.2106 * D^{2.6578})$
Nose Cone	$5.57 * (18.5 * D - 520.5)$

R…….…….…… Wind Turbine Radius [m]

D…..……..……Wind Turbine Diameter [m]

BCE ……..…Blade Material Cost Escalator [-]

$GDPE$ ……..…Labor Cost Escalator [-]

The blade material cost escalator is a factor that represents the escalation of the cost of the material from 2002 to the desired date. The labor cost escalator is a factor that represents the change in labor costs which trends with the gross domestic product (GDP). The rates are modifiable within the model depending on the simulation requirements. Further explanation of the BCE and $GDPE$ values can be found in the NREL Report [23].

4.2.1.2 Drive Train & Nacelle

The drive train is segmented into the low-speed shaft, main bearings, gearbox, brake and generator. The nacelle comprises of the remaining components that are positioned within the nacelle not considered part of the drive train. The remaining components are the variable speed electronics, yaw drive and bearing, the mainframe, platforms, railings, electrical connections within the turbine, hydraulic system, cooling system and the nacelle cover.

Table 4-2: Drive Train and Nacelle Component Costs

Drive Train and Nacelle Components	**Cost**
Low-speed Shaft	$0.01 * D^{2.887}$
Main Bearings	$0.3238 * (0.0133D - 0.033) * D^{2.5}$
Gearbox	$16.45 * P^{1.249}$
Brake	$1.9894 * P - 0.1141$
Generator	$P * 65$
Variable Speed Electronics	$P * 79$
Yaw Drive & Bearing	$2 * (0.0339 * D^{2.964})$
Mainframe	$9.489 * D^{1.953}$
Platforms & Railings	$2.4283 * D^{1.953}$
Electrical Connections (within turbine)	$P * 40$
Hydraulic & Cooling System	$P * 12$
Nacelle Cover	$11.537 * P + 3849.7$

P…..…Turbine Rated Power [kW]

The wind turbine configuration chosen for the model assumes that the gearbox is a three-stage planetary / helical configuration and the generator is a three-stage drive with a high-speed generator. Different configurations would require modifications to the cost function which can be seen in the reference [23].

4.2.1.3 Controls & Tower

This section includes the remaining components in the turbine system costs. The controls, safety system, condition monitoring and tower. The tower cost equation is separated from the others and is dependent on the turbine swept area, the hub height and the cost of steel. The controls section includes the safety system and condition monitoring and is a fixed cost per turbine estimated based on discussions with industry development partners of NREL.

Table 4-3: Controls and Tower Component Costs

Controls & Tower	Cost
Controls	55000
Tower	$(0.3973 * A * H - 1414) * COS$

A…..……Wind Turbine Swept Area [m^2]

H ……..…..…Hub Height [m]

COS ……..…Cost of Steel [$\$/kg$]

4.2.1.4 Marinization

The turbine system cost for offshore wind turbines is very similar to that of onshore wind turbines. The equations in Sections 4.2.1.1 to 4.2.1.3 are applicable to both onshore and offshore turbines, however offshore turbines do need some unique preparation and treatment. The marinization component covers special preparation for all components to increase their durability in the offshore environment. This includes for special paints and coatings, improved seals, and improved electrical connections. It is calculated using a percentage of the total turbine system costs. It is considered a rough estimate and it may vary between 10% and 15% depending on the design. Fingersh et al. elected to use 13.5% as its value, and this value was also used in this model.

Table 4-4: Marinization Cost

Marinization	Cost
Marinization	$0.135 * (Turbine + Tower\ cost)$

4.2.2 Balance of Station

The difference in the balance of station costs between onshore and offshore wind turbines varies much more than the turbine system costs. There is also potential for large variation in the balance of station costs for different offshore wind farm scenarios, be it shallow or deep water, floating or fixed foundations and the geology and meteorology of the wind farm site. To provide a level of consistency, the Fingersh model only handles shallow water installations. The data used by Fingersh et al. to create the scaling factors for the balance of station is primarily based on a 500 MW wind farm using 167 3-MW turbines. It assumes that the wind farm uses a mature turbine design with mature component production. Most of the data used to derive these equations were primarily based on magazine articles or private industry communications converted to scaling factors related to the turbine rated power.

Table 4-5: Balance of Station Component Costs

Balance of Station (BOS)	**Cost**
Offshore Support Structure	$300 * P$
Offshore Transportation	$P * (1.581E^{-5} * P^2 - 0.0375 * P + 54.7)$
Port & Staging	$20 * P$
Offshore Turbine Installation	$100 * P$
Electrical Interface & Connection	See Section 4.2.2.1
Offshore Permits, Engineering and Site Assessment	$37 * P$
Personnel Access Equipment	60000
Scour Protection	$55 * P$
Surety Bond	$0.03 * (ICC - Offshore\ Warranty\ Cost)$
Offshore Warranty Premium	$0.15 * (Turbine + Tower\ Cost)$

The offshore support structure is a simplified cost function that assumes a driven pile foundation that protrudes above the water line in which the turbine is bolted to. For different support structures, a new cost function may provide a more accurate cost estimation. The offshore transportation accounts for only the cost of bringing the components to the assembly site onshore. The offshore turbine installation accounts for the costs associated with the transportation of the turbine from shore to the installation site. Sites that are further offshore, in deeper water, will require a separate cost element. The transportation and installation costs are expected to become more cost effective as the wind farms increase in size and the industry becomes further developed. The cost functions for transportation and installation were taken from different NREL studies and communications with private industry that result in a scaling factor. The port and staging accounts for the unique facilities required to install and maintain operation.

This includes the costs for special ships and barges used for installing piles, setting towers and turbines, laying underwater cables and providing on-going service. The data available for port and staging costs is limited and is heavily reliant on communications with private industry.

4.2.2.1 Electrical Interface and Connection

The electrical interface and connection cost function that was expressed by Fingersh et al. included the cabling between turbines and the transmission system to the grid interconnect at shore. This presented a problem for inclusion into the present model as it required the intra-array cable costs to be dependent on the positions of the turbines (total collection cable length). This meant the Fingersh model was not sufficient and an additional cost function that included the same sub-components and yet was dependent on the total collection cable length was required.

There was a follow-up report published by NREL led by Green [46], that also once again included Fingersh. This report focused on electrical collection and transmission systems for offshore wind power. The report presents an example offshore wind farm and its electrical systems costs in which a number of cost factors for the different sub-components were acquired.

It should be noted that for the offshore and onshore substations, the cost factor was derived from the data from an example 500 MW wind farm presented by Green et al.

Table 4-6: Electrical Interface and Connection (Fixed) Component Costs

Electrical Interface & Connection (Fixed)	**Cost**
Turbine Transformer	50500
Offshore Substation	$81.04 * P$
Onshore Substation	$58.74 * P$
Transmission Cable	$755 * D_{trans}$
Cable Survey & Engineering (per windfarm)	1500000
Cable Installation Mobilization (per windfarm)	5000000

D_{trans}……Transmission Distance [m]

The transmission distance represents the distance from the offshore substation to the onshore substation. The remaining costs for the electrical interface and connection component are dependent on the total intra-array cable length and are covered in Section 4.3.

4.3 Variable Costs

The variable costs are all of the ICC's that are dependent on the variables that change throughout the optimization process, namely the wind turbine positions. The manipulation of the positions of the individual wind turbines, results in modified collection cable layouts and total collection cable length. For this reason, the cost function from Fingersh et al. could not be used as its only parameters were turbine dimensions and rating which are fixed throughout the optimization process. The NREL report by Green et al. presented the electrical interface and connection costs in a manner that a cost function could be derived. Section 4.2.2.1 covered the fixed costs acquired from this report. This section will discuss the costs of the collection cables per meter installed. Table 4-7 below outlines the material cost per meter of the collection cable and transmission cable based on conductor size. Table 4-8 shows the installation costs.

Table 4-7: Costs for cables by conductor sizes [46]

Conductor Size (mm2)	Company A ($/m)	Company B ($/m)
Collection System		
95	152	455
150	228	494
400	381	609
630	571	635
800	600	731
Transmission System		
630	755	860

** grey cells represent extrapolated values from data

Table 4-8: Installation cost breakdown [46]

	East Coast (North America)	West Coast (North America)
Marine Route Survey & Engineering ($ / Windfarm)	1500000	2000000
Cable Transport (From Europe) ($/m)	58	85
Mobilization / Demobilization ($ / Windfarm)	5000000	6000000
Cable Laying Operations ($/m)	94	103

The model was designed so that the collection cable cost values could be easily modifiable for adjustments between simulations as it was understood that these values are very dependent on each specific project.

4.4 Levelized Cost of Electricity

The objective of the thesis is to determine an optimal layout of a wind farm by directly comparing the array efficiency and the array cable costs. As this was the focus, all cost components relying on the layout of the wind farm were considered variables, and the remaining cost components were considered constants within the optimization function. In order to relate the contrasting array efficiency and cable costs, the full conversion to the LCOE is necessary. The LCOE is defined as the level sales revenue per unit of grid-tied electricity production needed for an electricity-generating venture to cover all capital operating expenses as well as satisfy a minimum rate of return for investors for the project lifetime [47]. The LCOE can be represented by Equation 4-1 and subsequently Equation 4-2 represents the annual operating expenses.

$$LCOE = \frac{ICC * FCR}{AEP} + AOE \qquad 4\text{-}1$$

$LCOE$…..……Levelized Cost of Electricity [$\$/kWh$]

ICC ……..…….....…Initial Capital Cost [$]

FCR ……..…….…….....…Fixed Charge Rate [-]

AEP ……..…...…Annual Energy Production [kWh]

AOE ……..…Annual Operating Expenses [$\$/kWh$]

$$AOE = BLC + \frac{O\&M + LRC}{AEP} \qquad 4\text{-}2$$

BLC ……..…Bottom Lease Cost [$\$/kWh$]

$O\&M$ ….....…Operations and Maintenance [$]

LRC……..…Levelized Replacement Cost [$]

- The Annual Energy Production (AEP) is provided to the economic model as an output from the physical model discussed in Chapter 3.

- The Initial Capital Costs (ICC) are defined as all the capital expenditures associated with the planning, design, manufacturing, deployment and project management of an electricity-generating venture. The ICC were described in depth in Sections 4.2 and 4.3 along with their equations.

The remaining variables and their equations/values that have yet to be discussed, can be seen in Table 4-9.

Table 4-9: Additional LCOE variables

Additional LCOE Variables	Value
Fixed Charge Rate	$.1158$
Offshore Levelized Replacement Cost	$17 * P$
Offshore Bottom Lease Cost	$.00108 * AEP$
Offshore Operations & Maintenance	$0.02 * AEP$

- The fixed charge rate is the annual return needed to meet the investor revenue requirements, represented as a fraction of the ICC. A value of 11.58% was used in the model which was suggested by Fingersh et al., but can be modified based on individual circumstances.
- The annual operating expenses (AOE) include for on-going expenses that occur on an annual basis, which include the BLC, O&M and LRC.
- The bottom lease cost (BLC) is the rental or lease fees charged for the turbine installation.
- The operations and maintenance (O&M) include for all scheduled and unscheduled maintenance, operations and monitoring activity.
- The levelized replacement cost (LRC) distributes the cost of major replacements over the life of a wind turbine.

Key assumptions from the cost model that were employed include:

- Maintenance costs were considered the same regardless of the layout of the individual turbines.
- Individual turbine installation costs are considered the same regardless of their position. This assumes each turbine has the same water depth, geology and soil characteristics.
- Electrical connections, transformers, relays and other electrical components were considered the same regardless of the layout.

Equation 4-1 provides the LCOE of a given wind farm based on the input parameters and assumptions outlined above. The LCOE results from the model will be compared to existing wind parks to determine its accuracy and sensitivity and then used in an optimization process to explore the advantages of wind farm layout optimization. It is important to consider that the comparison of LCOE between existing and optimized results from the model are relative results and not absolute.

Chapter 5

Model Validation

Chapters 3 and 4 detail the physical and economic components of the model that was developed to deliver the LCOE of an offshore wind farm. Chapter 5 details the validation procedure that was completed in order to ensure that all components interacted as expected and shows the model results compared to measured data from an existing offshore wind farm. This was a critical step in proving the validity and value of the current modelling because although the theories and equations were taken from previous reports and studies, the model was programmed entirely by the author.

5.1 Model Behaviour in the Design Space

Throughout the development process, analysis of the model behaviour in the design space was performed to observe how the sub-components of the model reacted to different inputs. This analysis was focused on ensuring expected trends between inputs and outputs and evaluating the magnitudes of the results. This type of analysis was used throughout the development stages of the model as consistent checks to help minimize errors.

Two components where this analysis was applied will be discussed in this section. The first was to observe how the wake model responded to different wind input data, and the second was to observe how the selected cable layout heuristic compared to a more traditional cable layout function for different wind turbine layouts.

5.1.1 Wake Model Behaviour Analysis

Developing the wake model was the most extensive part of the overall model. There were a number of different functions required to interact with one another. Two types of model behaviour analysis were used for preliminary validation of the wake model. The first was to modify the input wind characteristics related to the Weibull distribution scale and shape parameters to observe the annual energy production changes. The second type was to rotate the wind rose and observe the sensitivity of the annual energy production. A generic 8 by 8 turbine, rectilinear windfarm was used for analysis with 7 wind turbine diameters spacing between the rows and columns, as seen in Figure 5-1.

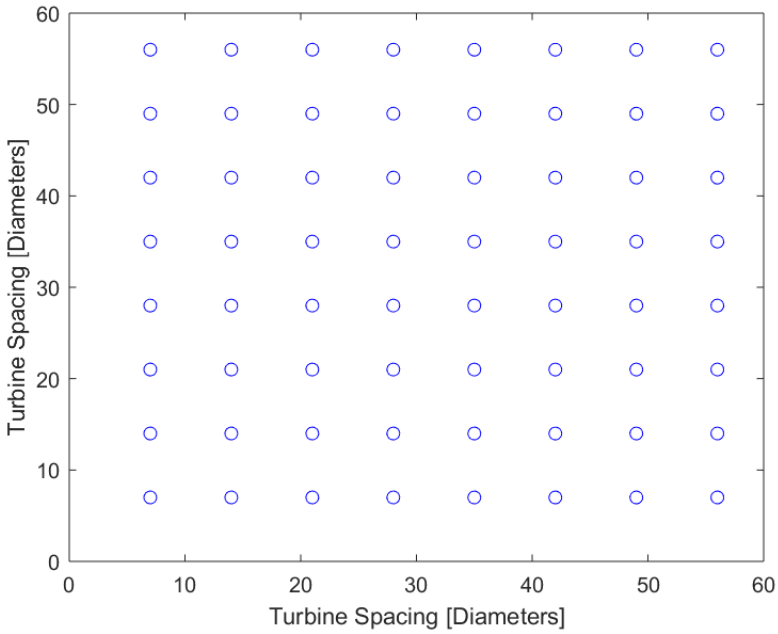

Figure 5-1: 8x8 rectilinear wind farm

5.1.1.1 Weibull Distribution Parameter Sensitivity

When simulating the wind farm shown in Figure 5-1, the effect of the two Weibull distribution parameters can be seen in Figure 5-2. Each parameter was isolated and varied while maintaining all other parameters constant to observe the variation of the AEP.

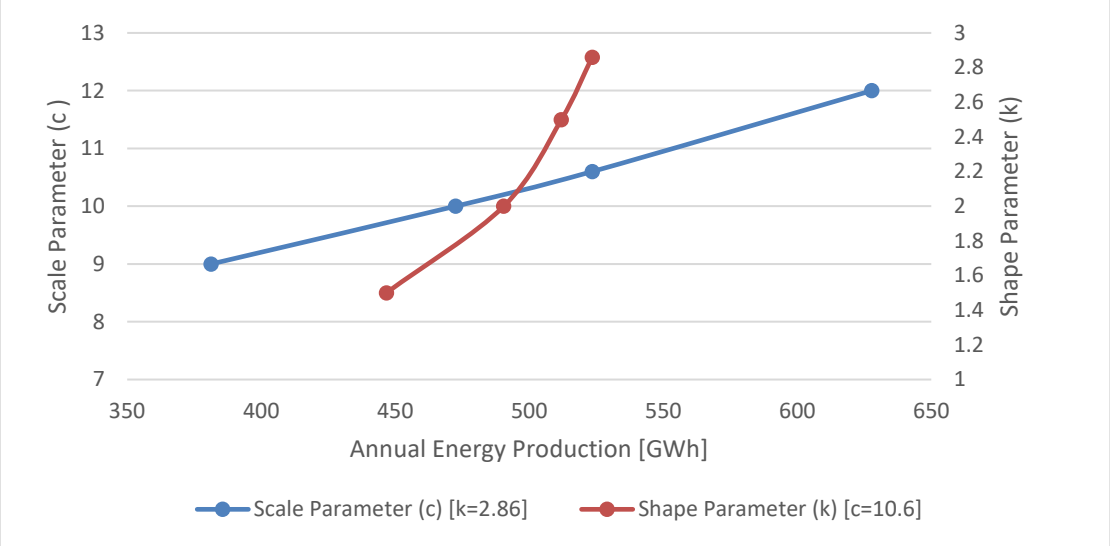

Figure 5-2: Weibull parameter effects on AEP

For the shape parameter, k, the value is typically between 1.5 and 3 and is dependent on the probability of occurrence of a given wind speed [48]. Shape parameter values closer to 1.5 are considered to have a smaller spread of wind speeds, whereas larger k values tend to have a larger spread. A shape factor of 2 is commonly considered when the value is unknown which is a typical value for the North Sea [49]. It can be seen in Figure 5-2 that a larger shape factor, which means a larger spread in 10-minute averaged wind speed occurrences, yields a higher AEP.

The results for same wind farm under the same parameters and only modifying the Weibull scale parameter, c, can also be seen in Figure 5-2. The Weibull scale parameter, which is related to the average wind speed [27], has a positive correlation with the AEP as well. From the results in Figure 5-2, variation of the scale parameter produces a larger variation in AEP than the shape parameter.

5.1.1.2 Wind Rose Rotation

To observe how the thesis model behaves with wind approaching from different directions and different frequencies, an arbitrary wind rose was applied to the wind farm in Figure 5-1. The wind rose (seen in Figure 3-4) was divided into 30° sections and was then rotated by various angles and the AEP was recorded.

For a rectilinear wind farm such as the one in Figure 5-1, which has two axes of symmetry, the

expectation is that the AEP will be the same in 90° rotations of the wind rose. This can be seen in Figure 5-3 below. The AEP values at different rotation angles between 0° and 90° are the same as the values between 90° and 180°. For the given conditions and considered wind farm rotation angles, the AEP peaks at 45° of rotation showing an increased AEP yield of 7.8% over the value at 60°.

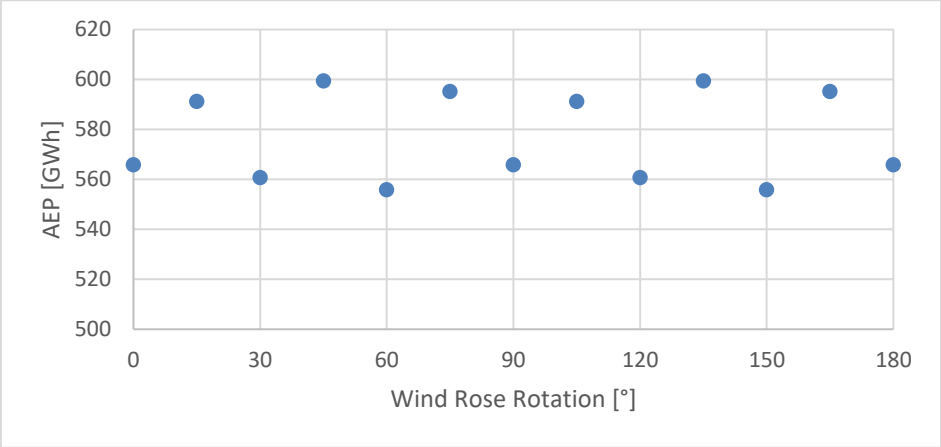

Figure 5-3: AEP results from wind rose rotation for 0°-180°

A more refined analysis was done to check the evolution between 0° and 90°, seen in Figure 5-4. It is observed that 45° was in fact still a peak and that there was still a jumpy nature to the relationship, exemplified by an AEP difference of 6.3% between 50° and 55° rotation. This behaviour between the AEP and the wind rose rotation (or in reality a wind park rotation with respect to the measured wind conditions) is caused by a combination of two factors; a rectilinear wind farm layout being modelled using the Jensen model which incorporates a linearly expanding wake and the implementation of a binary approach to modeling partially shadowed wind turbines.

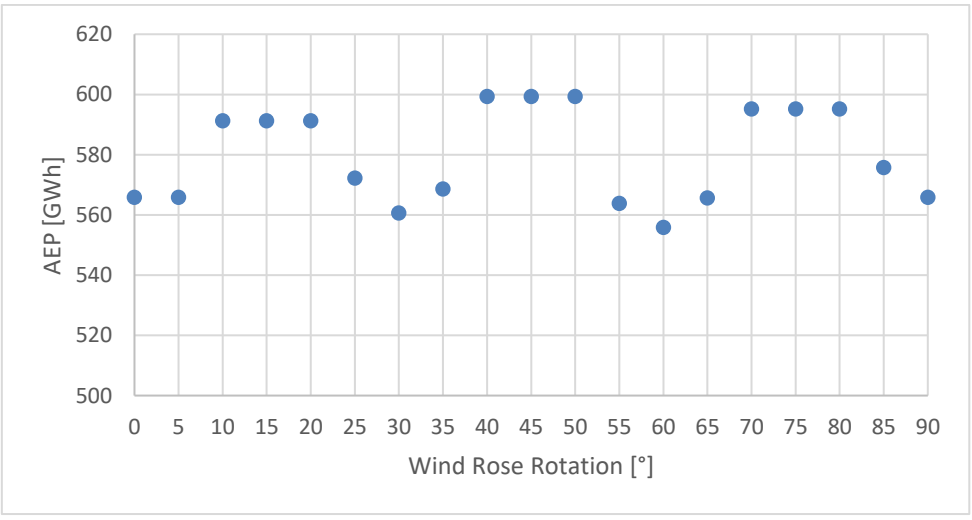

Figure 5-4: AEP results from wind rose rotation for 0°-90°

5.1.1.3 Wake Model Behaviour Observations

When applying a wind rose to a rectilinear wind farm layout there are wind directions where the wakes downstream may “just miss” or “just hit” many turbines in a row, or none at all, creating spikes in AEP for minimal changes in wind direction. As outlined in Section 3.2.3, a binary approach to a partial wake function was included in the wake model. This results in the consideration of a wake being defined by the turbine experiencing more or less than 50% of an upstream wake, which contributes to even larger spikes. An illustration of how many turbines can be affected by a wind rose rotation of only a few degrees can be observed in Figure 5-5 and Figure 5-6. In these figures you can see the wind rose rotation of 50° causes many wake effects downstream, where as the wind rose rotation of 55° causes fewer wake effects. This “all or nothing” effect is amplified when there are fewer wind rose bins as there is an increased emphasis on whether or not several wind turbines experience a wake or not for a specific wind direction. To create a smoother AEP response to the wind direction rotation for a rectilinear wind farm layout using the Jensen model, a more accurate partial wakes model should be implemented.

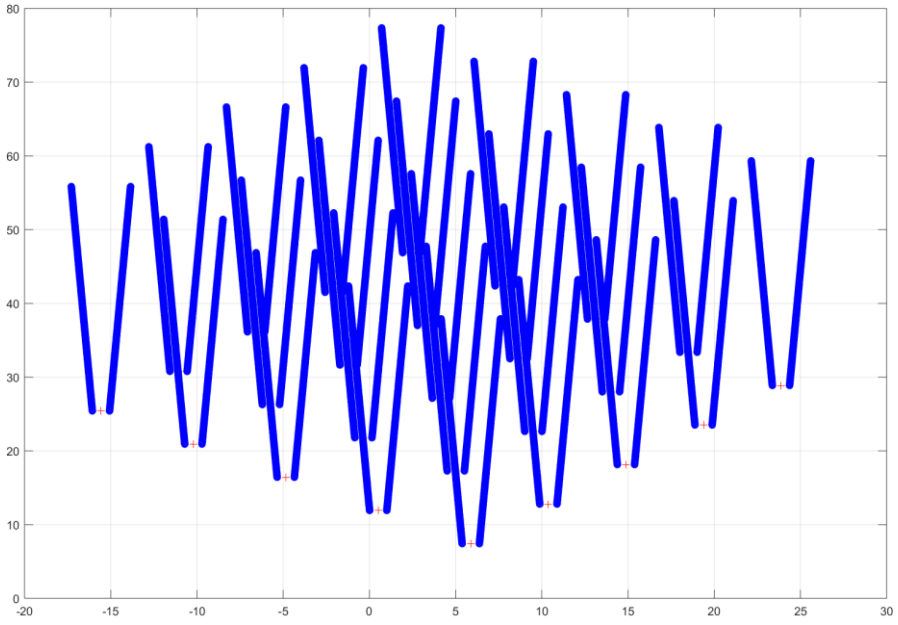

Figure 5-5: Rectilinear wind farm rotation of 50° (with wakes)

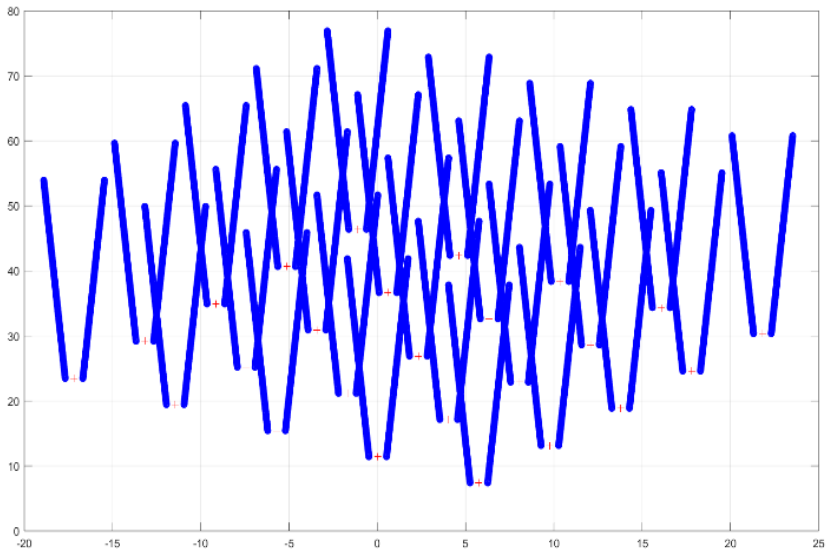

Figure 5-6: Rectilinear wind farm rotation of 55° (with wakes)

It is important to clarify that even though Figure 5-5 and Figure 5-6 show a wind rose rotation of 55° experiencing less wake effects than a wind rose rotation of 50°, it does not result in the AEP of a 55° rotation to be higher than a 50° rotation shown in Figure 5-4. This is because for the wind rose selected, the prevailing winds are not blowing from the North direction (0°). This means rotating the wind rose to the orientation of least wake effects relative the North does not result in a higher AEP.

A final observation of Figure 5-3 is the 7.8% increase in AEP yield based on a simple change in orientation of the wind farm. This increase in yield is why existing wind farms are oriented to an optimal angle with respect to the prevailing winds. This observation lead to the thesis investigation of improving the wind farm layouts further, by removing rectilinear constraints, to increase the AEP and improve the cost effectiveness of offshore wind energy.

5.1.2 Cable Layout Function Analysis

To analyze the effectiveness of the cable layout heuristic function, it was compared with a function that provided a traditional radial cable layout (developed by the author). The two functions were compared for both rectilinear and non-rectilinear wind farm layouts as it is paramount to have an effective cable design strategy that is consistent between different types of wind farm layouts that are being directly compared.

The cable layout heuristic was proven to be more effective than the traditional radial design that collects the power from all turbines in a column and transmits it to the substation. A visual comparison of the traditional layout and an improved layout from the cable layout heuristic on a rectilinear wind farm layout can be seen in Figure 5-7. The substation (blue circles) for the traditional design is in a different location than the heuristic design because of the constraint that cables cannot cross one another.

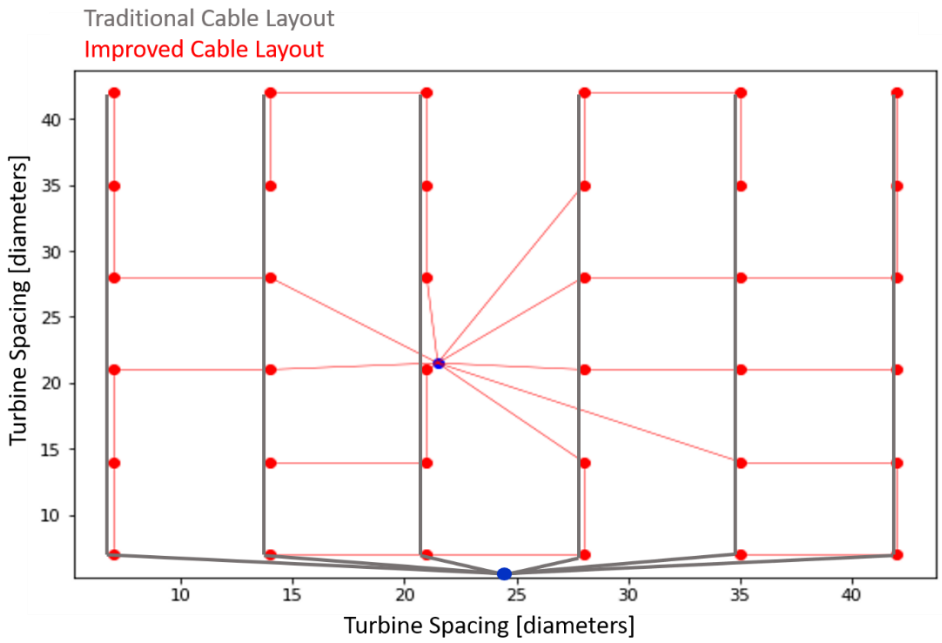

Figure 5-7: Cable layout comparison on a rectilinear wind farm layout

The heuristic results were compared with traditional designs for different numbers of turbines, different rows and column spacing and different intra-array cable capacities. In all scenarios the heuristic outperformed the traditional design for a rectilinear wind farm layout. Figure 5-8 shows the results for an 8 by 8 windfarm described above (Figure 5-1), that had various turbine spacing between rows and columns. The total collection cable length for the heuristic was between 81-89% of the traditional design for rectilinear wind farm turbine layouts tested. It should be noted that although the cable length decreased, the number of connections increased in some designs.

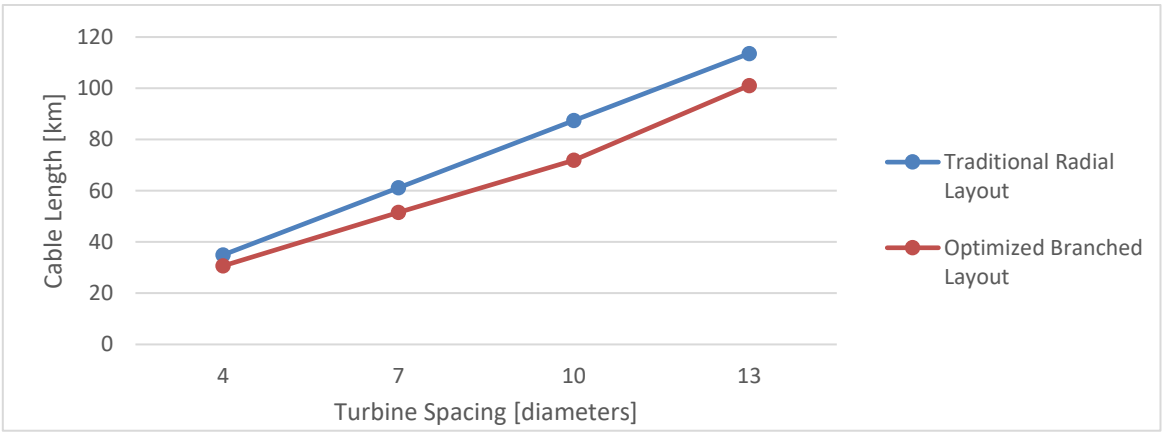

Figure 5-8: Cable length comparison of cable layout functions (8x8 Wind farm)

The cable layout heuristic becomes of increased value for non-rectilinear layouts where the function

developed for generating the traditional layout struggles to provide reasonable results. Figure 5-9 shows the traditional cable layout function results along with the improved cable layout results. The improved cable layout results in only 68% of the traditional cable length required.

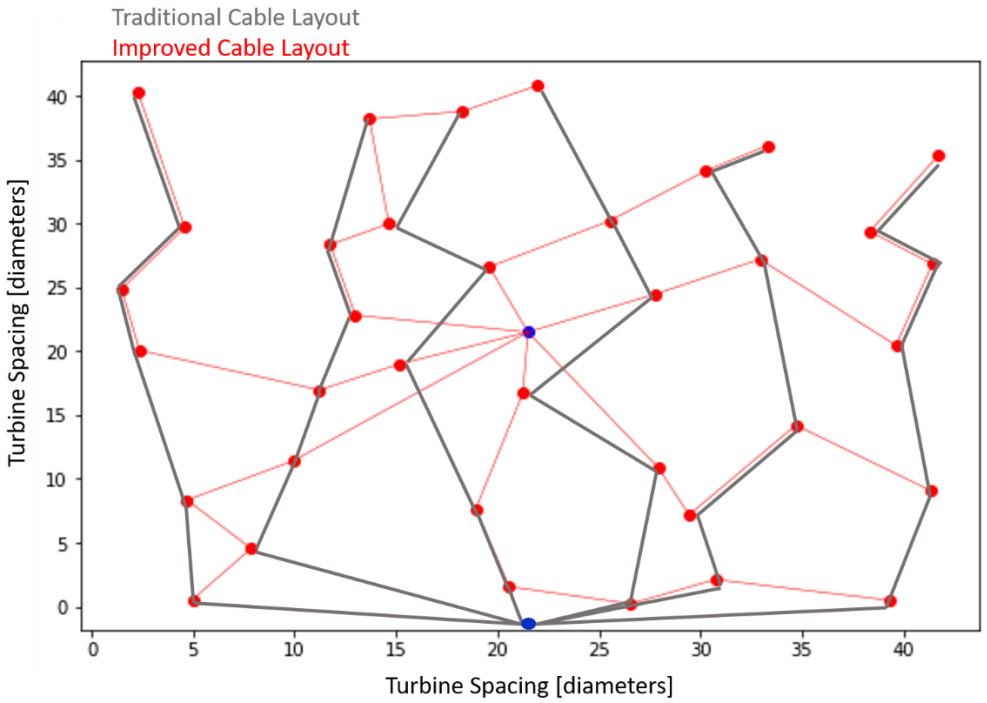

Figure 5-9: Cable layout comparison on a non-rectilinear wind farm layout

The cable layout heuristic function consistently provided a cable layout design with shorter overall cable length than the traditional layout function and was more robust and effective in dealing with non-rectilinear layouts.

5.2 Wake Model Validation

Validation was carried out once the model was completed and model behaviour within the design space was analyzed. The wake model validation compares results from the present model with measured data from an existing wind farm. Acquiring data for model validation is difficult as most wind farm data is considered proprietary [34]. This limited the number of wind farms that the model could be validated against. Sufficient data was obtained to validate the wake model with the Horns Rev wind farm.

5.2.1 Horns Rev Wind Farm

Horns Rev was one of the largest wind farms developed when it was first connected to the grid and

provided one of the first and most complete data sets available to analyze the wake effects in large offshore wind farms [34]. Horns Rev wind farm was used for model validation because there was the necessary data available for the model inputs, as well as measured power data for individual machines to analyze specific turbines in different locations within the wind farm.

The physical model required data for the wind farm layout characteristics, wind turbine characteristics and the wind characteristics, all of which were obtained from a variety of references [50] [51] [24].

Horns Rev wind farm consists of an 8 row (east to west) by 10 column (north to south) matrix of 80 turbines as seen in Figure 5-10. The columns are at an angle approximately 6 degrees with the North direction which forms a parallelogram, and the rows and columns are spaced apart by 7 wind turbine diameters (560 meters). Figure 5-10 also shows the numbering system that is used to identify each of the individual wind turbines.

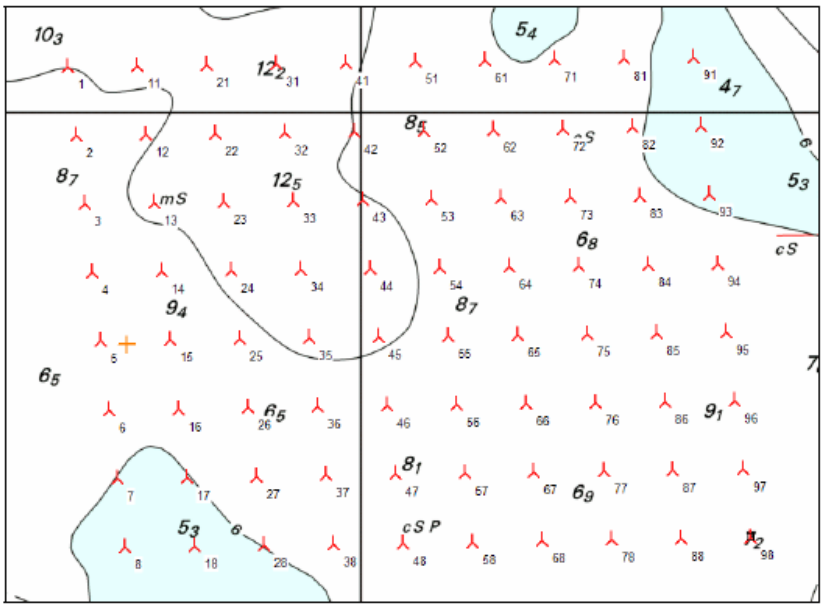

Figure 5-10: Horns Rev wind farm turbine layout [24]

The wind turbines installed at Horns Rev are Vestas V80 turbines, which are variable-pitch, variable-speed machines. The hub height is 70 meters, the rotor diameter is 80 meters and the power and thrust coefficient curve for the Vesta V80 can seen in Appendix B. As a pitch-controlled variable-speed turbine, the Vestas V80 has a similar control schedule and power/thrust curve to that in Figure 3-3.

The wind characteristics are described by the wind rose in Figure 3-4 and Weibull parameters in Table 5-1. The wind data is from the same time period in which the normalized power data was analyzed [24].

Table 5-1: Weibull parameters for Horns Rev [24]

Weibull Parameter	Value
Shape Factor (c_w)	10.86
Scale Factor (k_w)	2.86

5.2.2 Horns Rev Measured Data Analysis

Beyond the model input parameters outlined above, there are two more wake effect parameters that define the results from the wake model, the wake dissipation length (WDL) and the wake decay constant (k).

The wake dissipation length is not a theoretical value used in wake effect equations, but is simply a value required for actual model implementation. Computing wake effects that extend to the boundaries of the wind farm is computationally demanding. Due to the limits in computational power for the thesis, different lengths of the wake (the distance downstream in which it causes a wind deficit) were tested to observe its effect on the results and to determine an effective trade-off between computational time and model accuracy.

The wake decay constant, as seen in Equation 3-6, relates to both the extent at which the wake decays, and the angle at which it expands linearly. The wake decay factor is typically considered to be 0.075 for onshore wind farms and 0.04 for offshore wind farms [34]. Multiple values between 0.04 and 0.075 were tested to determine which wake decay constant fits the measured data the best.

5.2.2.1 Wind farm data acquisition

The scope of the validation process was limited by available data. The only data available was acquired second hand, and subsequently the reference is being relied upon for the examination of the validity and uncertainty of the data [24]. The individual turbine data was provided in the form of normalized power without the direct wind rose. This data required modifications in order to validate the wake model by comparing the wind deficits experienced at multiple turbines rather than the normalized power. Normalized power represents the power output of the wind turbine being analyzed divided by a wind turbine experiencing free stream wind velocities. In order to determine the relative wind velocity deficit (wind velocity experienced by a given wind turbine divided by a wind turbine experiencing free stream wind velocities) at each turbine, the cubed-root of the normalized power was calculated (as per Equation 3-15).

The measured data was obtained for two turbines, Turbine 17 and Turbine 45 from Figure 5-10, in order to analyze the wake effects from different positions within the wind farm. The measured data pertained to wind speeds between 7-10 m/s over a one-year time span. As the specific frequency of occurrence

of each wind speed was not available, the validation procedure assumed a Weibull distribution for the wind speeds between 7-10 m/s in 0.25 m/s bins for calculating the average wind speed deficit for a given direction.

5.2.2.2 Wake decay constant analysis

The results for comparing the model wake deficits with different wake decay constants of Turbine 17 with the measured data can be seen in Figure 5-11 and the results from Turbine 45 in Figure 5-12. The wind direction convention is the wind approaching from 0° is from the North.

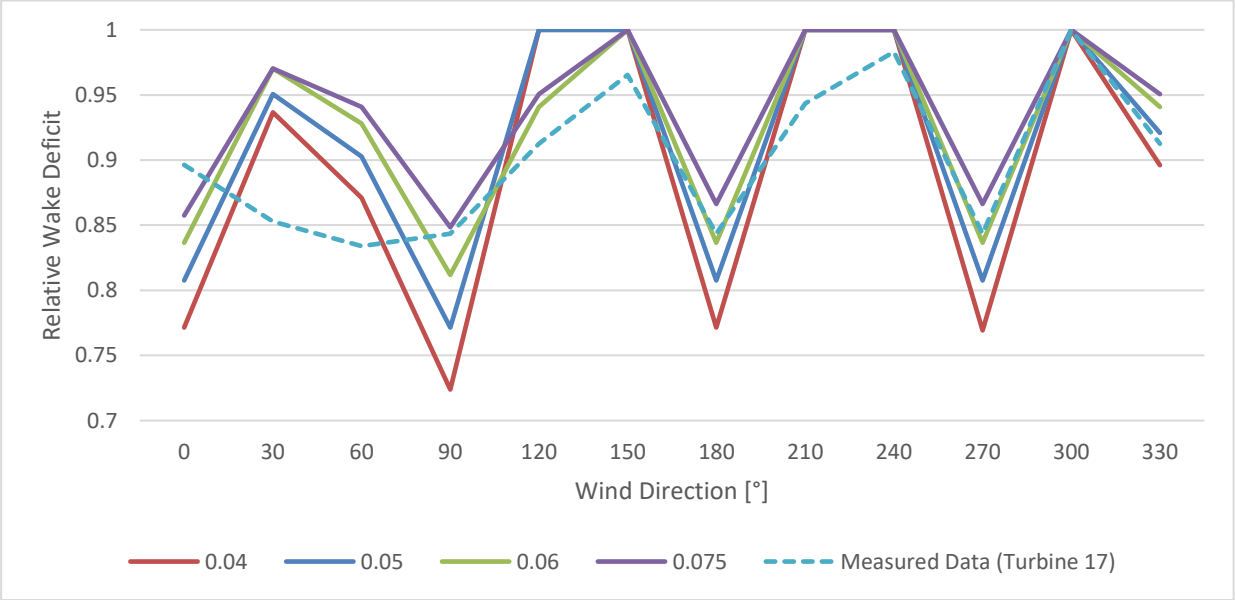

Figure 5-11: Wake decay constant sensitivity (WDL = 30 D) – Turbine 17

While analyzing Figure 5-11, the model results show a trend where the highest wake effects occur when the wind approaches from 0°,90°,180° and 270°, which is expected with this rectilinear layout. In between these angles the wind deficits at the turbines tested are less, with the model results showing some orientations even experiencing no wake losses.

Between 0° and 90°, the measured data does not trend with the model results. Firstly, the measured wind deficit at 0° is much less than the measured wind deficit for 90°, 180° and 270°. This discrepancy is unexpected, as when the wind is approaching from 0°, Turbine 17 is near the back of the wind farm, compared to at 180° Turbine 17 is in the second row. The model results indicate that Turbine 17 would experience greater wake effects when the wind approaches from 0°, however the measured data does not show this. Additionally, between every 90° the model results indicate a peak where Turbine 17 experiences less wake effects, however between 0° and 90°, the measured data show no such peak, although it does show the peak between the other axes. An explanation for this may be that in this orientation, Turbine 17 is near the back of the wind farm and the Jensen model, with a binary approach

to partial shadowing, may not accurately represent the wind deficits. Additionally, Sorensen [34] indicates that for large wind farm arrays, the Jensen model over estimates the wake effects in the first rows and underestimates the wake effects in the back rows, even without the inclusion of a wake dissipation length.

With regards to a comparison between wake decay constants, a wake decay constant of 0.075 always underestimates the wake effects, whereas a wake decay constant of 0.04 tends to both over estimate and underestimate depending on the direction of the wind approaching. As expected, the wake decay constants trend in the same order with larger wake decay constants providing lower wind deficit estimates and smaller wake decay constants providing higher wind deficit estimates. However, as the wind approaches from 120°, wake decay constants of 0.06 and 0.075 provide higher wind deficit estimations than the lower constants because of the wake expansion angle. At 120°, Turbine 17 does not experience any wakes for wake decay constants of 0.04 and 0.05. These results may differ with a more accurate partial wake model.

Finally, the last difference between the measured and modelled data to note is the results when the wind approaches from 90° and 270°. The model indicates that Turbine 17 should experience larger wake effects at 90° than at 270°, which corresponds with the turbine position being closer to the rear of the wind farm. However, the measured data shows similar wake effects for Turbine 17 when the wind approaches from either direction, which cannot be explained.

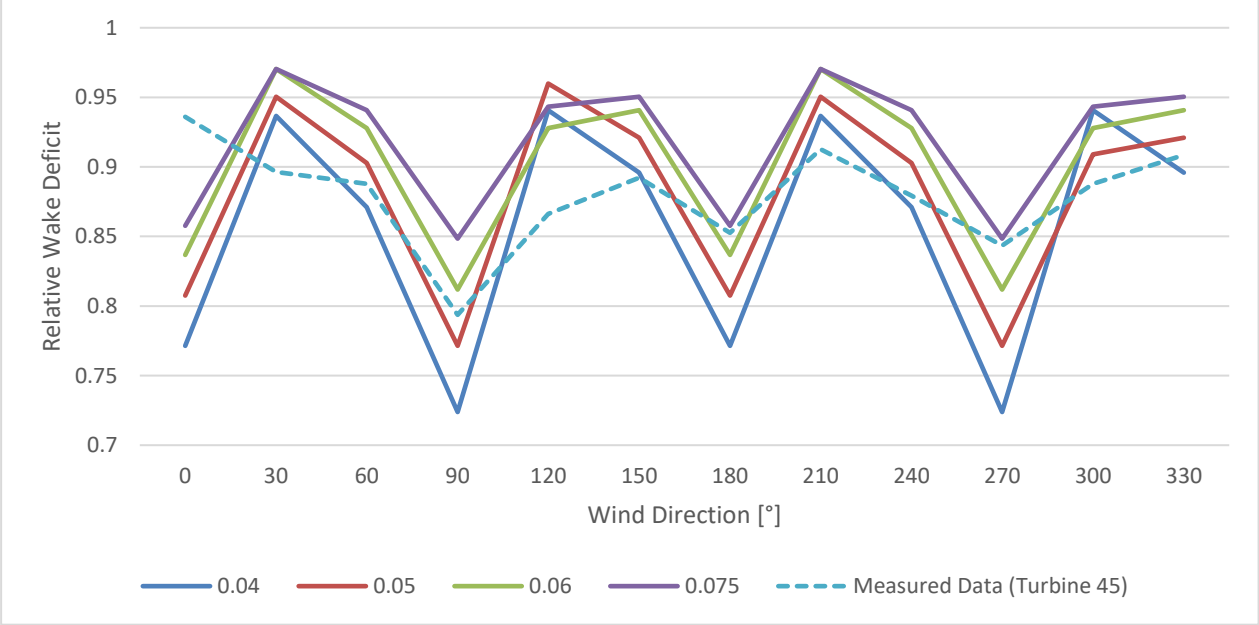

Figure 5-12: Wake decay constant sensitivity (WDL = 30 D) – Turbine 45

Figure 5-12 shows the wake decay constant results for Turbine 45 and displays similar features at wind directions of 0° and 180° to Turbine 17. It also displays the similar trend of the wake effects being stronger (when they are experienced) for smaller wake decay constants. Again, there are two areas of

note that do not abide by this trend at 120° and 300°. At 120° you can see the wind speed deficits of wake decay constants of 0.04 and 0.05 paired in order, and the wind speed deficits of wake decay constants 0.06 and 0.075 in order with each other, but not with 0.04 and 0.05. This can be explained because being in the center of the wind farm, Turbine 45 experiences increased wake interaction and with a wake decay constant of 0.06 and 0.075, the wake expansion causes multiple wakes to interact with Turbine 45 where as this increased wake interaction does not occur with 0.04 and 0.05.

The results between 0° and 90° correlate better for Turbine 45 than Turbine 17 because it remains relatively near the center of the wind farm for all wind directions and doesn't experience as much of an underestimation. However, again the measured data with the wind approaching from the North does not correspond with the model data, nor the trends in the measured data at 90°, 180° or 270°. Partial wake effects may explain the large difference in the model and measured data however, the measured data indicates the 0° is the orientation with the lowest wind deficits which does not match its mirrored orientation of 180°. Considering the position of Turbine 45, it would be expected the wakes experienced from an orientation of 0° and 180° would be similar.

Figure 5-12 also shows that for Turbine 45 the measured data indicates greater wake losses at 90° orientation than at 270°, which is not what is expected based on the turbine position within the wind farm and does not correspond with the model results.

5.2.2.3 Wake dissipation length analysis

Figure 5-13 and Figure 5-14 display the effect of different wake dissipation lengths for a wake decay constant of 0.04.

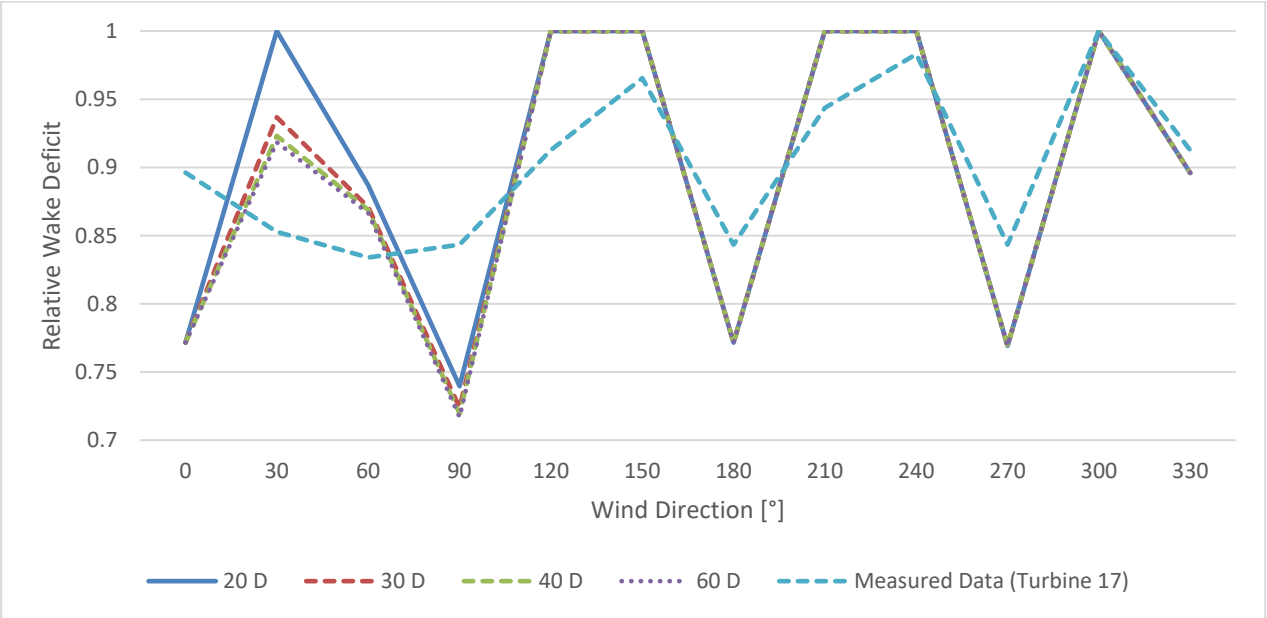

Figure 5-13: Wake dissipation length sensitivity (k = 0.04) – Turbine 17

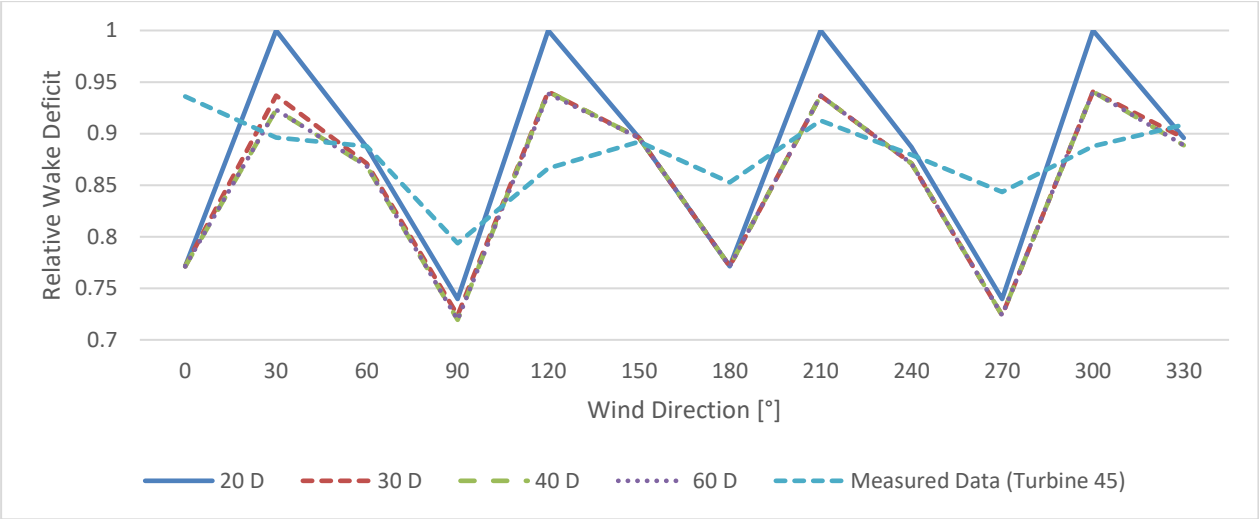

Figure 5-14: Wake dissipation length sensitivity (k = 0.04) – Turbine 45

The results for both Turbine 17 and Turbine 45 are similar when varying the wake dissipation lengths between 20 and 60 diameters. The results for Turbine 17 showed that there was little effect caused by varying the wake dissipation length, with only having noticeable differences between 0° and 90° for a wake dissipation length of 20. Turbine 45 results displayed a larger and more consistent discrepancy between a wake dissipation length of 20 and the greater values. As the results from altering the wake dissipation length between 30 and 60 diameters did not change significantly, and 30 diameters did outperform 20 diameters, a wake dissipation length of 30 diameters was selected.

The present model results are compared with another implementation of the Jensen Wake Model (VL Wake Model) [24] that used a standard offshore wind farm wake decay constant of 0.04 in Figure 5-15 and Figure 5-16.

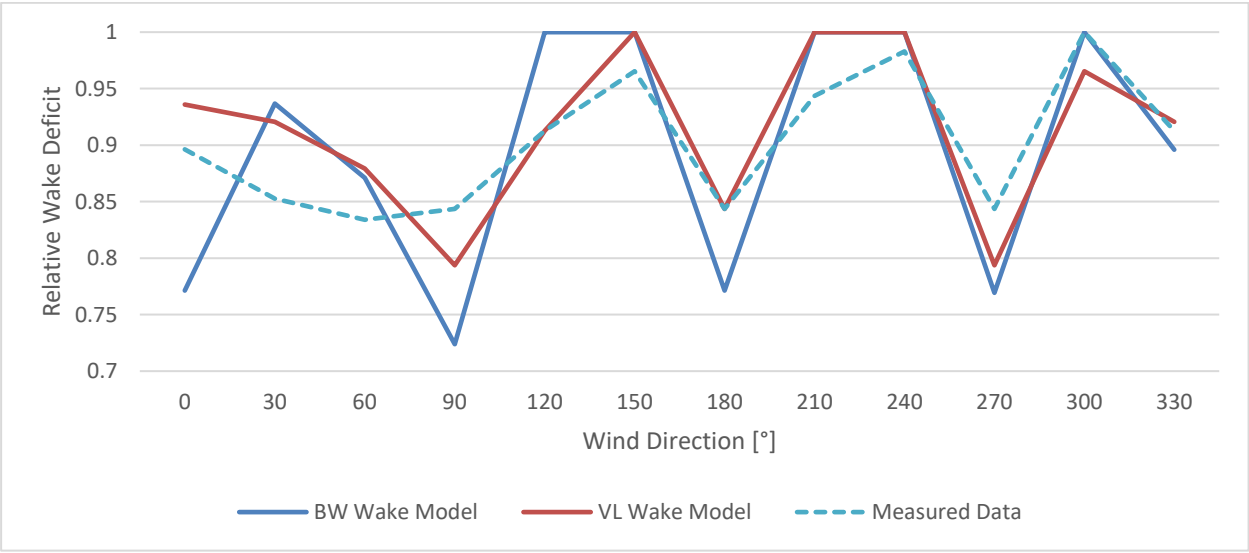

Figure 5-15: Model validation (k = 0.04, WDL = 30D) - Turbine 17

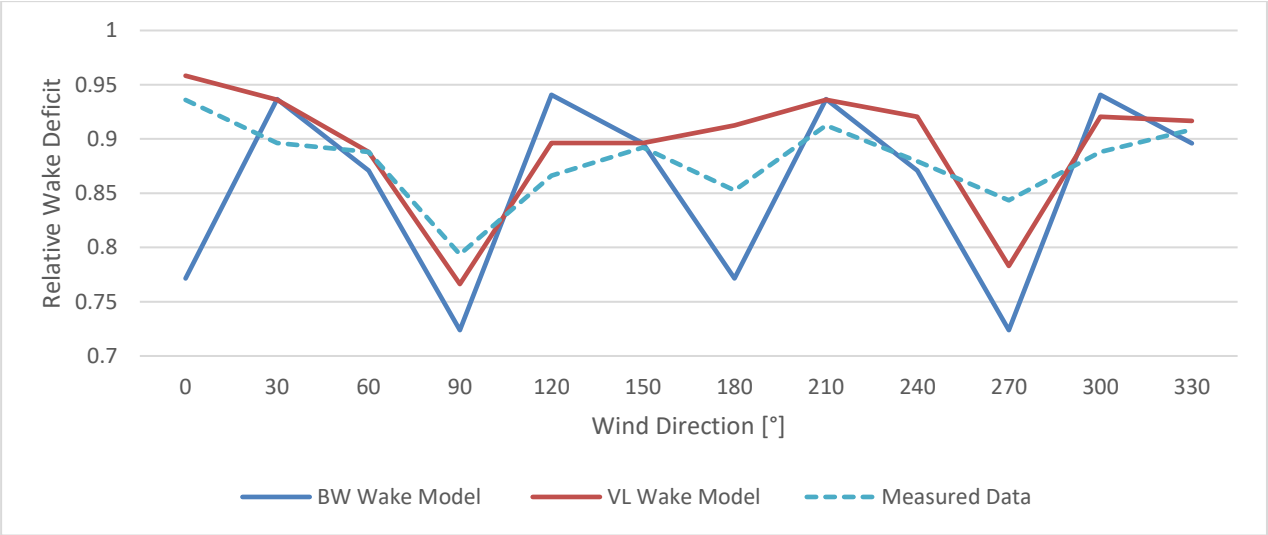

Figure 5-16: Model validation (k = 0.04, WDL = 30D) - Turbine 45

The model results for a wake decay constant of 0.04 have a similar fit as the VL model results, however the VL model is closer to the measured data at 0° and 180°, which may be a result of a more accurate partial wake model.

5.2.2.4 Limitations in Validation

The model results do not match the measured data exactly for a number of reasons:

- Including a simplified binary partial wakes function creates larger discrepancies between model results and measured data at certain angles. This is exemplified when the measured data shows that certain turbines experience wake losses and the model indicates either much higher wake losses or no wake losses depending on if 50% of the turbine experiences the wake or not.
- A potential influence on the difference between the measured and model results could be attributed to the Weibull distribution parameter assumption for the wind distribution between 7-10 m/s. As for a given wind direction, the wind frequency may be substantially closer to 10 m/s than 7 m/s for the majority of the time period that was measured, resulting in the normalized power and therefore the derived wind deficit being much lower than the averaged data would suggest.
- Inconsistencies in the measured data that cannot be explained by relying on second-hand data. Validation with more data would provide more conclusive results.

The wind deficit validation observations indicated that including a partial wake model would most likely increase the accuracy of the model, as would more accurate wind information. Beyond this, further model validation would be valuable with other offshore wind farm data sets which were not available.

5.2.3 AEP Validation

The Horns Rev wind farm was simulated with the input data outlined in Section 5.2.1. The simulations used a wake dissipation length of 30 diameters and multiple wake decay constants to determine a value that fit the measured results best. The results for the simulation are displayed in Table 5-2 along with an approximation of the measured AEP for the Horns Rev wind farm that was obtained for the same time period [24]. An availability factor of 95% was implemented into the model as this was the availability for the Horns Rev wind farm in 2005 according to the operator [34].

Table 5-2: AEP comparison between model results and measured data for Horns Rev

k	AEP (GWh)	Relative AEP
Measured Data (Approximation)	630	100.00%
0.04	626.90	99.5%
0.05	640.50	101.7%
0.06	653.14	103.7%
0.075	665.47	105.6%

Applying a wake decay constant of 0.075 provided an AEP that is 105.6% of the measured AEP which corresponds to the expected overestimation. Utilizing a wake decay constant of 0.04 provided results that were 99.5% of the measured AEP results, which was the closest to the measured data of the values tested. It is important to emphasize that the measured AEP was an approximate value obtained from [24], and it was not quantified how accurate the approximation was. The AEP results obtained from the model using a wake decay constant of 0.04 were also compared with the results from VL Wake Model implementation of the Jensen model and differed by 1.5%.

The LCOE information was not available for the Horns Rev wind farm in 2005. The model results for the LCOE can be seen in Table 5-3.

Table 5-3: LCOE results for Horns Rev wind farm

k = 0.04 ($/kWh)	k = 0.05 ($/kWh)	k = 0.06 ($/kWh)	k = 0.075 ($/kWh))	Horns Rev Measured ($/kWh)
0.0904	.0891	0.0880	0.0869	-

The average LCOE for offshore wind farms in 2016 was 0.14 US$/kWh and is expected to decrease to a range of 0.06-0.10 US$/kWh by 2020-2022 [52]. The LCOE results from the model are within an

acceptable range of the current costs for offshore wind energy. For the purpose of this model it is important to recognize that the LCOE function is dependent on the financial variables that are specific to each site. Therefore, the tool is valid for comparison on a relative basis and not necessarily on an absolute basis. The model results may be used for comparison while using the same financial parameters, for the same wind farm, under different orientations.

5.2.4 Wake Model Validation Summary

The wake model correlated within an acceptable range of the measured data, although the results suggested that the inclusion of an improved partial wake model would increase the accuracy. Beyond this area of improvement, it was understood that even with professional software, determining the best wake decay constant for an offshore wind farm can be difficult, especially with limited availability of measured data [34]. Therefore, moving forward in the optimization and analysis, a wake decay constant of 0.04 was selected for the following reasons; it is considered the industry standard value in wake model software [34], it fit the measured wind speed deficit data to an acceptable degree and provided an AEP that best fit the measured results.

Chapter 6

Optimization Framework

Chapter 3,4,5 discuss the model that was created to simulate the annual energy production and LCOE of an offshore wind farm. Chapter 6 lays out the framework for the optimization component that uses the model to determine the optimal layout of wind turbines within the wind farm.

6.1 Wind Farm Layout Optimization

The current state of wind farm layout optimization was outlined in Section 2. The focus of this work was to follow the second track of research outlined, which was to focus on improving the performance modelling of wind farms. The goal was to develop an inclusive model that incorporated a wake model component, a cable layout component and an economic component. The work was conducted in such a way that sub-components could be improved, modified or added to improve the accuracy of the overall results. Analyzing different optimization methods was not a key focus of this work, but inclusion of an effective optimization technique was required and selected based on previous WFLOP research.

When creating a framework for optimization, it is important to consider the constraints that are required, the number of variables that are involved and the potential shape of the function result surface. The selected framework was a hybrid between a continuous optimization (where there are no internal wind farm constraints) and an optimization that imposes rectilinear constraints. The result is a wind farm that is sectioned into tiles which contain only one wind turbine, but the turbine can be placed anywhere within the tile. This hybrid framework is useful when the perimeter of the windfarm is defined, the capacity of the wind farm is fixed and there is a requirement for limited internal constraints.

6.1.1 Turbine Micro-siting Optimization (Non-rectilinear Topology)

Genetic algorithms are probabilistic search algorithms which are designed to mimic the logic of natural selection. Genetic algorithms work by generating populations of individuals (wind farm layouts) that consist of a set number of variables (x and y coordinates for each turbine). The objective function for each individual (LCOE of each windfarm layout) is calculated for the entire population. The population is evaluated based on the desired stopping criteria for the optimization and if the criteria is satisfied, the optimization process is complete. If the stopping criteria is not met, the population goes through a genetic manipulation process where the elite individuals (wind farm layouts with lower LCOE) are passed on to the following population and other individuals are selected to become parents in the following generation. Once the parent individuals have been selected, a crossover operation is used to combine the traits of the parent individuals. The final step in the genetic manipulation process is the mutation phase in which there are random alterations made to the population. These random alterations are important for incorporating new information into the population that increase the likelihood of testing more of the result surface [53]. A schematic of the genetic algorithm process can be seen in Figure 6-1.

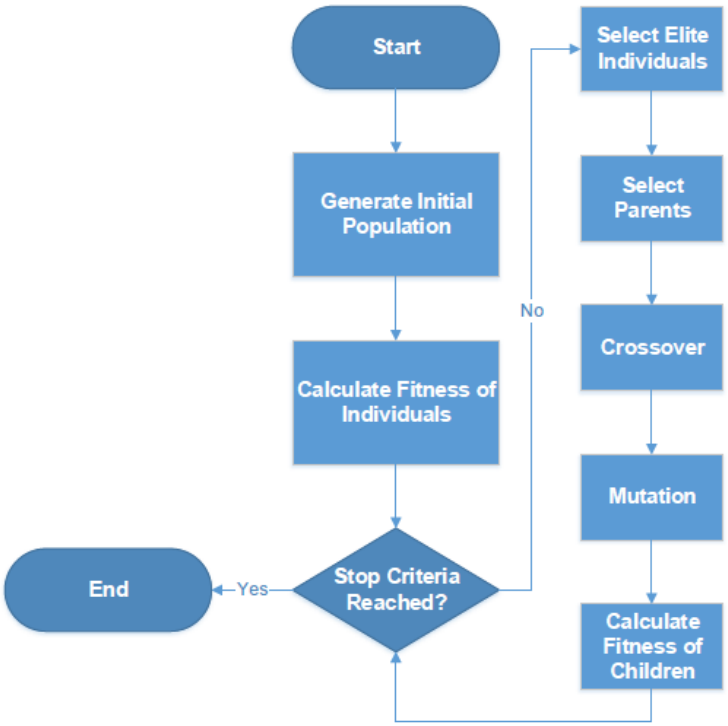

Figure 6-1: Genetic algorithm schematic [44]

The children individuals that were created from the parent individuals are then evaluated against the optimization stopping criteria to determine whether or not another genetic manipulation process is required. There are different parameters and strategies that can be implemented for each stage of the genetic manipulation which is described further by Pohlheim [54].

Genetic algorithms are effective for discovering a global minimum for a function result surface that is not expected to be a smooth convex shape but have several local minima. A function result surface with many local minima is expected when the relationships between all of the variables are not always direct, which is the case with micro-siting optimization.

External constraints were applied to the genetic algorithm that sectioned the wind farm into tiles where only one turbine could be micro-sited within each tile as seen in Figure 6-2. The wind turbine could be placed anywhere within each tile so long as it also satisfied the additional Jensen model constraint which ensures no turbines were closer than 3 diameters to one another. This feature provided some structure to the wind farm which may be desirable for designers, but more importantly it limited the function result surface which reduced the computational demand of the optimization process. When analyzing an existing wind farm, the tile size can be set by the spacing between rows and columns.

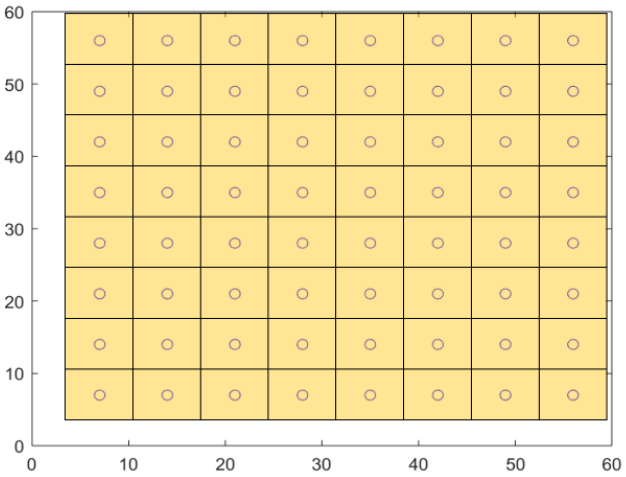

Figure 6-2: Turbine positioning constraint tiles

A graphic representation of how the optimization component utilizes the developed model to generate populations can be seen in Figure 6-3. The external data that is inputted into the model at the beginning of the simulation and remains unchanged is in yellow. The variables that the model components (in blue) generate throughout the simulation are in green. This cycle continues until the optimization stopping criteria is achieved.

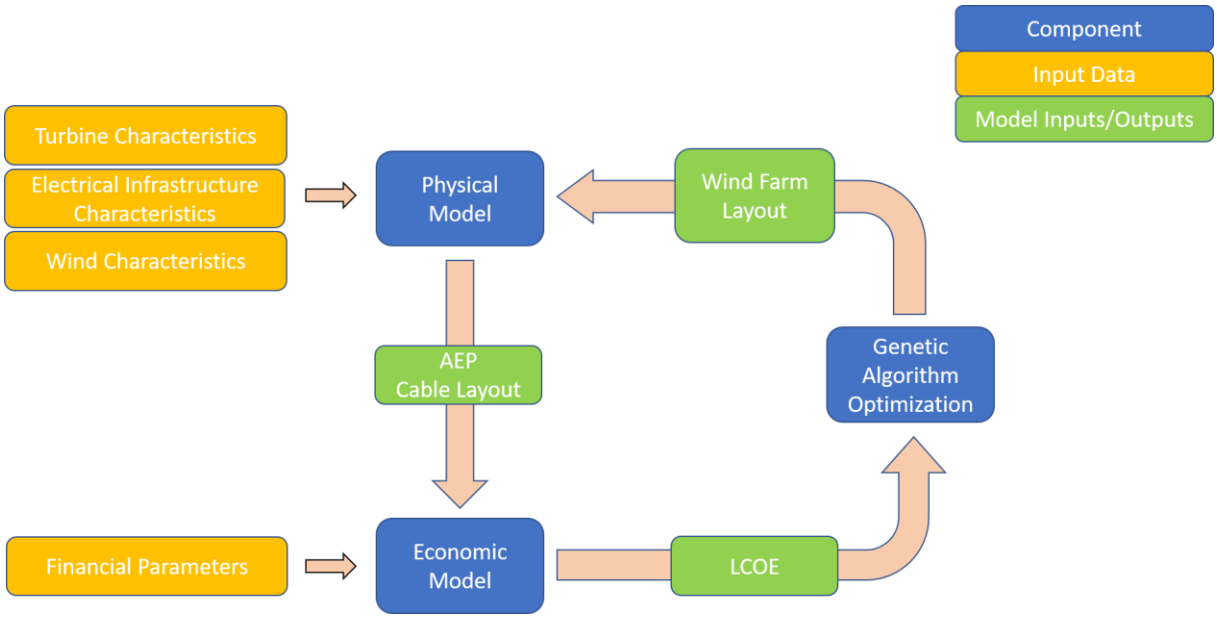

Figure 6-3: Optimization framework schematic

Chapter 7

Wind Farm Optimization Analysis

Chapter 7 applies the optimization strategy outlined in Chapter 6 to the model detailed in Chapters 3 through 5 to analyze how removing rectilinear constraints on offshore wind farm layouts affect the LCOE of wind farms in two case studies.

7.1 Case Study I: Horns Rev Wind Farm

Horns Rev was selected as one of the wind farms to be analyzed within this thesis because, as outlined in Section 5, it fit the criteria of being a large offshore wind farm with a rectilinear layout and it had the available input data required for the model.

The optimization algorithm outlined in Section 6.1 was applied to the Horns Rev wind farm and the results were analyzed.

7.1.1 Input Parameters

Application of the optimization strategy for micro-siting of the Horns Rev wind farm was restricted due to project time constraints. The optimization parameters applied to the Horns Rev wind farm layout (outlined in Appendix B in Table B-2) were not representative of a comprehensive optimization simulation with a near optimal result. The population (100) and maximum number of generations (10) were restricted due to the estimated simulation time required. Increasing the number of individuals in the population and increasing the number of generations would increase the likelihood of an improved design. The outcome from the simulation under the parameters outlined in Table B-2 results in evaluations of 900 ‘irregular’ wind farm layouts that show improvements from the existing rectilinear layout and provide insight into the potential value of wind farm layout optimization.

The wind rose applied to the Horns Rev wind farm was shown in Figure 3-4 and the Weibull parameters in Table 5-1. The wake dissipation length applied was 30 diameters and the wake decay constant selected was 0.04 as determined in Section 5. A full list of the model inputs can be found in Appendix B.

7.1.2 Simulation Results

The optimization of the Horns Rev Wind Farm evaluated 900 individual wind farm layouts in total, over 9 generations and determined an optimal layout after the minimum LCOE from 4 consecutive generations averaged a difference of less than 0.0001. It is understood that the limited nature of this optimization simulation does not necessarily provide a true optimum, but these were the best results available due to time. The existing Horns Rev wind farm is shown in Figure 7-1 with a cable layout that was designed using the hybrid cable layout heuristic. The cable layout heuristic was used instead of the installed cable layout to provide a valid comparison between the different wind farm layouts due to assumptions that were made in the cable cost sub-model. The improved wind farm layout can be seen in seen in Figure 7-2.

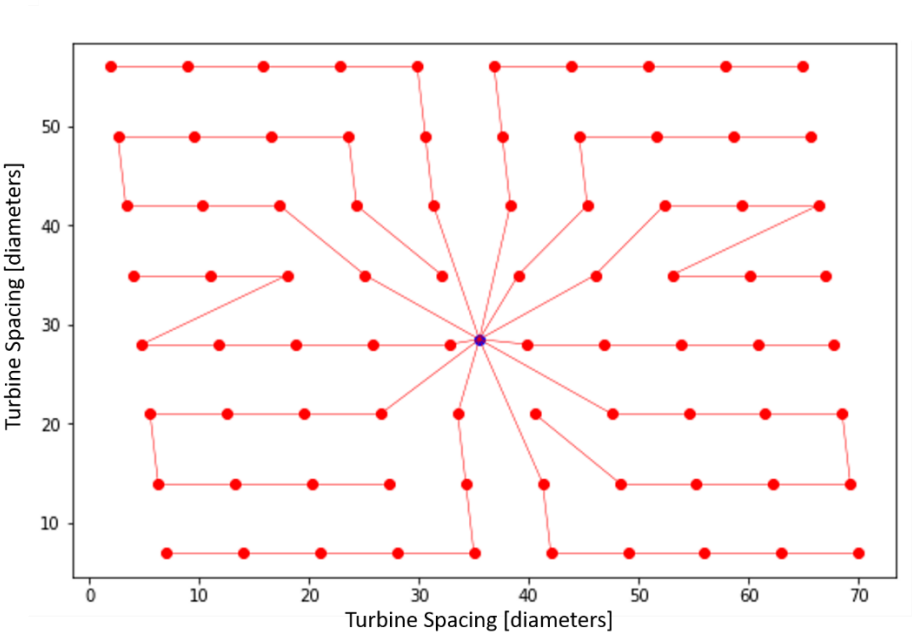

Figure 7-1: Horns Rev existing (rectilinear) wind farm layout

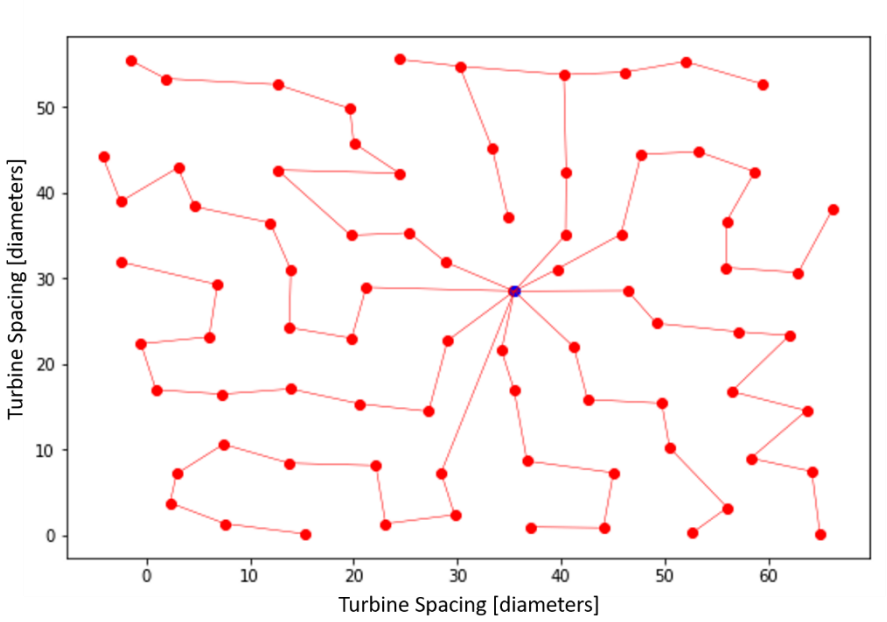

Figure 7-2: Horns Rev improved wind farm layout

It is observed that both constraints implemented in the optimization strategy, namely limiting one turbine per defined tile and turbine distance limited to at least 3 diameters, were abided by. This is evident by the relatively even spread of turbines throughout the wind farm, with no dense clusters. In the improved layout there is still visual similarities to rows and columns in some places, particularly the turbines along the bottom edge of the wind farm. It is uncertain that if with more generations, a more optimal layout would have similarities to the existing wind farm layout.

The final layout selection provided the lowest LCOE of the 900 individuals that were evaluated throughout the optimization process. Figure 7-3 displays the minimum, average and maximum LCOE value for each generation. None of the individuals that were evaluated resulted in an LCOE as high as the LCOE from the existing layout (0.0904 $/kWh). If the number of wind farm layouts in the population were to increase, there is a chance that some wind farm layouts would result in an LCOE comparable to the original design. However, from the wind farm layouts evaluated, the result from the existing Horns Rev wind farm layout is considered very poor.

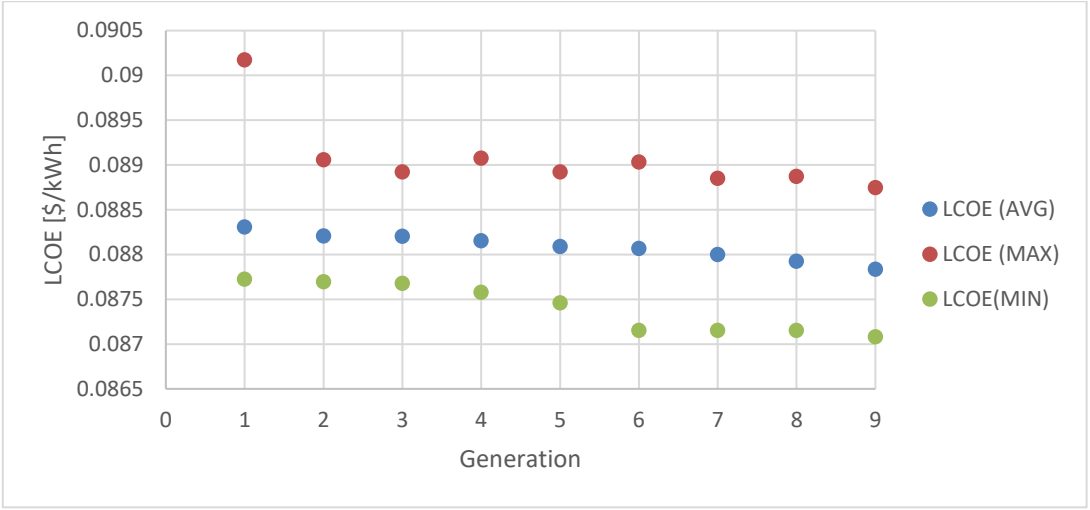

Figure 7-3: LCOE results for Horns Rev wind farm layouts

Figure 7-4 shows the minimum, average and maximum results from each generation for the AEP. The AEP for the optimal wind farm layout was near the maximum of the individuals that were evaluated. The difference between the minimum and maximum AEP values calculated for all individuals was only 5%. The genetic algorithm selected its initial individual in the first generation to be very close to the existing wind farm layout which is why the minimum result from the first generation is similar to the existing layout. Besides this point, all AEP results were higher than the existing layout indicating that a rectilinear layout is not optimal when considering wake effects for the Horns Rev wind farm. The AEP results trended slightly upwards as the generations increased due to the top individuals being selected to move onwards and thus be considered in the next generation. It is expected with an increased number of generations this trend would continue until it approaches the global optimum.

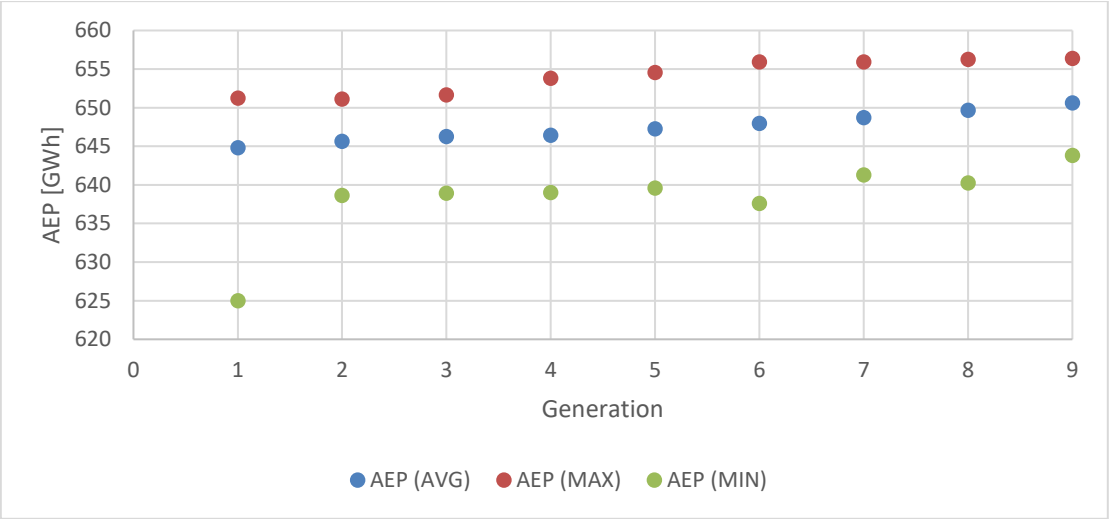

Figure 7-4: AEP results for Horns Rev wind farm layouts

The cable cost results were more widely spread than the AEP results, varying by nearly 18% between minimum and maximum values. The optimal cable layout had a cable cost near the lowest of the individuals evaluated, however the cable cost data did not trend downwards over the generations. The results from Figure 7-4 and Figure 7-5 indicate that the LCOE is more sensitive to the AEP than the cable cost for the Horns Rev wind farm. This conclusion will be discussed further in Section 7.3.

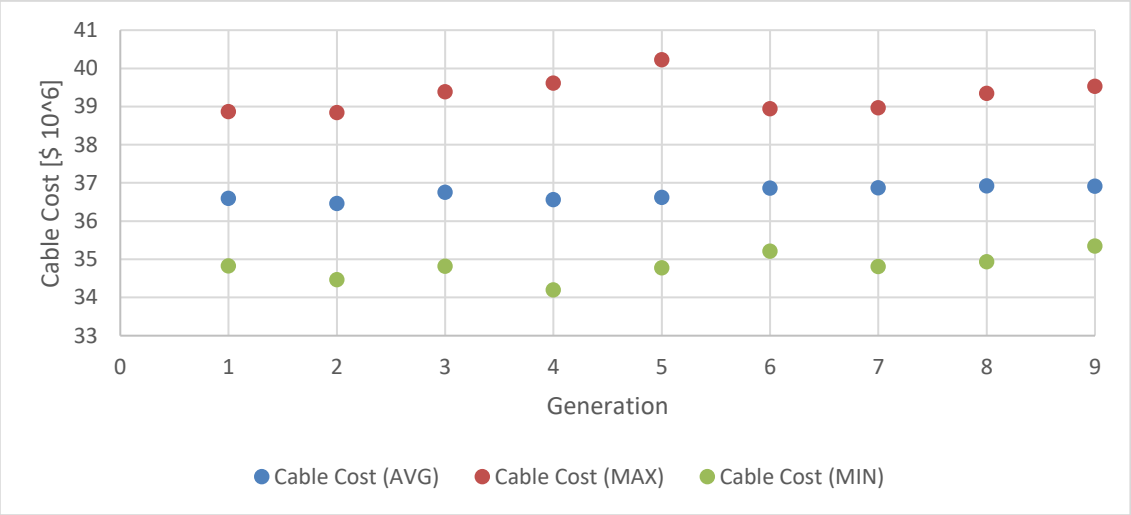

Figure 7-5: Cable cost results for Horns Rev wind farm layouts

The array efficiency for the final design is 90.5% compared to the existing design which was 86.5%. A comparison of the cable length, AEP and LCOE of the two layouts can be seen in Table 7-1.

Table 7-1: Horns Rev Wind Farm Layout Results Comparison

Parameter	**Existing Layout**	**Improved Layout**
Cable Length [m]	65611	59943 (91.4%)
Cable Cost [$10^6$$]	38.96	35.59 (91.4%)
AEP [GWh]	626.91	656.37 (104.7%)
LCOE [$/kWh]	0.0904	.0871 (96.3%)

The total collection cable length of the improved wind farm layout design is 8.6% shorter than the existing wind farm layout (which used the hybrid heuristic for the cable design). The improved wind farm layout design results in an estimated 4.7% increase in AEP. As both the cable length and AEP improve, the resulting LCOE for the improved layout is 3.7% lower than the existing Horns Rev layout.

7.2 Case Study II: Borssele Wind Farm

The second case study analyzed the Borssele Wind Farm. The Borssele wind farm zone is divided into 5 smaller wind farm sites. Borssele III and Borssele IV are considered for this thesis and will be referred to as the Borssele Wind Farm. What is different about the Borssele wind farm compared to Horns Rev is that the Borssele wind farm has not yet been constructed. So, although an existing design cannot be validated like it was for Horns Rev in Section 5, the data made available for the design tender [55] is used along with a proposed baseline wind farm design obtained from Perez-Moreno et al. [56] to analyze different layouts.

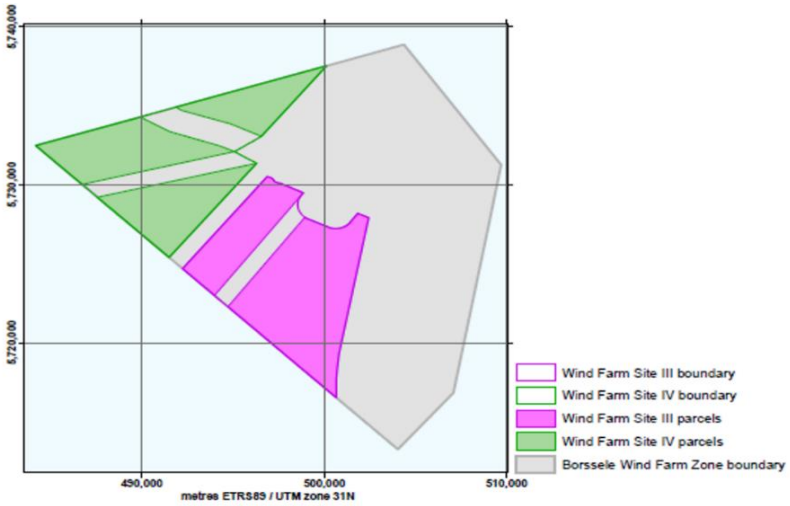

Figure 7-6: Borssele Wind Farm Zone – Sites III & IV [55]

Perez-Moreno et al. proposed a baseline windfarm layout to compare different design strategies, which can be seen in Figure B-1 in the appendices. The baseline layout was a rectilinear layout that comprised of 74 10-MW turbines and disregarded the existing pipe/cable restraints. The expected turbine size at Borssele is 9.5 MW, however Perez-Moreno et al. elected to use the DTU 10-MW reference turbine [57] as their motivations were not to meet all of the design criteria. Similar to Perez-Moreno et al., a 74-turbine design was used, though alternatively a 5-MW wind turbine was implemented in the present model because of the data readily available for the NREL reference wind turbine [58], seen in Table B-5 in the appendices.

The results for the baseline design were obtained and compared with the results from the application of the wind farm layout optimization.

7.2.1 Input Parameters

The optimization input parameters can be seen in Table B-6 in the appendices. As was mentioned in Section 7.1.1, the parameters were selected in consideration of the time required for the optimization. Improved results would be expected if the optimization evaluated more wind farm layouts over a longer duration of time.

The wind rose applied in this case study can be seen in Figure 7-7.

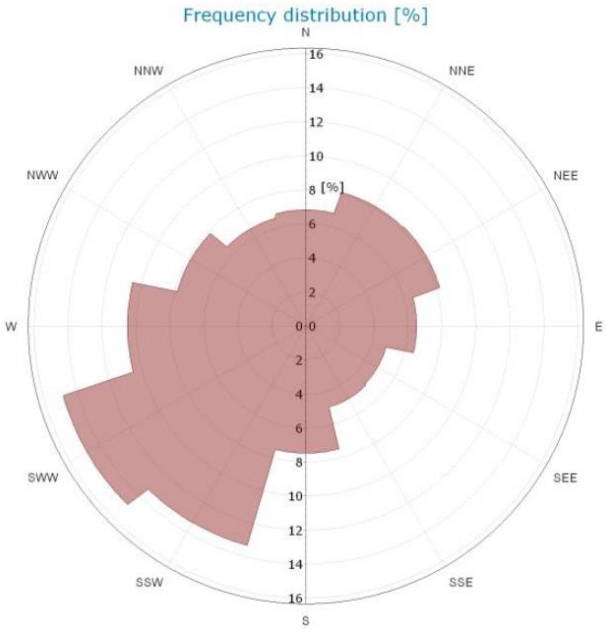

Figure 7-7: Borssele wind rose [59]

A full list of the model input parameters can be seen in Appendix B.

7.2.2 Simulation Results

Similar to the first case study, the analysis of Borssele wind farm was also limited by the computational constraints on the optimization. In the case for Borssele wind farm, 600 individual wind farm layouts were evaluated over 6 generations, with the best seen in Figure 7-9. The optimization ran for 6 generations before achieving 4 consecutive generations with an average objective function difference of the best layout of 0.0001. As mentioned for the first case study, the limited time that was available for the optimization was unlikely to provide a true optimum, however it did evaluate 600 wind farm layouts without rectilinear constraints which can be compared to the baseline wind farm layout seen in Figure 7-8. The baseline wind farm layout had a cable layout that was designed using the cable layout heuristic to provide a valid comparison between the different wind farm layouts.

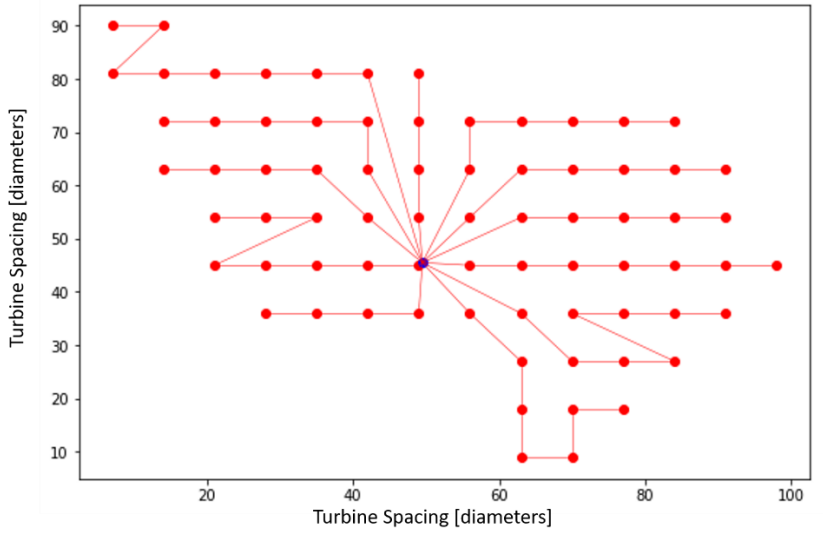

Figure 7-8: Borssele baseline (rectilinear) wind farm layout (rotated 210°)

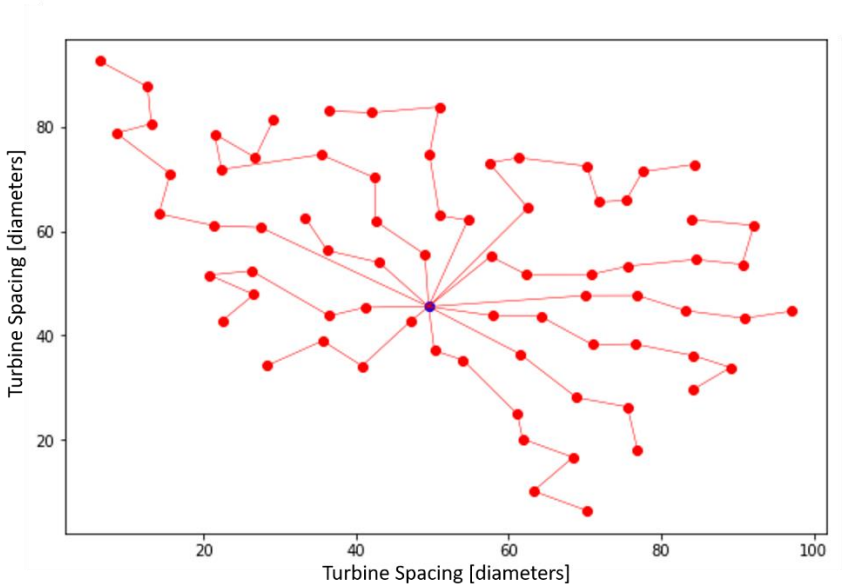

Figure 7-9: Horns Rev improved wind farm layout (rotated 210°)

The perimeter of Borssele wind farm provided a very different layout than Horns Rev. Figure 7-10 shows the minimum, average and maximum LCOE result for each generation, all of which are lower than the LCOE for the baseline layout (0.0970 $/kWh). Much like Case Study I, the initial individual simulated was very similar to the baseline layout which is why the maximum value in the first generation is similar to the LCOE of the baseline layout. It should be noted that the LCOE cost for the Borssele wind farm does not consider transmission costs (or losses) because the transmission was provided by another project. Also, the project proposal has a maximum bid for the cost of electricity of 0.11975 €/kWh [55], which indicates that the results from the model are within an appropriate range of expectations.

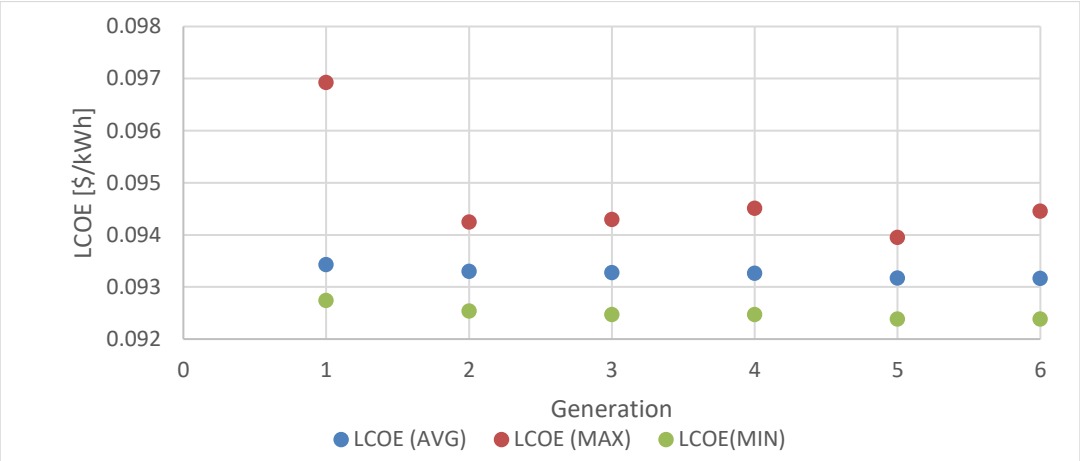

Figure 7-10: LCOE results for Borssele wind farm layouts

The minimum, average and maximum AEP results for each generation are shown in Figure 7-11. The results vary by approximately 5% between the minimum and maximum result from all 600 individuals, and trend slightly upwards over the generations. The AEP for the optimal layout is 1506.9 GWh which is near the maximum that was obtained.

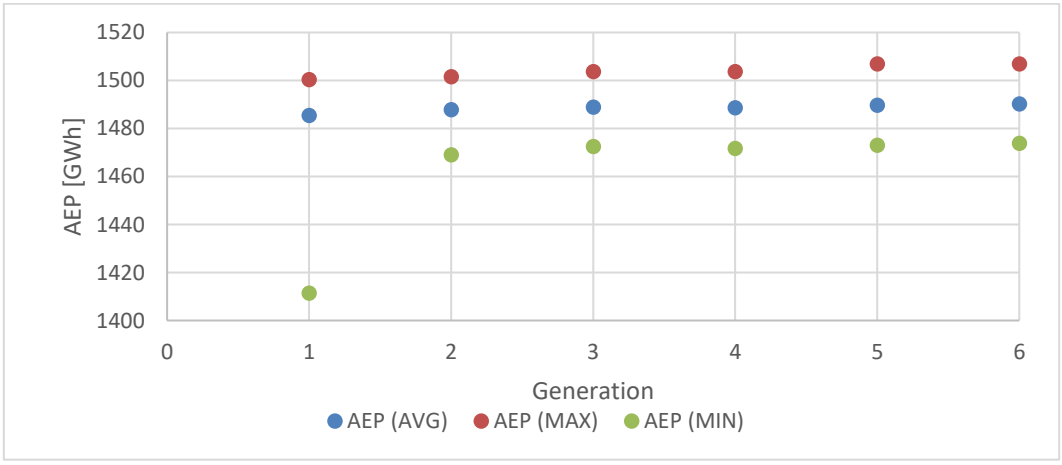

Figure 7-11: AEP results for Borssele wind farm layouts

The cable cost results were again more varied than the AEP results, varying by nearly 17%, as shown in Figure 7-12. The cable layout of the optimal design had a cost below the average of the generation, but was 5.8% higher than the lowest result of the individuals evaluated. The cable costs for Borssele had a slight trend downwards over the generations.

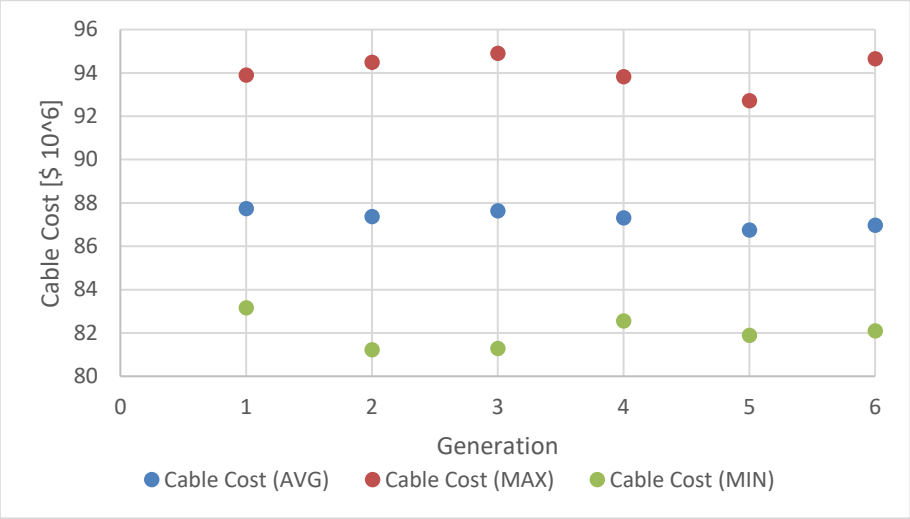

Figure 7-12: Cable cost results for Borssele wind farm layouts

The array efficiency for the final design is 93.0% compared to the existing design which was 87.1%. A comparison of the cable length, AEP and LCOE of the two layouts can be seen in Table 7-2.

Table 7-2: Borssele Wind Farm Layout Results Comparison

Parameter	**Existing Layout**	**Improved Layout**
Cable Length (m)	107540	103560 (96.3%)
Cable Cost (10^6\$)	89.40	86.09 (96.3%)
AEP (GWh)	1411.3	1506.9 (106.8%)
LCOE (\$/kWh)	0.0970	0.0924 (95.3%)

The total collection cable length of the improved design is 3.7% shorter than the baseline layout. The improved design results in an estimated 6.8% increase in AEP. As both the cable length and AEP improve, the resulting LCOE for the improved layout is 4.7% lower than the baseline Borssele rectilinear layout. The influence of each parameter on the LCOE will be explored further in the observations in the following section.

7.3 Case Study Observations

Analysis was limited to two case studies for two reasons: limitations in available data, and focus of the thesis was on development of the model that allowed for the analysis. The scope was limited to analysis of the two case studies and therefore broader trends could not be determined. With the limited results available from the two case studies, the following observations were made.

In both case studies results indicate that optimizing the positions of the individual turbines within the wind farm provides both a higher AEP and lower cable costs. The original expectation was that these two variables were contrasting and that one may have to worsen in order for the other to improve and lower the LCOE. It wasn't considered that both may improve within the optimal layout and as this is the case, at first glance it is difficult to know which variable impacts the LCOE more.

However, upon analysis of Figure 7-13 and Figure 7-14, the average AEP results for each generation trend upwards (improves) as the optimization continues for both wind farms. The average cable cost on the other hand, trends downwards (improves) over generations for Borssele but trends upwards (worsens) for Horns Rev. This would indicate that in the case of Horns Rev, increasing the AEP was of more influence than lowering cable costs in an effort to minimize the LCOE.

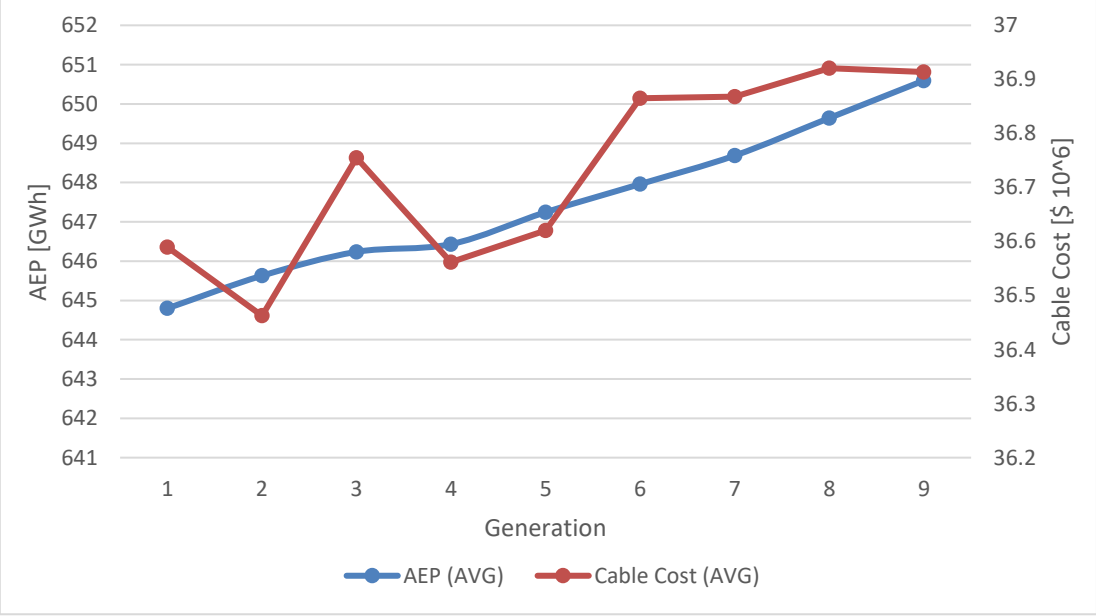

Figure 7-13: Average AEP and cable cost trends for Horns Rev

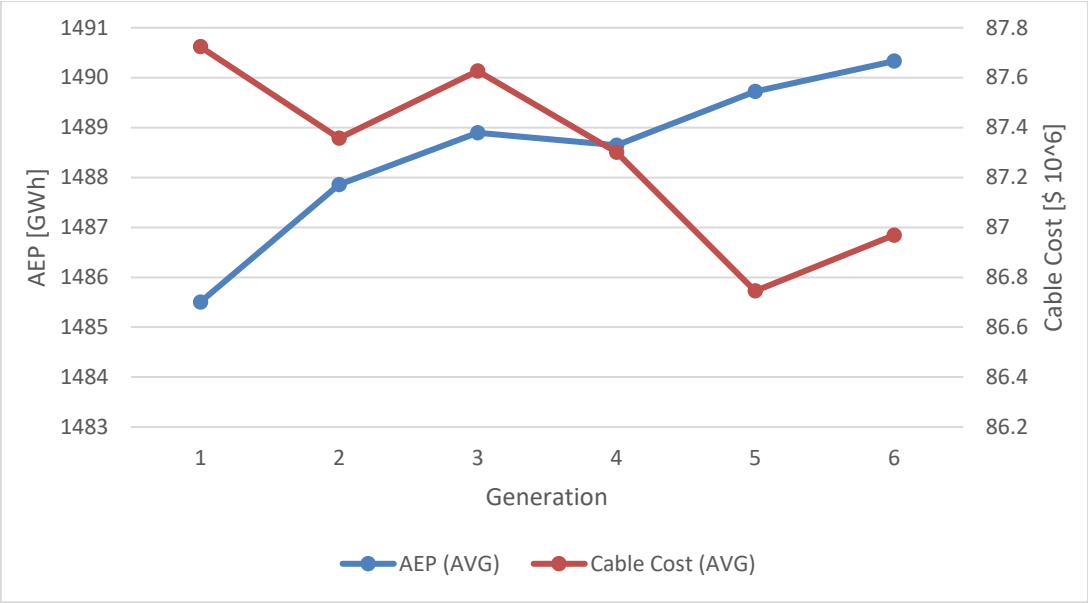

Figure 7-14: Average AEP and cable cost trends for Borssele

This relationship can be observed in Equation 7-1 (same as Equation 4-1) and Figure 3-9. Equation 7-1 shows that the LCOE corresponds to the relationship of the ICC divided by the AEP. Figure 3-9 shows that the intra-array cable costs are only a fraction of the ICC. Therefore, the LCOE is more sensitive to variations in the AEP than the collection cable costs.

$$LCOE = \frac{ICC * FCR}{AEP} + AOE \qquad 7\text{-}1$$

With more time and access to wind farm data, further analysis would be performed in order to observe trends of how much influence the cable cost has on the wind farm layout design.

The AEP for each wind farm varied no more than 5% once the optimization had abandoned the original rectilinear layout. The cable costs varied much more than the AEP, varying 18% and 17% for the Horns Rev and Borssele wind farms respectively.

As both the AEP increased and the cable cost decreased for each design relative to the existing layouts, both wind farms saw a decrease in the LCOE which was the expected outcome from the optimization. The optimized layout for Horns Rev experienced a decrease in LCOE of 3.7% and Borssele 4.7%. The difference in the WFLO-driven LCOE decrease between the present work and the results of Pillai et al. [18] may be attributed to the fact that both Horns Rev (80 turbines, 160 MW) and Borssele (74 turbines, 370 MW) are much larger than Middelgrunden (20 turbines, 40 MW) and would experience much more wake interaction. The increased wake interaction and variability for cable design of the larger farms would be expected to provide larger potential for savings if the layout is optimized.

In the limited number of individual wind farm layouts that were evaluated, none of them beyond the first individual evaluated in each case provided values near the existing rectilinear layout. An argument could be made that if the wind farm layout optimization populations were larger, there may be more individuals that provide an AEP or cable cost value that compare to the baseline rectilinear layout. Regardless of this fact, it was evident from the results of two case studies that rectilinear wind farm designs were not optimal with regards to minimizing the LCOE. The values for the existing rectilinear wind farm designs for AEP, cable cost and LCOE for both case studies would be considered outliers relative to the individuals evaluated in the optimization.

Despite the findings of this thesis and the prior research, rectilinear wind farm layouts are still the industry standard for offshore wind farms. This may be a result of the industry being conservative in nature and as such, slow to transition away from the traditional designs. As the observations from the thesis indicate that the traditional designs are not optimal from a cost of energy standpoint, they may be considered optimal for variables other than the cost of energy, for example easier planning or aesthetics. This trend may change in the future as more accurate models are developed that provide more information on new design strategies to help the industry become more economically viable.

Chapter 8

Conclusions

Chapter 8 finalizes this work by drawing conclusions, discussing the key assumptions and limitations, and recommending areas for development in future work.

The objective of the thesis was to explore the advantages of optimizing the positions of the individual wind turbines within an offshore wind farm. In order to perform analysis on different wind farms, a model was developed that is capable of simulating an existing offshore wind farm by converting external input data into a representative LCOE. The model which outputs LCOE is used in an optimization framework to optimize the positions of the individual turbines within the wind farm with the objective of minimizing the LCOE. Upon consideration of accuracy, availability of data and computing restrictions, the Jensen Wake-deficit Model and a hybrid cable layout heuristic were incorporated into the physical sub-model and the NREL cost scaling model was included into the economic sub-model. A genetic algorithm was selected for the wind farm layout optimization component.

Horns Rev and Borssele wind farms were used as case studies to explore the advantages of optimizing the positions of the individual turbines within an offshore wind farm. The wind farm layout optimization results show that:

- Optimized wind farm layouts resulted in a reduction of collection cable length relative to the baseline rectilinear layout of 8.6% for Horns Rev and 3.7% for Borssele.
- Optimized wind farm layouts resulted in an increase in the Annual Energy Production relative to the baseline rectilinear layout of 4.7% for Horns Rev and 6.8% for Borssele.
- Optimized wind farm layouts resulted in a decrease in the Levelized Cost of Electricity relative to the baseline rectilinear layout of 3.7% for Horns Rev and 4.7% for Borssele.

The initial expectation was that the contrasting nature of the wake effects and the collection cable costs would result in the improvement of one value at the expense of the other that would ultimately lead to an improved LCOE. However, the results from the model indicate that both the wake effects and collection cable costs were improved by applying an optimized layout in both case studies. The LCOE savings were higher than the results of Pillai et al. for Middelgrunden wind farm (1-3.5%). This difference may be explained by the size and shape of the Horns Rev and Borssele wind farms relative to the Middelgrunden wind farm. The larger wind farms studied in this thesis provide increased potential for savings through farm layout optimization layout because of the increased wake interaction and cable design variability.

The results observed from the model in both case studies indicate that there is potential for reducing the levelized cost of electricity for offshore wind farms by optimizing the positions of individual wind turbines within the layout. However, it is important to consider the assumptions and limitations of the implementation of the model used for analysis.

The following assumptions and limitations should be considered as they relate to the validity of the model and the qualitative results:

- The model was validated against the measured data from one wind farm due to limitations on available data. It is important that the current model is compared with measured data from more wind farms in order to compare the results and determine the model's accuracy.
- The model assumed a 'binary' partial wake effect model which was observed to provide inaccurate wind deficit results compared to the measured data at certain wind directions.

- The assumption that the foundation costs for each turbine were the same regardless of the bathymetry and soil conditions may cause large discrepancies in the LCOE results. However, as it was outlined in Section 3.1.3, the rectilinear constraints are unlikely to provide a better result if the individual turbine foundation costs are considered.

The subsequent assumptions and limitations should be considered as they relate to the accuracy of the model and the quantitative results:

- The optimization framework was constrained by time which limited the effectiveness of the application of the genetic algorithm. Using a more powerful computing device and having longer simulation times would allow for improved optimization results.
- The accuracy of the LCOE results are limited by the uncertainty of the input values incorporated into the economic model which vary based on the existing market and wind farm location. This is less relevant for relative comparisons, however could provide increased value by having the model LCOE be representative of the actual wind farm LCOE.
- The application of a simplified cable loss sub-model provides limited accuracy for the total electrical losses experienced in the collection cable network. However, in both case studies the cable length was reduced relative to the existing layout, therefore it is expected that improving this sub-model would result in increased value for optimizing the turbine locations.

Despite the limitations and assumptions, the results still provide valuable insight into the benefits of micro-siting as the same parameters and conditions were applied to each simulation.

8.1 Recommendations

In order to improve the validity and accuracy of the results obtained throughout the thesis and draw stronger conclusions that could be applied in practice, the following improvements are recommended:

- Inclusion of an improved partial wake effect model. This addition is expected to improve the accuracy of the wake model results and provide increased precision for the optimization algorithm.
- Inclusion of an improved collection cable loss model. Implementing a sub-model that could perform a power flow calculation of the collection cable network would allow for more accurate loss calculations which would improve the accuracy of the AEP.
- Validate the model against multiple existing wind farms to improve credibility / accuracy.
- Implement a more recent economic model that is representative of the recent advancements in offshore wind technology.
- Improve the existing physical model to be more robust for inclusion of external wind farm constraints. These developments would include improvements to the wind turbine boundary constraints that are implemented into the genetic algorithm to better represent

the wind farm perimeter, as well as improvements to the cable layout heuristic that would account for external cable layout constraints such as pipes or existing cables. This would provide more valuable results for wind farms similar to Borssele.

- Include a sub-model that accounts for the changes in foundation costs with regards to the changes in water depth and soil conditions.
- Improve the cable layout sub-model to include the ability to incorporate a ring design which would allow the model to be used in comparison with more existing wind farms that include power transmission redundancy.

Appendix A

Cable Layout Heuristic Algorithms

Appendix A provides the algorithm structure for the different cable layout heuristics that were used.

A.1 Planar Open Savings (POS) Heuristic

Inputs

Turbines: $T = \{t_1, ..., t_T\}$, $t_i = (x_i, y_i)$
Substations: $S = \{s_1, ..., s_S\}$, $s_i = (x_i, y_i)$
Infield Cables: $R = \{r_1, ..., r_R\}$, $r_i = (n_i, c_i)$
Transmission Lines: $((s_{x_0}, s_{y_0}),(s_{x_1}, s_{y_1}))\ \forall\ s \in S$
Pipelines/Cables: $((a_{x_0}, a_{y_0}),(a_{x_1}, a_{y_1}))$
Crossing penalty: p
Switchgear: $sw = 2$ or 3

Outputs

Connections: $P = \{(u_{k_1}, u_{v_1}, r_i^{kv})_1, ..., (u_{k_p}, u_{v_p}, r_i^{kv})_p\}$
Cable Length: $L = \{l_1, ..., l_R\}$
Cable Cost: C
Number of crossings: N

Figure A-1: List of heuristic inputs and outputs [40]

POS1 (Graph $(T \cup S, P)$, distance $d(k,u)\ \forall\ (k,u) \in P$, Capacity n):

1 foreach $i \in T$ **do** $s_i = argmin_{s \in S}\{d(i,s)\}$
2 $P \leftarrow \bigcup_{i \in T}\ (i, s_i)$
3 foreach $k,u \in T$, *if* $s_k \equiv s_u$ **do** $sv_{ku} = d(k,s_k) - d(k,u)$
4 $SV \leftarrow$ sorting of sv_{ku} according to decreasing saving
5 repeat
6 *(k,u)* $\leftarrow$ *next element in SV*
7 **if** *k and u are in different routes,*
8 *and* $(k, s_k) \in P$
9 *and u has only one neighbour in P,*
10 *and the total number of turbines in the routes containing k and u does not exceed n,*
11 *and (k,u) does not cross any connection in P* **then**
12 $P \leftarrow P \setminus ((k, s_k) \cup (k, u))$
13 until *end of SV is reached*
14 return P

Figure A-2: POS heuristic algorithm structure [6]

A.2 Esau-Williams (EW) Heuristic

EW Multiple Cable Types
(Graph $(T \cup S, P)$, distance $d(k,u)\ \forall\ (k,u) \in P$, Cables $r_1 = (n_1, c_1)$, $r_2 = (n_2, c_2)$):

foreach $i \in T$ **do** $s_i = argmin_{s \in S}\{d(i,s)\}$
$P \leftarrow \bigcup_{i \in T}\ (i, s_i, r_1)$
foreach $k,u \in T$, *if* $s_k \equiv s_u$ **do** $sv_{ku} = (d(k,s_k) - d(k,u)) * c_1$
$SV \leftarrow \bigcup_{k,u \in T}\ sv_{ku}$
repeat
    (k,u) $\leftarrow$ *maximum saving* sv_{ku} *in* SV
    if *k and u are in different routes,*
    and the total number of turbines in the routes containing k and u does not exceed n_1,
    and (k,u) does not cross any connection in P **then**
        $i \leftarrow$ last client in the route containing k
        $j \leftarrow$ last client in the route containing u
        $P \leftarrow P \setminus ((i, s_i, r_1) \cup (k, u, r_1))$
        foreach *client z of the merged route* **do**
            if $n \in T$ and $sv_{zn} \in SV$ **do**
                $sv_{zn} \leftarrow (d(j, s_j) - d(z, n)) * c_1$ *and update SV acccordingly*
        delete sv_{ku} **from** SV
    elif *k and u are in different routes,*
    and the total number of turbines in the routes containing k and u exceeds n_1
    and does not exceed n_2,
    and (k,u) does not cross any connection in P **then**
        $i \leftarrow$ last client in the route containing k
        $j \leftarrow$ last client in the route containing u
        $P_{tmp} \leftarrow P \setminus ((i, s_i, r_1) \cup (k, u, r_1))$
        Upgrade connections in P_{tmp} where necessary
        Downgrade connections in P_{tmp} where necessary
        $sv_{ku} \leftarrow Cost(P) - Cost(P_{tmp})$ *and update SV acccordingly*
        if $sv_{ku} = max_{sv \in SV}\{sv\}$ **then**
            $P \leftarrow P_{tmp}$
            foreach *client z of the merged route* **do**
                if $n \in T$ and $sv_{zn} \in SV$ **do**
                    $sv_{zn} \leftarrow (d(j, s_j) - d(z, n)) * c_1$ *and update SV acccordingly*
            delete sv_{ku} **from** SV
        else continue
until $sv_{ku} < 0$
return P

Figure A-3: EW heuristic algorithm structure [6]

A.3 Hybrid Heuristic

foreach $i \in T$ **do** $s_i = argmin_{s \in S}\{d(i,s)\}$
$P \leftarrow \bigcup_{i \in T} (i, s_i, r_1)$
foreach $k,u \in T$, *if* $s_k \equiv s_u$ **do** $sv_{ku} = (d(k,s_k) - d(k,u)) * c_1 + (N_{ks_k} - N_{ku}) * p$
$SV_1, SV_2 \leftarrow$ sorting of $sv_{ku} > 0$ according to decreasing saving
repeat
    (k,u) $\leftarrow$ *next element in* SV_1
    turbines $\leftarrow$ *the total number of turbines in the routes containing k and u*
    if *k and u are in different routes* **and** $(k, s_k) \in P$ **and** *u has only one neighbour in P,*
    and *turbines* $\leq n_1$,
    and *(k,u) does not cross any connection in P and transmission line* **then**
        $P \leftarrow P \setminus ((k, s_k, r_1) \cup (k, u, r_1))$
until *end of* SV_1 *is reached*
repeat
    (k,u) $\leftarrow$ *maximum saving* sv_{ku} *in* SV_2
    turbines $\leftarrow$ *the total number of turbines in the routes containing k and u*
    if *k and u are in different routes,*
    and *the number of (t,u) connections in P* **foreach** $t \in T < sw - 1$,
    and *(k,u) does not cross any connection in P and transmission line* **then**
        $i, j \leftarrow$ last clients in the routes containing k and u respectively
        if *turbines* $\leq n_1$ **then**
            $P \leftarrow P \setminus ((i, s_i, r_1) \cup (k, u, r_1))$
        elif *turbines* $> n_1$ **then**
            $n_i \leftarrow$ cable capacity for which $n_{i-1} <$ *turbines* $\leq n_i$
            $P_{tmp} \leftarrow P \setminus ((i, s_i, r_1) \cup (k, u, r_1))$
            upgrade and **downgrade** connections in P_{tmp} where necessary
            $sv_{ku} \leftarrow Cost(P) - Cost(P_{tmp}) + (N_{is_i} - N_{ku}) * p$ *and update* SV_2
            if $sv_{ku} = max_{sv \in SV_2}\{sv\}$ **then**
                $P \leftarrow P_{tmp}$
    if *P was updated* **then**
        foreach *client z of the merged route* **do**
            if $n \in T$ and $sv_{zn} \in SV_2$ **do**
                $sv_{zn} \leftarrow (d(j, s_j) - d(z, n)) * c_1 + (N_{js_j} - N_{zn}) * p$ *and update* SV_2
        delete sv_{ku} **from** SV_2
    elif *P and* sv_{ku} *were not updated* **then**
        delete sv_{ku} **from** SV_2
until $sv_{ku} < 0$
$P \leftarrow$ **RouteOpt** (radial parts of the routes for which cable r_1 is used)
$L = \{\sum_{(u_k,u_v,r_1^{kv}) \in P} d(u_k, u_v), ..., \sum_{(u_k,u_v,r_R^{kv}) \in P} d(u_k, u_v)\}$
$C = \sum_{l_i \in L} l_i * c_i$
$N = \sum_{(u_k,u_v,r_i^{kv}) \in P} N_{u_k u_v}$
return P, L, C, N

Figure A-4: Hybrid heuristic algorithm structure [40]

Appendix B

Case Study Model Input Data

The following appendix consists of tables of input data for each of the case studies in Chapter 7.

B.1 Horns Rev Wind Farm Inputs

B.1.1 Vestas V80 Power / Thrust Curve

Table B-1: Vestas V80 wind turbine power and thrust curve [24] [50]

Wind Speed [m/s]	Turbine Power [kW]	Thrust Coefficient [-]
0	0	0
1	0	0
2	0	0
3	0	0
4	66.60	0.818
5	154.00	0.806
6	282.00	0.804
7	460.00	0.805
8	696.00	0.806
9	996.00	0.807
10	1341.00	0.793
11	1661.00	0.739
12	1866.00	0.709
13	1958.00	0.409
14	1988.00	0.314
15	1997.00	0.249
16	1999.00	0.202
17	2000.00	0.167
18	2000.00	0.140
19	2000.00	0.119
20	2000.00	0.102
21	2000.00	0.088
22	2000.00	0.077
23	2000.00	0.067
24	2000.00	0.060
25	2000.00	0.053
26	0.00	0.000

B.1.2 Optimization Input Parameters

Table B-2: Horns Rev Optimization Parameters

Optimization Parameter	**Value**
Population Size	100
Max Generations	10
Max Stall Generations	4
Max Stall Tolerance	0.0001
Elite Count	.05*Population
Crossover Fraction	.8

B.1.3 Horns Rev Wind Park Input Data

Table B-3: Horns Rev Input Data

Parameter	Value	Units
Hub Height	70	m
Rotor Diameter	1	diameters
Rated Power of the Turbine	2000	kW
Rotor Diameter	80	m
Initial Turbine spacing in the x direction	7	diameters
Initial Turbine spacing in the y direction	7	diameters
Initial Number of turbines in each row	10	-
Initial Number of turbines in each column	8	-
Initial Total number of turbines in the array	80	-
Wake Decay Parameter	0.04	0.04
Wake Dissipation Length	30	diameters
Collection Cable Voltage	36	kV
Collection Cable Capacity	10	turbines
Collection Cable Efficiency	98.8	%
Transmission Cable Efficiency	100	%
Initial Collection Cable Length	76237	m
Wind Farm Availability	95	%
Fixed Charge Rate	11.58	%
Average Water Depth	20	m
Distance Offshore to Onshore Substation	13000	m

B.1.4 Horns Rev Cost Data

Table B-4: Horns Rev Cost Data

Parameter	Value	Units
Collection Cable Material Cost	381	$/m
Cable Transport (Transatlantic)	0	$/m
Cable Installation Cost	94	$/m
Cost of Steel ($/kg)	1.5	$/kg
Blade Material Cost Escalator	139.3	%
Labor Cost Escalator	139.3	%
Conversion from 2002->2018 US Dollars	139.3	%
Conversion from 2003->2018 US Dollars	137	%
Conversion from 2006->2018 US Dollars	125	%
Number of Offshore Substation Transformers	3	-
Transformer Cost per Turbine	50500	$/turbine
Offshore Substation and Transformer Cost	81.04	$/kW
Onshore Substation and Transformer Cost	58.74	$/kW
Transmission Cable Material Cost	755	$/m
Marine Route Survey & Engineering Cost	1500000	$/windfarm
Cable Installation Mobilization/Demobilization	5000000	$/windfarm

B.2 Borssele Wind Farm Inputs

B.2.1 NREL Reference Turbine Power / Thrust Curve

Table B-5: NREL reference wind turbine power and thrust curve

Wind Speed [m/s]	Turbine Power [kW]	Thrust Coefficient [-]
0	0	0
1	0	0
2	0	0
3	0	0
4	178	0.818
5	404	0.806
6	738	0.804
7	1187	0.805
8	1771	0.806
9	2519	0.807
10	3448	0.793
11	4562	0.739
12	5000	0.709
13	5000	0.409
14	5000	0.314
15	5000	0.249
16	5000	0.202
17	5000	0.167
18	5000	0.140
19	5000	0.119
20	5000	0.102
21	5000	0.088
22	5000	0.077
23	5000	0.067
24	5000	0.060
25	5000	0.053
26	0	0.000

B.2.2 Borssele Optimization Input Parameters

Table B-6: Borssele Optimization Parameters

Optimization Parameter	**Value**
Population Size	100
Max Generations	10
Max Stall Generations	4
Max Stall Tolerance	0.0001
Elite Count	.05*Population
Crossover Fraction	.8

B.2.3 Borssele Wind Park Input Data

Table B-7: Borssele Wind Farm Input Data

Parameter	Value	Units
Hub Height	90	m
Rotor Diameter	1	diameters
Rated Power of the Turbine	5000	kW
Rotor Diameter	126	m
Initial Turbine spacing in the x direction	7	diameters
Initial Turbine spacing in the y direction	9	diameters
Initial Number of turbines in each row	Varies	-
Initial Number of turbines in each column	Varies	-
Initial Total number of turbines in the array	74	-
Wake Decay Parameter	0.04	0.04
Wake Dissipation Length	30	diameters
Collection Cable Voltage	66	kV
Collection Cable Capacity	8	turbines
Collection Cable Efficiency	98.8	%
Transmission Cable Efficiency	-	%
Initial Collection Cable Length	107540	m
Wind Farm Availability	95	%
Fixed Charge Rate	11.58	%
Average Water Depth	30	m
Distance Offshore to Onshore Substation	0	m

B.2.4 Borssele Cost Data

Table B-8: Borssele Cost Data

Parameter	Value	Units
Collection Cable Material Cost	571	$/m
Cable Transport (Transatlantic)	0	$/m
Cable Installation Cost	94	$/m
Cost of Steel ($/kg)	1.5	$/kg
Blade Material Cost Escalator	139.3	%
Labor Cost Escalator	139.3	%
Conversion from 2002->2018 US Dollars	139.3	%
Conversion from 2003->2018 US Dollars	137	%
Conversion from 2006->2018 US Dollars	125	%
Number of Offshore Substation Transformers	3	-
Transformer Cost per Turbine	50500	$/turbine
Offshore Substation and Transformer Cost	81.04	$/kW
Onshore Substation and Transformer Cost	58.74	$/kW
Transmission Cable Material Cost	755	$/m
Marine Route Survey & Engineering Cost	1500000	$/windfarm
Cable Installation Mobilization/Demobilization	5000000	$/windfarm

B.2.5 Proposed Borssele baseline wind farm layout

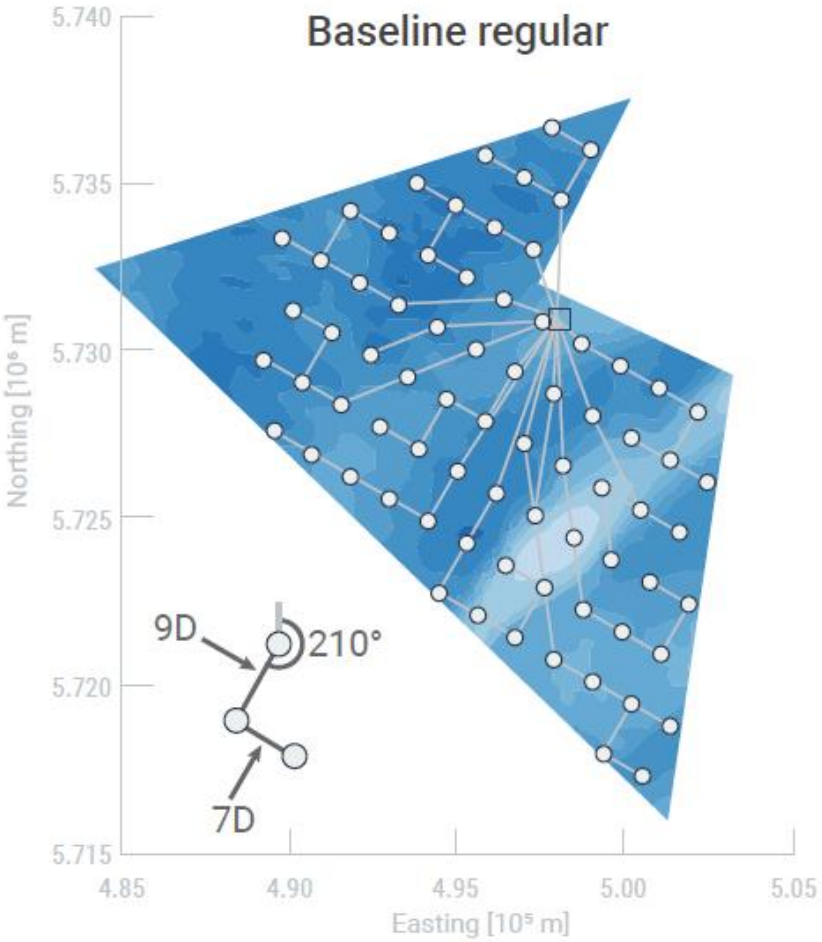

Figure B-1: Borssele baseline wind farm layout [56]

References

[1] R. Perveen, N. Kishor and S. Mohanty, "Offshore wind farm development: Present status and challenges," *Renewable and Sustainable Energy Reviews (29),* pp. 780-792, 2014.

[2] S. Rodrigues, C. Restrepo, E. Kontos, R. T. Pinto and P. Bauer, "Trends of offshore wind projects," *Renewable and Sustainable Energy Reviews (49),* pp. 1114-1135, 2015.

[3] M. Bilgili, A. Yasar and E. Simsek, "Offshore wind power development in Europe and its comparison with onshore counterpart," *Renewable and Sustainable Energy Reviews (15),* pp. 905-915, 2011.

[4] S. Pfeifer, "Subsidy-free renewable projects on 'cusp of breakthrough'," Financial Times, 28 March 2018. [Online]. Available: https://www.ft.com/content/1960c6fe-2dea-11e8-a34a-7e7563b0b0f4. [Accessed 1 October 2018].

[5] S. Krohn, P.-E. Morthorst and S. Awerbuch, "The Economics of Wind Energy," European Wind Energy Association, Belgium, 2009.

[6] J. Bauer and J. Lysgaard, "The offshore wind farm array cable layout problem: a planar open vehicle routing problem," *JORS (66),* pp. 360-368, 2015.

[7] J. Herbert-Acero, O. Probst, P.-E. Rethore, G. Larsen and K. Castillo-Villar, "A Review of Methodological Approaches for the Design and Optimization of Wind Farms," *Energies (7),* pp. 6930-7016, 2014.

[8] I. Katic, J. Hojstrup and N. Jensen, "A Simple Model For Cluster Efficiency," in *European Wind Energy Association Conference and Exhibition*, Rome, 1986.

[9] M. A. Lackner and C. N. Elkinton, "An Analytical Framework for Offshore Wind Farm Layout Optimization," *Wind Engineering,* vol. 31, no. 1, pp. 17-31, 2007.

[10] G. Mosetti, C. Poloni and B. Diviacco, "Optimization of wind turbine positioning in large windfarms by means of a genetic algorithm," *Wind Engineering and Industrial Aerodynamics (51),* pp. 105-116, 1994.

[11] S. Grady, M. Hussaini and M. Abdullah, "Placement of wind turbines using genetic algorithms," *Renewable Energy (30),* pp. 259-270, 2005.

[12] C. M. Ituarte-Villarreal and J. F. Espiritu, "Optimization of wind turbine placement using a viral based optimization algorithm," *Procedia Computer Science,* vol. 6, pp. 469-474, 2011.

[13] C. Wan, J. Wang and Z. X. Yang G., "Optimal Micro-siting of Wind Farms by Particle Swarm Optimization," in *Advances in Swarm Intelligence ICSI 2010*, Berlin, Heidelberg, Springer, 2010, pp. 198-205.

[14] K. Chen, M. Song, Z. He and X. Zhang, "Wind turbine positioning optimization of wind farm using greedy algorithm," *Journal of Renewable and Sustainable Energy ,* vol. 5, pp. 023128 1-15, 2013.

[15] A. Tesauro, P.-E. Rethore and G. Larsen, "State of the art of wind farm optimization," in *European Wind Energy Conference & Exhibition*, 2012.

[16] R. Shakoor, M. Y. Hassan, A. Raheem and Y. Wu, "Wake effect modeling: A review of wind farm layout optimization using Jensen's model," *Renewable and Sustainable Energy Reviews,* pp. 58 1048-1059, 2016.

[17] P. Pardalos and e. al., Handbook of Wind Power Systems, Energy Systems, Berlin Heidelberg: Springer-Verlag, 2013.

[18] A. Pillai, J. Chick, M. Khorasanchi, S. Barbouchi and L. Johanning, "Application of an offshore wind farm layout optimization methodology at Middelgrunden wind farm," *Ocean Engineering (139),* pp. 287-297, 2017.

[19] C. Elkinton, J. Manwell and J. McGowan, "Algorithms for Offshore Wind Farm Layout," *Wind Engineering Volume 32,* pp. 67-83, 2008.

[20] C. Elkinton, Offshore Wind Farm Layout Optimization, Ph.D Thesis, University of Massachusetts Amherst, 2007.

[21] T. Burton, D. Sharpe, N. Jenkins and E. Bossanyi, Wind Energy Handbook, Chichester: John Wiley & Sons Ltd, 2001.

[22] Wind Power Program, "14. Wind Turbine power output variation with steady wind speed," 16 September 2018. [Online]. Available: http://www.wind-power-program.com/turbine_characteristics.htm.

[23] L. Fingersh, M. Hand and A. Laxson, "WindTurbine Design Cost and Scaling Model," National

Renewable Energy Laboratory, Golden CO, 2006.

[24] D. R. VanLuvanee, "Investigation of Observed and Modeled Wake Effects at Horns Rev using WindPRO," Technical University of Denmark (Master Thesis), 2006.

[25] S. Pena, P. Rethore and M. van der Laan, "On the application of the Jensen wake model using a turbulence dependent wake wake coefficient: The Sexbierum case," *Wind Energy,* 2015.

[26] M. Bencherif, B. Brahmi and A. Chikhaoui, "Optimum selection of wind turbines," *Science Journal of Energy Engineering,* pp. 2(4): 36-46, 2014.

[27] S. Akdag and A. Dinler, "A new method to estimate Weibull parameters for wind energy applications," *Energy Conversion and Management,* pp. (50) 1761-1766, 2009.

[28] F. Amar and M. Elamouri, "Wind Energy Assessment of the Sidi Daoudi Wind Farm - Tunisia," in *Wind Farm - Technical Regulations, Potential Estimation and Siting Assessment*, InTech (ISBN: 978-953-307-438-2, 2011, pp. 115-140.

[29] F. Gonzalez-Longatt, P. Wall and V. Terzija, "Wake effect in wind farm performance: Steady-state and dynamic behaviour," *Renewable Energy (39),* pp. 329-338, 2012.

[30] Vattenfall, "Wind turbine wake effects," 17 September 2018. [Online]. Available: http://www.windaction.org/posts/24269-wind-turbine-wake-effects#.W59_Feip2Uk.

[31] M. Samorani, "The Wind Farm Layout Optimization," in *Handbook of Wind Power Systems*, Berlin Heidelberg, Springer-Verlag, 2013, pp. 21-37.

[32] J. Vermeer, J. Sorensen and A. Crespo, "Wind turbine wake aerodynamics," *Progress in Aerospace Sciences (39),* pp. 467-510, 2003.

[33] B. Sanderse, "Aerodynamics of wind turbine wakes literature review," Energy Research Center of Netherlands ECN-E-09-016, 2009.

[34] T. Sorensen, M. L. Thogersen and P. Nielsen, "Adapting and calibtration of existing wake models to meet the conditions inside offshore wind farms.," EMD International A/S, Aalborg, Denmark, 2008.

[35] M. Zaaijer, "Great expectations for offshore wind turbines," TU Delft (PhD Thesis), Delft, 2013.

[36] IRENA Secretariat, "Renewable energy technologies: Cost Analysis series - Wind Power," International Renewable Energy Agency, 2012.

[37] S. Lundberg, "Performance comparison of wind park configurations," Department of Electric Power Engineering, Chalmers University of Technology, 2003.

[38] A. Madariaga, J. Martin, I. Zamora, I. Martinez de Alegria and S. Ceballos, "Technology trends in electric topologies for offshore wind power plants," *Renewable and Sustainable Energy Review (24),* pp. 32-44, 2013.

[39] P. Bresesti, W. Kling, R. Hendricks and R. Vailati, "HVDC Connection of Offshore Wind Farms to the Transmission System," *Energy Conversion, IEEE Transactions on, (22),* pp. 37-43, 2007.

[40] G. Katsouris, "Infield Cable Topology Optimization of Offshore Wind Farms," Delft University of Technology (Master Thesis), Delft, 2015.

[41] S. Lumbreras and A. Ramos, "Offshore wind farm electrical design: a review," *Wind Energy (16),* pp. 459-473, 2013.

[42] L. Esau and K. Williams, "On teleprocessing system design: part ii a method for approximating the optimal network," *IBM Systems Journal ,* vol. 5, no. 3, pp. 142-147, 1966.

[43] J. Schachner, "Power connections for offshore wind farms," Delft University of Technology (Diploma Thesis), Delft, 2004.

[44] L. Amaral and R. Castro, "Offshore wind farm layout optimization regarding wake effects and electrical losses," *Engineering Applications of Artificial Intelligence,* no. 60, pp. 26-34, 2017.

[45] A. Gonzalez-Rodriguez, "Review of offshore wind farm cost components," *Energy for Sustainable Development (37),* pp. 10-19, 2017.

[46] J. Green, A. Bowen, L. Fingersh and Y. Wan, "Electrical Collectione and Transmission Systems for Offshore Wind Power," National Renewable Energy Laboratory, Golden CO, 2007.

[47] US Department of Energy, "Standardized Cost and Performance Reporting for Marine and Hydrokinetic Technologies," US DOE, 2014.

[48] J. Seguro and T. Lambert, "Modern estimation of the parameters of the Weibull wind speed distribution for wind energy analysis," *Journal of Wind Engineering and Industrial Aerodynamics ,* no. 85, pp. 75-84, 2000.

[49] P. Eecen, J. Wagenaar, N. Stefanatos, T. Pedersen, R. Wagner and K. Hansen, "Final Report - Upwind 1A2 Metrology," ECN, 2011.

[50] L. Jensen, C. Morch, P. Sorensen and K. Svensen, "Wake Measurements from the Horns Rev wind farm," in *EWEC 2004 Proceedings*, London UK, 2004.

[51] M. Mechali, R. Barthelmie, S. Frandsen and P. Rethore, "Wake effects at Horns Rev and their influence on energy production," in *EWEC 2006 Proceedings*, Athens Greece, 2006.

[52] International Renewable Energy Agency, "Renewable Power Generation Costs in 2017," IRENA, Abu Dhabi, 2018.

[53] MathWorks, "How the Genetic Algorithm Works," [Online]. Available: https://www.mathworks.com/help/gads/how-the-genetic-algorithm-works.html. [Accessed 1 October 2018].

[54] H. Pohlheim, "GEATbx Introduction - Evolutionary Algorithms: Overview, Methods and Operators, Version 3.8," 2006. [Online]. Available: www.geatbx.com. [Accessed 25 September 2018].

[55] Netherlands Enterprise Agency, "Borssele Wind Farm Zone: Wind Farm Sites III & IV - Project and Site Description," Utrecht, The Netherlands, 2016.

[56] S. S. Perez-Moreno, K. Dykes, K. O. Merz and M. B. Zaaijer, "Multidisciplinary design anlysis and optimization of a reference offshore wind plant," *Journal of Physics Conf. Ser. 1037 042004,* pp. 1-15, 2018.

[57] C. Bak and e. al., "The DTU 10-MW Refernce Wind Turbine," Sound/Visual production, 2013.

[58] J. Jonkman, S. Butterfield, W. Musial and G. Scott, "Definition of a 5-MW Reference Wind Turbine for Offshore System Development," NREL, Golden, Colorado, 2009.

[59] B. Bulder, E. Bot, E. Wiggelinkhuizen and F. Nieuwenhout, "Quick scan wind farm efficiencies of the Borssele location," ECN (ECN-E--14-050), Petten, The Netherlands, 2014.